

THESIS ON MECHANICAL ENGINEERING E79

Disintegrator Milling System Development and Milling Technologies of Different Materials

DMITRI GOLJANDIN

TUT
PRESS

TALLINN UNIVERSITY OF TECHNOLOGY
Faculty of Mechanical Engineering
Department of Materials Engineering

Dissertation was accepted for the defence of the degree of Doctor of Philosophy in Engineering on June 27, 2013.

Supervisors: Prof. Priit Kulu, Department of Materials Engineering, TUT

Prof. Jaan Kers, Department of Polymer Materials, TUT

Opponents: Prof. Viktors Mironovs, Laboratory of Powder Technology,
Riga Technical University, Latvia

Dr. Ph.D. Boris Kipnis, Desintegraator Tootmise OÜ,
Chief Technologist, Estonia

Defence of the thesis: August 28, 2013 at 11:00
Room No.: VI-425
Tallinn University of Technology,
Ehitajate tee 5, Tallinn, Estonia

Declaration:

Hereby I declare that this doctoral thesis, my original investigation and achievement, submitted for the doctoral degree at Tallinn University of Technology has not been submitted for any academic degree.

/Dmitri Goljandin/



Copyright: Dmitri Goljandin, 2013
ISSN 1406-4758
ISBN 978-9949-23-519-3 (publication)
ISBN 978-9949-23-520-9 (PDF)

MEHHANOTEHNIKA E79

**Desintegraatorjahvatussüsteemi arendus ja
erinevate materjalide desintegraator-
jahvatustehnoloogiad**

DMITRI GOLJANDIN

CONTENTS

LIST OF PUBLICATIONS	6
LIST OF ABBREVIATIONS AND SYMBOLS	7
INTRODUCTION	9
1. THEORY OF THE MILLING BY COLLISION	12
1.1 Theoretical aspects of milling	12
1.1.1 Size reduction by collision	12
1.1.2 Stresses on collision	13
1.1.3 Collision of particle with another particle or plate	16
1.1.4 Size reducing model	18
1.2 Basics of separation	20
1.2.1 Separation of particles in inertial classifier	20
1.2.2 Centrifugal classifier	21
2 DEVELOPMENT OF DISINTEGRATOR MILLING SYSTEM FOR	
MATERIALS TREATMENT	25
2.1 Design of disintegrator	25
2.2 Design of classifier	28
2.3 Prediction of wear resistance of steels for grinding media	31
3 TREATMENT OF DIFFERENT MATERIALS	33
3.1 Pretreatment of metallic materials	34
3.1.1 Production of metallic powders from steel chips	34
3.1.2 Production of ultrafine Co- and Ni- based alloy powders	36
3.2 Grindability of mineral materials	40
3.3 Pretreatment of composite materials	41
3.3.1 Production of hardmetal powders	41
3.3.2 Reprocessing of metallic-GFRP laminated plastic composite ...	43
3.4 Potential areas of application of produced metallic powders	45
CONCLUSIONS	47
REFERENCES	49
ACKNOWLEDGEMENTS	56
ABSTRACT	57
KOKKUVÕTE	59
PUBLICATIONS	61
Publication I	61
Publication II	89
Publication III	97
Publication IV	105
Publication V	113
ELULOOKIRJELDUS	121
CURRICULUM VITAE	123

LIST OF PUBLICATIONS

The present dissertation is based on the following papers, which are referred in the text by their Roman numerals I–IV.

- I Zimakov, S.; Goljandin, D.; Peetsalu, P.; Kulu, P. (2007). Metallic powders produced by the disintegrator technology. *International Journal of Materials and Product Technology*, 28(3/4), 226 - 251.
- II Goljandin, D.; Kulu, P.; Käerdi, H.; Bruwier, A. (2005). Disintegrator as device for milling of mineral ores. *Materials Science (Medžiagotyra)*, 11(4), 398 - 402.
- III Käerdi, H.; Goljandin, D.; Kulu, P.; Sarjas, H.; Mikli, V. (2013). Characterization of Mechanically Milled Cermet Powders Produced by Disintegrator Technology. Hussainova, I. (Toim.). *Key Engineering Materials and Tribology*, 148-153.
- IV Goljandin, D.; Sarjas, H.; Kulu, P.; Käerdi, H.; Mikli, V. (2012). Metal-Matrix Hardmetal/Cermet Reinforced Composite Powders for Thermal Spray. *Materials Science (Medžiagotyra)*, 18(1), 84 - 89.
- V Kers, J., Kulu, P., Goljandin, D., Kaasik, M., Ventsel, T., Vilsaar, K., Mikli, V. (2008). Recycling of Electronic Wastes by Disintegrator Mills and Study of Separation Technique of Different Materials. *Materials Science (Medžiagotyra)*, 14(4), 296 - 300.

Autors contribution to the publications

Paper I Development of theoretical model for the size reduction of ductile materials by collision, calculation of impact parameters, development of special multipurpose disintegrator milling system - disintegrator DSL-175 with a combined inertial-centrifugal classifier for the production of micrometrical powders, disintegrator milling of different metallic materials

Paper II The study of the grindability of different mineral materials using milling by collision in a disintegrator.

Paper III Procession of TiC-based cermets scrap by semi-industrial and laboratory disintegrator milling system. Estimation of properties of recycled cermet powders by sieving analysis. Grindability estimating using specific energy parameter E_s .

Paper IV Studying grindability of hardmetal/cermet using milling by collision in disintegrator mills. Influence clarifying of particle size reduction on specific energy of treatment.

Paper V Studying grindability of metallic and composite materials containing printed circuit board electronic wastes. Influence clarifying of particle size reduction on specific energy of treatment parameter E_s . Characterization of milled product. Separation of metallic and non-metallic materials with different methods.

LIST OF ABBREVIATIONS AND SYMBOLS

Abbreviations:

Alloy	– Ni-based powder Alloy 59 (MBC Metal Powders Ltd.)
CC	– centrifugal classifier
DESI	– experimental disintegrator
DS	– disintegrator milling system
DSL	– laboratory disintegrator milling system
GFRP	– glass fibre reinforced plastics
HSS	– high speed steel
IC	– inertial classifier
PCB	– printed circuit board
Ultimet	– Co-based powder Anval Ultimet (Carpenter Powder Products Ltd.)

Symbols:

AS	– aspect ratio, ellipticity of the particle, ratio between major and minor axes of the Legendre ellipse
B, H	– grid parameters, mm
c_1, c_2	– velocities of elastic waves, m/s
d	– particle size, mm
d_{50}	– median diameter (the median of the mass density function of Rosin-Rammler), mm
d_m	– mean diameter, μm
d_{min}	– boundary grain size, μm
E	– modulus of elasticity, MN/mm^2
E_s	– specific energy of milling in disintegrator mill, kWh/t or kJ/kg; depends on disintegrator construction
EL	– elongation, ellipticity of the particle
F	– contact forces in the collision, N
F_a	– air resistance force
F_i	– inertia force
F_{in}	– centrifugal force
f_m	– modified Rosin-Rammler distribution function
F_{st}	– resistance force of the air environment
H_a	– abrasive hardness, HV
HV	– Vickers hardness
IP	– irregularity parameter, ratio between minimum circumscribed and maximum inscribed circles of the particles cross-section
n_i	– number of loadings
Q	– air performance; productivity of separative air aspirated through the grid, m^3/min
R	– qualifier grid radius, m
r	– radius of the curvature, mm

r_k	– contact area radius; radius of the contact patch, μm
R_0	– initial radius of colliding bodies
R_1, R_2	– radii of colliding bodies, mm
SF	– shape factor
SPQ	– spike parameter – quadratic fit; angularity parameter
$\text{wt}\%$	– weight percentage
α	– approach of the centres; convergence centres, μm
α_{max}	– maximum convergence centres, μm
δ	– thickness of flake; parameter in the model of size reduction by collision of ductile materials, μm
Δp	– pressure differential
ε	– wear resistance
μ	– Poisson's ratio; is the negative ratio of transverse to axial strain
μ_a	– dynamic viscosity of air
v_a	– velocity vector of air, m/s
v_C	– velocity of blades of centrifugal separator, m/s
v_i	– current particle relative velocity, m/s
v_k	– radial velocity of particles in gas environment at movement through a centrifugal classifier, m/s
v_{max}	– maximum speed of air in the separation system, m/s
v_p	– velocity vector of particles, m/s
v_{rel}	– tangential (relative) velocity; relative speed of the flow separation, m/s
ρ	– material density, g/cm^3
ρ_a	– air density, g/cm^3
ρ_1, ρ_2	– densities of colliding bodies, g/cm^3
σ	– stress in the contact area in the collision, GPa
σ_{av}	– average stress, GPa
σ_H	– Hertz model stress; stresses of collision according to the Hertz model, GPa
σ_m	– maximum stress, GPa
σ_W	– wave model stress, GPa
ω	– angular velocity of rotor rotation, s^{-1}

INTRODUCTION

Big variety of physical mechanical properties of grinded materials and many different requirements towards grinding products demand using different types of grinding devices [1].

Mills of intensive action with high load speed such as vibration, jet, disintegrators and other types are widely used by industries to produce finely dispersed powders. Out of all these machines the most perspective devices are mills of percussive type [2].

Grinding is an energy-intensive process [3, 4]. The problem of specific energy is addressed globally as grinding consumes up to 3–4% of the whole energy produced on the planet. Considering that it is very important to know the relation between specific energy of grinding and grinding method used [5, 6].

Energy consumed while grinding using impact of materials like coal, quartz, cement, plaster, rubber, grain etc. is much lower than in case of crushing by compression, and is 5–6 times lower than in case of crushing by impact (ball mill or vibration mill) [5–8].

At collision speeds of 90–120 m/s specific energy of grinding is 30 times lower than in case of grinding using compression [9]. It is registered in work [10] that during impact grinding the force needed to destroy materials is increased twice while specific energy of crushing is 2.5 times lower.

The whole cost of the grinding process is 1.5–2 times lower with machines using impact than with machines using rolls and 3.5–5.5 times lower than with machines using cheek plates.

In comparison with other mills disintegrators have a number of advantages:

- They are compact
- They allow to grind materials with very wide hardness range while having very low contamination of products (which is very important when producing the solid-phase materials with structure sensitive properties)
- By swapping rotors, adjusting engine rotation speed and using separating systems they allow to vary the specific energy of processing the materials being grinded.
- To produce the same amount of new surface units of materials being grinded they use twice less energy than vibration mills and 10 times less energy than ball mill, not to mention jet or whirlwind mills
- The aerodynamic conditions in grinding chamber provide a way to pneumatically transport materials to the next technological device or receiving bin and also when needed support operating the aerial separator without additional air delivery systems (fans or compressors)
- During simultaneous grinding of multiple materials they allow almost ideal mixing of all materials being processed [11, 12]

- Modern devices of this type have a very wide range of productivity: starting from a few kilograms up to dozens of tons per hour
- They have a relatively low specific energy consumption
- They are able to perform grinding of materials with natural moistness

However, disintegrators also have disadvantages limiting their use. First of all, they have higher wearing of work surfaces, especially when used to grind materials of medium and high hardness.

What is more, the current disintegrator calculation and construction methods are not yet completed, preventing effective use of the whole spectrum of advantages because of constructive shortcomings.

The analysis performed on literary data indicates that there is currently no common technique of calculation in the area of disintegrator theory and construction.

These shortcomings can be explained by a wide variety of disintegrator designs based on different material grinding principles. In reality constructional design of disintegrators, their working conditions and materials used for elements of construction are mostly chosen by trial-and-error method.

The aims of the current thesis:

1. Developement of new laboratory disintegrator milling system for production of ultrafine powders with determined granularity
2. Study of grindability of different materials (brittle and plastic, metallic and non-metallic, composites)

The following research activities were conducted:

1. Performing analysis of existing constructions and developing disintegrator design which will contribute to rational acceleration of particles towards rows of percussive elements (flat fingers)
2. Describing the model of grinding ductile and brittle materials using impact
3. Calculating the basic constructive-technological parameters of disintegrator
4. Developing centrifugal separation system of disintegrator and determining the basic patterns of separation process; optimizing parameters and factors which affect disintegrator's grinding mode and separation
5. Determining rational modes of material disintegrating and separating process
6. Treating materials of different groups using created disintegrator milling system and characterizing produced powders

The scientific novelty of this work is the following:

- in the obtained formulas for calculation of particle movement speed in accelerating unit of disintegrator while taking into account its constructional design features; and determination of trajectory of particle movement in grinding chamber, used to determine rational amount of percussive elements and distance between their adjacent rows;
- determination of specific energy of material grinding; and algorithms for calculation of disintegrator's efficiency
- production of powders with desired size and shape – ultrafine powders and spherical powders from plastic metallic materials

The practical value of this work lies in creation of improved disintegrator design and separator based on theory of grinding and experimental researches, allowing to improve the efficiency of grinding process.

1. THEORY OF THE MILLING BY COLLISION

1.1 Theoretical aspects of milling

1.1.1 Size reduction by collision

Milling by collision is an effective method of materials size reduction, and the disintegrator, a grinding machine for brittle materials, has been known for over a century [13]. It was introduced in Estonia in the 1960s by Johannes Hint [14] and later Tymanok [15].

A systematic research of grinding by collision was conducted by Hans Rumpf's school [7]. The process of breaking single particles to pieces by collision was described by Priemer [16], who also proved Rumpf's model of fracture. Reiners [17] investigated grinding mixtures of different materials in a wide range of collision velocities (up to 950 m/s) and showed high selectivity of grinding at certain velocities. Lenkewitz [18] invented a mill with one-collision grinding action. The collision velocity was increased up to 400 m/s. Drögemeier and Leschonski [19] treated ultrafine grinding with separation of highly pure limestone in a two-stage collision mill. Disintegrator is one of the few devices for materials treatment by collision.

Rumpf [7] and Primer [16] were the first to use collision for brittle materials. The materials size reduction occurs as a result of fracturing of the treated material. By collision of the particle with a grinding element, from the point of contact an intensive pressure wave spreads (Figure 1.1b). Stresses are approximately an order higher than the strength of the material [20] in comparison with traditional grinding methods (Figure 1.1(a)) and equipment (jaw crusher, mortar, hand-mill, quern, vibro- and ballmill).

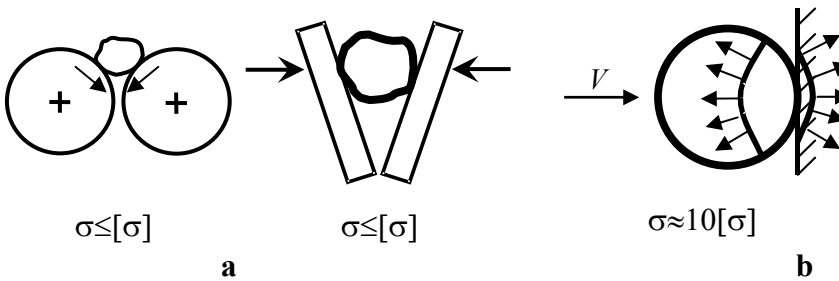


Figure 1.1 Stresses in the particle: a – traditional grinding methods and b – grinding by collision; $[\sigma]$ – strength of material

The parameters of materials treatment in the disintegrator are essentially different (Table 1.1).

Table 1.1 Comparison of the parameters of materials treatment by traditional methods and by collision

Parameter	Traditional method	Collision
Loading velocity, m/s	0.1 – 10	30 – 200
Loading time, s	$10^{-2} - 10^{-1}$	$10^{-6} - 10^{-5}$
Time spent in active zone, s	1 – 10000	10^{-2}
Ratio of the stresses to material strength, $\sigma/[\sigma]$	≤ 1	≈ 10

1.1.2 Stresses on collision

The investigations in [7 and 16–19] were mainly experimental, whereas in [14] a quasistatic case was derived on the basis of the Hertz static model. Ibidem, the corresponding formulae for calculating collision forces and contact time for a quartz sand particle colliding with a plane grinding surface were presented.

The stresses generated in the particle at collision have not been measured experimentally until today. They cannot be calculated exactly, but it is possible to estimate them by two extreme models: either according to the quasistatic *Hertz model* applied to a spherical particle or according to the *Wave model* where the particle with a plane side hits the target exactly with the same side [7].

The stress wave parameters can be calculated from Hertzian contact theory [21, 22, 29]. The Hertz contact model is both elastic and quasistatic; it does not consider either radiated elastic waves or anelastic effects, such as plasticity and viscoelasticity. The Hertz law has been used beyond the limits of its validity on the basis that it accurately predicts those impact parameters which can be experimentally verified [23].

With growing precision of test methods, and theoretical and numerical studies becoming more detailed, the Hertzian impact model tries to experimentally validate and to quantitatively evaluate its limits [24–27].

The measurements [28] are compared with theoretical estimates derived from elastic wave propagation and indicate a close match between the experiment and Hertz theory.

According to the ***Hertz model***, both colliding particles are spheres. The stresses σ_H of collision for the general case:

$$\sigma_H = 0.279 \cdot A^{-3/5} \cdot B^{1/5} \cdot C^{4/5} \cdot v^{2/5} \quad (1.1)$$

where

$$A = R_1 \cdot R_2 / (R_1 + R_2)$$

$$B = \rho_1 \cdot R_1^3 \cdot \rho_2 \cdot R_2^3 / (\rho_1 \cdot R_1^3 + \rho_2 \cdot R_2^3)$$

$$C = (1 - \mu_1^2)/E_1 + (1 - \mu_2^2)/E_2$$

and

v – velocity of collision,

R_1, R_2 – radii of colliding bodies,

ρ_1, ρ_2 – densities of colliding bodies,

E_1, E_2 – Young's module,

μ_1, μ_2 – Poisson's coefficient.

In case spherical particle collides with a plane surface, stresses can be calculated by equation (1.1) provided $R_2 \rightarrow \infty$ in (1.2).

$$\sigma_H = 0.279 \cdot \rho^{2/5} \cdot C^{4/5} \cdot v^{2/5} \quad (1.2)$$

The stresses are independent from the radius of particle; although in the formula (1.1) the stress depends on the radius through A , but the dependence is weak.

According to the ***Wave model*** it is supposed that the particles collide mainly with their plane surfaces (Figure 1.2). The stress waves begin to propagate in both particles to the opposite directions from the contact surface.

Historically, the first mention of stress waves produced by rapidly changing forces at the surface of an elastic half space was made by Lamb [30]. Extension of the theory for specific geometries and loading situations has been improved by many researchers [31–33], and today displacements produced by forces acting on the surface of a material are widely known [34, 35]. Agreement between theoretical, numerical, and experimental results is demonstrated in [35, 36].

Using the law of momentum of motion for stressed parts of particles, the formula of stresses in contact surfaces can be derived:

$$\sigma_W = \rho_1 \cdot c_1 \cdot \rho_2 \cdot c_2 / (\rho_1 \cdot c_2 + \rho_2 \cdot c_1) \quad (1.3)$$

where

c_1 and c_2 – velocities of elastic waves

$$c_i = E_i / \rho_i, \quad i = 1, 2 \quad (1.4)$$

Stresses σ_W are called *Wave model* stresses.

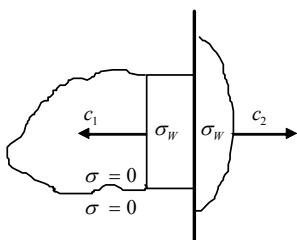


Figure 1.2 Collision of particles at wave model: c_1 , c_2 – velocities of elastic waves, σ_W – wave model stresses

Since real particles differ from ideal spheres, and they do not collide precisely with plane surfaces, *Hertz model* and *Wave model* should be observed as boundary cases, and the actual real stresses occur between these limit values (Figure 1.3)

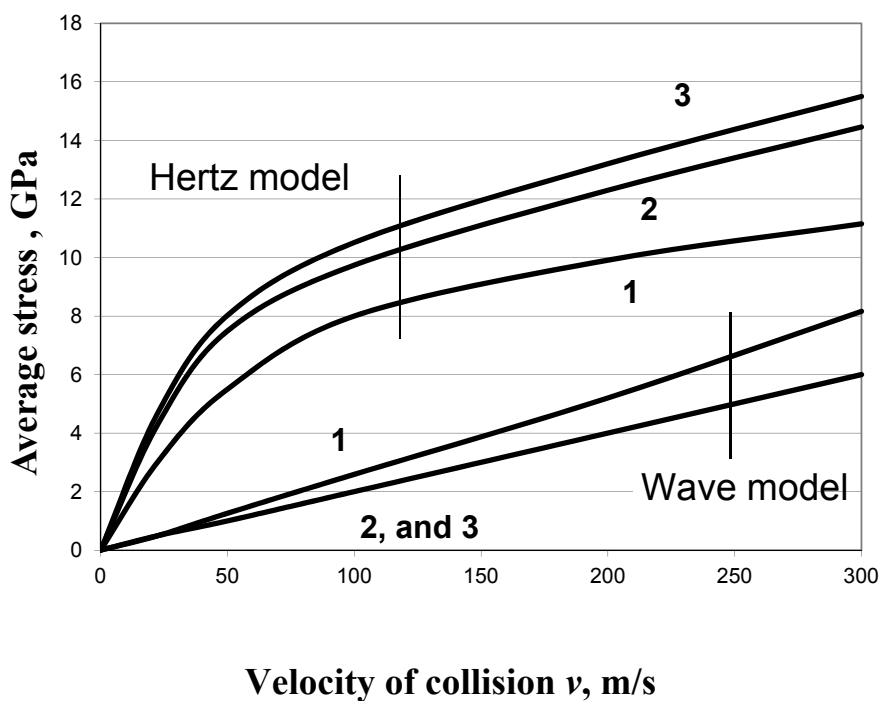


Figure 1.3 Dependence of maximum of average stress on velocity of collision. AISI316 steel particle ($d=2\text{mm}$) collision to: 1 – hardmetal WC-6Co plate; 2 – plate of same steel; 3 – same equal another particle.

Figure 1.3 indicates the change of the stresses in a steel particle with diameter 2 mm depending on collision velocity and on target (grinding element). Three

grinding elements were tested: a hard metal WC-6Co plate, a steel AISI 316 plate and a steel particle of the same size.

1.1.3 Collision of particle with another particle or plate

Initially, metal chips are loose and the metal is hardened. At collision its behaviour is nearly similar to brittle material. With reduction of size the chip's particles approach isometric and even spherical form. In the process of getting powder from metal chips the principal part of energy is used up to the last stage of reducing spherical particles to powder. On the last stage the particles, produced by collision, in size of 1–3 mm have a spherical form.

On basis of quasistatic Hertz theory the stresses given by formulas (1.1 – 1.3) were derived. On collision the particles deform (Figure 1.4).

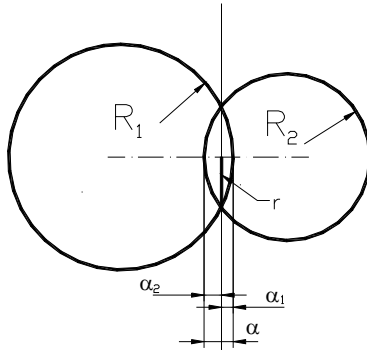


Figure 1.4 Collision of two spherical particles: α - approach of the centres, α_1 , α_2 - approach of each particle, r_k - contact area radius

Their contact area is a circle with the radius r_k . From quasistatic consideration of collision the approach of the centres of the particles can be derived

$$\alpha = 1.729 \cdot A^{1/5} \cdot B^{2/5} \cdot C^{2/5} \cdot v^{4/5} \quad (1.5)$$

where marks are the same as (2.2). If the particle collides with a plate, the formula (1.5) takes the form

$$\alpha = 1.729 \cdot \rho^{1/5} \cdot C^{2/5} \cdot R_1 \cdot v^{4/5} \quad (1.6)$$

The approach of particle is proportional with the particle's radius. Contact area radius is derived and can be expressed by formulas corresponding to general and plate case

$$r_k = 1.86 \cdot \rho^{2/5} \cdot C^{1/5} \cdot R_1 \cdot v^{2/5} \quad (1.7)$$

It is notable that, both approach α_1 and radius r_k , are proportional to the size of particle.

Maximum stress σ_m and average stress σ_{av} can be expressed as follows

$$\sigma_{\max} = \frac{3}{2} \cdot \sigma_{av} \text{ and } \sigma_{av} = \frac{F}{\pi \cdot r^2} \quad (1.8)$$

The material is plastica deformation in a certain area smaller than the contact area. As on collision the order of stresses is high, it can be assumed that the radius of plastic deformation area is equal to the contact area (Figure 1.5).

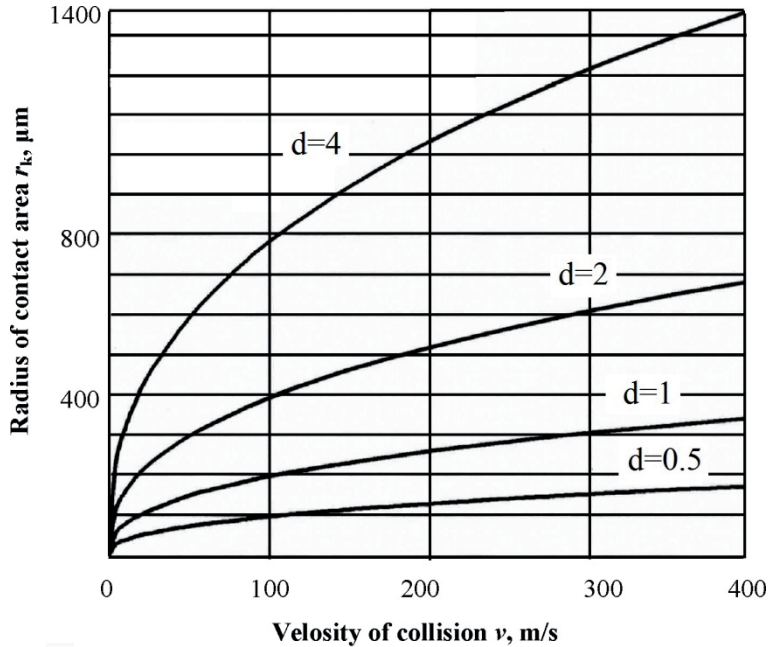


Figure 1.5 Dependence of radius of contact area between AISI316 particle and hard metal WC-6Co plate on velocity of collision and size of particle d , mm

Numerical values of impact parameters for some materials during the collision of particles with the grinding body are indicated in Table 1.2

Table 1.2 Properties of some materials and values in Eqs. (1.5), (1.6), and (1.7)

Material	ρ g/cm ³	E GPa	μ	$(1-\mu^2)/E$ ms ² /kg	Values $(1-\mu_1^2)/E_1+(1-\mu_2^2)/E_2$, ms ² /kg			
					Quartz sand	WC 6	Steel St3	
Quartz	2.6	36	0.2	$2.8 \cdot 10^{-11}$	Quartz	$5.5 \cdot 10^{-11}$	$3 \cdot 10^{-11}$	$3.2 \cdot 10^{-11}$
WC-6	15	72	0.2	$1.9 \cdot 10^{-12}$	WC-6	$3 \cdot 10^{-11}$	$3.9 \cdot 10^{-12}$	$6.1 \cdot 10^{-12}$
Steel St3	7.8	22	0.3	$4.2 \cdot 10^{-12}$	St3	$3.2 \cdot 10^{-11}$	$6.1 \cdot 10^{-12}$	$8.3 \cdot 10^{-12}$

A graphical representation of calculation results is shown in Figure 1.6

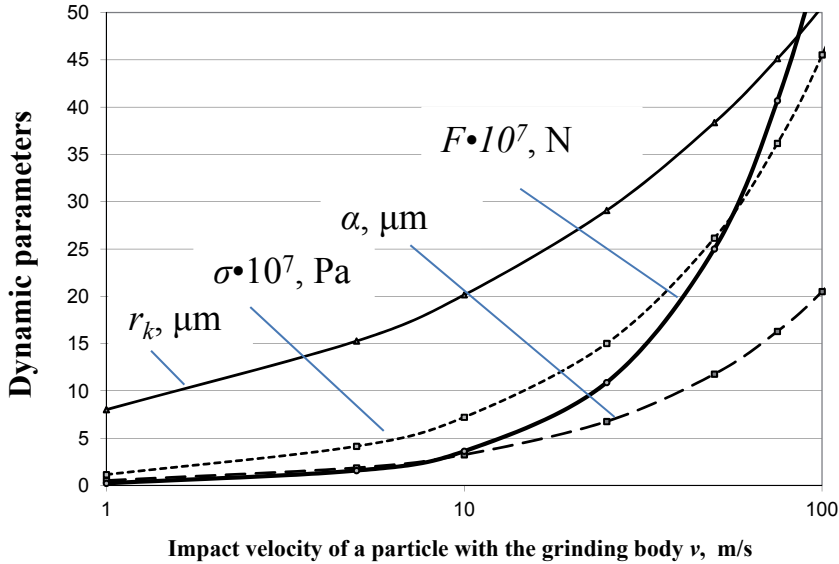


Figure 1.6 Dynamic parameters of collision particles with a diameter $d = 250 \mu\text{m}$, where σ - stress in the contact area in the collision; F - contact forces in the collision; α - convergence centres; r_k - radius of the contact patch

Thus, the impact of a particle with $d = 2 \cdot R_1$, if the particle has a size $= 125 \mu\text{m}$, is characterized by the following parameters:

Approach of centres

$$\alpha_{\max} = 0.00412 \cdot R_1 \cdot v^{4/5}, \mu\text{m} \quad (1.9)$$

Contact area radius

$$r_k = 0.0642 \cdot R_1 \cdot v^{2/5}, \mu\text{m} \quad (1.10)$$

Contact forces in collision

$$F = 18.3 \cdot R_1 \cdot v^{6/5}, \text{N} \quad (1.11)$$

Stress in the contact area

$$\sigma = 91.5 \cdot R_1 \cdot v^{4/5}, \text{Pa} \quad (1.12)$$

1.1.4 Size reducing model

The reduction of ductile metal particles size occurs by low cyclic fatigue fracture [Paper I]. When the particle of radius $R_i < R$ is loaded with an enormous number of collisions, a small plastic deformation area develops at each loading [37]. After a certain number n_i of loadings the surface of particles will be completely covered with plastic deformations.

$$n_1 = \frac{4 \cdot \pi \cdot R^2}{\pi \cdot r_K^2} = \left(\frac{2 \cdot R}{r} \right) = 1.15 \cdot \rho^{-2/5} \cdot C^{2/5} \cdot v^{-4/5} \quad (1.13)$$

It can be stated that n_1 depends on collision velocity, elastic properties of materials and thickness of particles, but not on radius R of the particle. By repeating such series many times (a great number of cycles) the area will be deformed continuously. As a result of repeated collision loading and fatigue breaking of particles surface, small pieces with size δ will be detached. After a certain number n_2 of loading series a layer with thickness δ will be separated. The size of particles is reduced by 2δ . A simple differential equation can be written as follows

$$\frac{dR}{d\delta} = - \frac{n}{n_1 \cdot n_2} \quad (1.14)$$

The solution of the equation, where R_0 is the initial radius of the particle, takes the form

$$R = R_0 - \frac{n \cdot \delta}{n_1 \cdot n_2} \quad (1.15)$$

The particle will be ‘ground’ when radius R approaches the boundary size to be separated in the classifier by separative milling. If the boundary size is equal to δ , it gives a necessary number of collision loadings for grinding the particle of size $2R_0$.

$$n = n_1 \cdot n_2 \cdot \left(\frac{R_0}{\delta} - 1 \right) \text{ or } n \cong n_1 \cdot n_2 \cdot R_0 / \delta \quad (1.16)$$

The depth of plastic deformation is of the same order as the approach $\alpha_1 = \alpha$.

The separated size of δ is smaller but of the same order of size as α . It is assumed that

$$\delta = \alpha / k \quad (1.17)$$

where $k = 2 - 8$

Actually, grinding AISI316 steel particles of size $d = 2 - 2.5$ mm at velocity $v = 150$ m/s the approach $\alpha = 80$ μm , the ground particles in the product are of the order $\delta = 20$ μm and $k = 4$ [38, 39].

On the other hand, AISI 316 steel particles with the above described size will be fully ground by separative grinding with approximately $n = 30,000 - 40,000$ number of cycles collision loadings [41] and [40–42]. From equation (1.14) number n_2 of loading for fatigue fracture can be found.

In our cases, from equations (1.13) and (1.16)

$$n_1 = 17 \text{ and } n_2 = \frac{n \cdot \delta}{n_1 \cdot R_0} = 17.6 \div 18.8 \quad (1.18)$$

It can be concluded that by impact on the same place of the surface the particle of AISI 316 steel must be loaded $n_2 \cong 20$ times before fatigue breaking occurs. Low-cycle fatigue breaking is referred to, which occurs owing to the high rate of intensity of stresses at high velocity of collision. While stresses at collision minimally depend on the size of particle, n_1 does not depend on the size of particle, and in the first approximation n_2 does not depend on the size of particle. Instead it depends on properties of materials and velocity of collision.

1.2 Basics of separation

1.2.1 Separation of particles in inertial classifier

The inertial classifier [43] used in the disintegration system DSL-160 [44], works as follows: air (A) and particle mixture (M) enter the classifier; the air has to make a sharp turn passing through the grid, resulting in drop of pressure. Fine particles (FM) make a sharp turn together with the air (A), and they are directed into the collector of the finished product. Large particles (CM) together with the remaining air (A) continue their direct movement by inertia and are directed for the second round of processing.

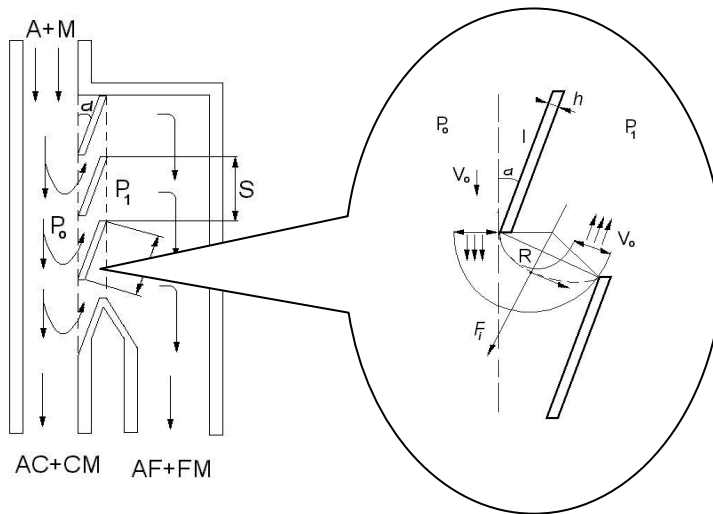


Figure 1.7 Flow model of air and particle mixture in the gap grid of inertial separator

If the airflow moves with speed v along the grid of the separator and the pressure differential $\Delta p = p_0 - p_1$ on it, air layer with the thickness of δ passes through the grid slit. The air layer can be considered as a jet changing its flow

direction because of the pressure differential. The dynamic pressure of the layer must be equal to the pressure differential on the surface of the jet curvature.

$$\Delta p = \frac{\rho_a \cdot v^2 \cdot \delta}{r}, \quad (1.19)$$

where ρ_a is air density

Layer thickness δ , radius of the curvature r and angles φ_0 , ψ (Figure 1.7) are determined in accordance with the law of sines in the system of equations:

$$\frac{\cos(\varphi_0 - \psi)}{r - \delta} = \frac{\cos \psi}{r} = \frac{\sin \varphi_0}{l_0} \quad (1.20)$$

When the pressure increases, the layer thickness δ decreases, and the outer turning radius r increases accordingly. The inner curvature radius of the layer $r - \delta$ decreases. When the pressure decreases, curves r and δ join. Thus, the outer curvature radius is equal to the layer thickness δ , the inner curvature radius nears zero, and the curvature centre moves to the edge of the grid. The layer flow is reduced to an ordinary airflow through the grid. The particle trajectory differs from the air trajectory. The inertia force F_i and the air resistance force F_a affect the particles. Since the fine particles speed is low, relative to the speed of the air, the air resistance is calculated by Stokes

$$F_a = 3 \cdot \pi \cdot \mu_a \cdot d \cdot (v_p - v_a) \quad (1.21)$$

where:

μ_a is the dynamic viscosity of air,

v_a and v_p are velocity vectors of air and particles, respectively, and

d is particle size.

The location of particles is determined by polar coordinates R and φ .

The movement of boundary particles leads to the numerical solution of a differential equation system,

$$\ddot{R} = R \cdot \dot{\varphi}^2 - \frac{\dot{R}}{\tau} \quad \text{and} \quad (1.22)$$

$$\ddot{\varphi} = \frac{1}{R^2} \left(k - \frac{y_0 \cdot \delta}{2} \exp\left(-\frac{t}{\tau}\right) \right), \quad (1.23)$$

where it can be assumed that the boundary particle is the particle with size d_1 , the trajectory of which crosses the imaginary line of the plate in the front edge of the plate.

1.2.2 Centrifugal classifier

Design background

It appears from the calculations that particles of submicron sizes collide.

However, the inertial separator cannot stably separate the produced fine fraction [38, 45] of less than 40 – 60 μm .

The separation of finer material from the total weight of ground material is complicated by the increasing influence of adhesion force with the decrease of particle size. Furthermore, particles acquire an electric charge.

The inertial classifier can separate the material particulates up to one micron in size [46–50], but it has several disadvantages: they operate effectively only for the separation of particles of high density $\rho = 7 - 15$, such as metal and tungsten carbide particles.

That can be explained by the direct dependence of inertial separation on the mass of the particle. Consequently, the ability to control parameters of the separation as described below (dependence of separation boundary d_1 , on the longitudinal speed of airflow v , on the coefficient of particle shape k_{sh} ; or the inclination of grid plate of classifier α , performance of the separation air through grid slits) is limited. The reason is the high resistance of environment gases, which does not allow the boundary particle to exit the boundary layer of the airflow turned by the classifier, and therefore the large particles are moved with air into the collector of the fine product.

Therefore, the inertial separator was modified. To this end, the mathematical model of separation of particles by centrifugal forces was developed.

Design parameters

Next, the main factors affecting separation are considered [51].

The separation boundary of the slit inertia classifier is significantly affected by:

- performance of air Q in the fine material path. It is the main factor for regulation of the separation boundary.
- shape of the particles,
- grid parameters B and H ,
- longitudinal speed of air flow v .

Of the above factors, the particle shape and the geometry of the classifier blades

(optimum where $\frac{B_1 \sin \alpha}{H - B_1 \cos \alpha} \approx 0.5$) do not change.

Only Q – air performance (0 – max) and the flow speed v (0 – v_{\max}) can be regulated as it can be seen, the regulation of these parameters has its limits:

$$\bar{d} = f(v, 1/Q)$$

where:

v_{\max} – the maximum speed of air in the system depends on angular velocity ω of rotor rotation (in this case $\omega_{\max} = 1200 \text{ s}^{-1}$).

Q_{\min} – almost completely stops air passing through the classifier, thus it reduces the performance of classification and leads to agglomeration of fine material path due to the effect of electrostatic and adhesion forces. Consequently, the material adheres to the blades and the walls of the classifier. On the other hand, it does not prevent accidental slippage of large particles.

To solve this problem, it is proposed to use a rotating grid in the classifier, which allows to:

1. unrestrictedly increase the relative speed of inertial (air with particles) flow v
2. to introduce a really important factor of separation – the centripetal force (artificial gravity)

The idea of using the centrifugal classifier is the following [Paper I].

It may be assumed that along with the effect of the above classification factors, the particles will be cast away to the walls of rotating blades of the classifier by the centrifugal force, and the fine particles will be discharged into finished product collector.

By our assumption the centrifugal force affecting the “boundary grain” with flow force moving in radial direction. The speed of particles is assumed to be the same as the speed of air flow.

To simplify calculations, we disregard the mutual influence of particles and the effect of Coriolis forces on them. In addition, we disregard the particle shape.

The centrifugal force F_{in} , affecting the particle on the part of rotating blades of the centrifugal classifier, is determined by the formula

$$F_{in} = \frac{\pi d^3}{3} \rho_m \frac{v_{rel}^2}{R}, \quad (1.24)$$

where:

R – classifier grid radius

v_{rel} – tangential (relative) velocity, equal to $v_1 + \omega_{CC} \cdot R$, i.e. the relative speed of the flow separation is equal to the amount of material speeds v_1 in the classifier and the speed $\omega_{CC} \cdot R$ of the classifier blade.

d – particle diameter

ρ_m – material density

The force of radial flow, preventing the movement of the “boundary grain” out of separation zone under the centrifugal force due to resistance of air environment, can be determined by the Stokes formula

$$F_{st} = 3 \cdot \pi \cdot d \cdot v_k \cdot \mu, \quad (1.25)$$

where:

d – particle diameter

v_k – radial velocity of particles in gas environment at movement through a centrifugal classifier

μ – gas environment viscosity

For the balance of “boundary grain” it is necessary

$$F_{in} = F_{st} \text{ or } \frac{\pi \cdot d^3}{3} \rho_m \cdot \frac{v_{rel}^2}{R} = F_{st} = 3\pi d v_k \mu \quad (1.26)$$

Having solved the equation for the “boundary grain” we get

$$d_{min} = \sqrt{\frac{9v_k \cdot \mu \cdot R}{v_{rel}^2 \cdot \rho_m}} \quad (1.27)$$

The formula (1.27) shows the dependence of the “boundary grain” size of flow speed (air + material), material density, and rotating grid parameters.

The calculated values of the “boundary grain” size are specified for the disintegrator DSL–175 and are indicated in Figure 1.8

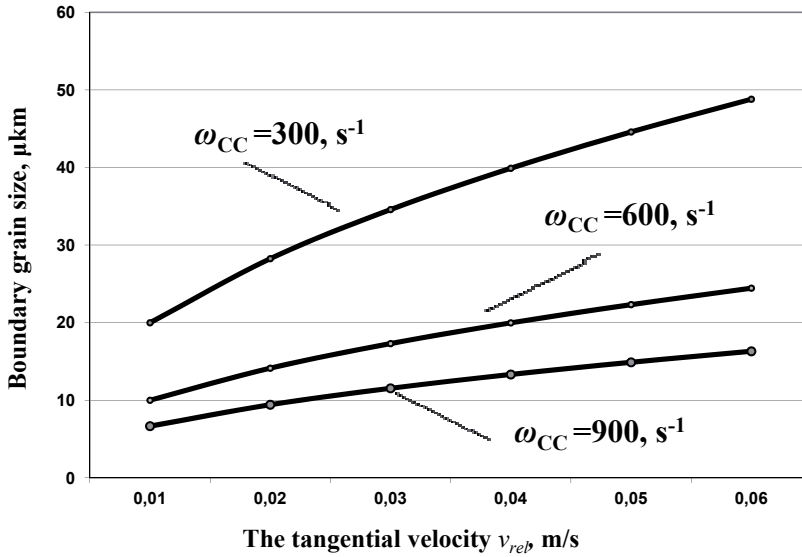


Figure 1.8 Dependence of "boundary grain" size on flow velocity v_k (air and material) at centrifugal separator speed

2 DEVELOPMENT OF DISINTEGRATOR MILLING SYSTEM FOR MATERIALS TREATMENT

2.1 Design of disintegrator

Disintegrators or mills of percussive type are the utmost perspective for industry and laboratory practices.

Disintegrator is a grinding mill consisting of two rotors rotating in opposite direction treating materials by collision. The principal scheme of disintegrator equipment is indicated in Figure 3.1.

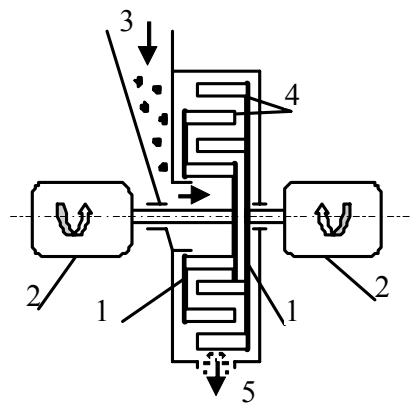


Figure 2.1 Schematic representation of the disintegrator equipment: 1 – rotors; 2 – electric drives; 3 – material supply; 4 – grinding elements; 5 – output

These rotors are equipped with one or more concentric rings (Figure 3.2), with a row of grinding bodies on each ring. The grinding bodies are effective as targets for the colliding particles and as accelerators for the next collision.

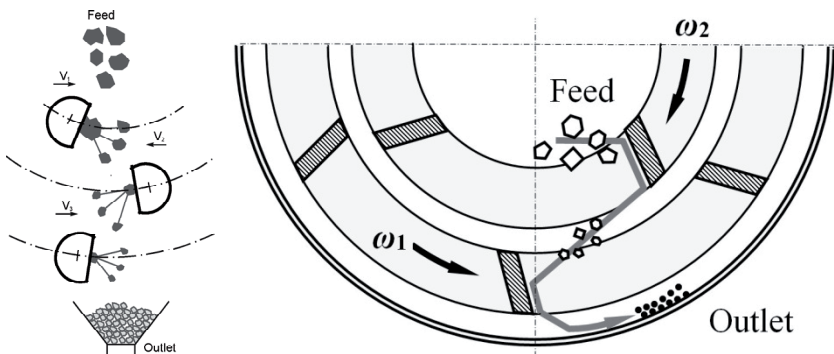


Figure 2.2 Principal scheme of disintegrator rotors equipped with grinding bodies

On the basis of theoretical investigations, the corresponding mills, the DS-series disintegrator, have been designed and developed at TUT [52]. They operate in a system of direct, separative (closed), selective or selective–separative grinding (Figure 2.3).

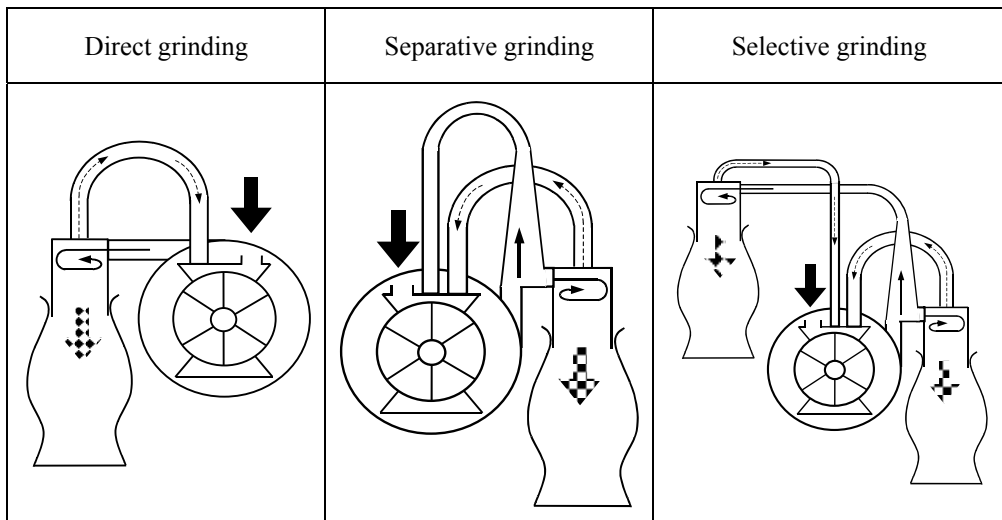


Figure 2.3 Different modes of disintegrator grinding of materials

In the DS-series disintegrator systems, the ground material ejected from rotors carries significant kinetic energy [53–55] that can be used for further transportation of the material. This is taken into account in disintegrators of direct grinding (for transportation of the material into the bunker or into the classifier for separative or selective grinding).

The DS-series disintegrators and disintegrator systems have been designed on the basis of the following principles:

- modular design
- convenience of operating and service
- possibility to use an autonomous and ecologically clean closed gas system
- possibility to realise direct, separative, selective and selective–separative grinding
- modes with simplicity of switching from one mode to another
- elastic support of motors with a possibility to use automatic balancing of the rotor system
- high level of safety

The DS-series disintegrator is designed for certain technologies and aims. Therefore, rotors, classifiers and other auxiliary devices ought to be designed accordingly. With small modifications, the DS-series disintegrators can be adjusted for different purposes, such as:

- maximum output of certain size of ground material
- maximum volume density of ground product
- high level of activation of materials
- mixing, homogenisation and alloying of materials

At high abrasivity of materials to be treated, the grinding media is subjected to intensive wear. Rotors with a special configuration of working blades [52, 56 and 57] are designed. Thus, portions of materials fall periodically on working surface, covering it with a thick layer of the treated material. This layer is formed from fine and coarse particles of materials [58–62], and it protects the working surface against wear.

For the production of micronized powders, a special multipurpose disintegrator milling system – the disintegrator DSL-175 with a combined inertial–centrifugal classifier – was developed (Paper I and III), (Figure 2.4).

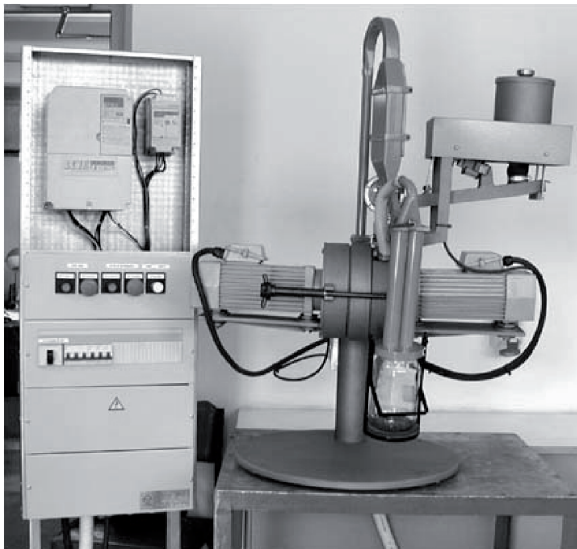


Figure 2.4 Laboratory disintegrator milling system DSL-175 with inertial air classifier

The main kinetic parameter in materials treatment is the specific energy of treatment [63] both regarding the grinding effect (grindability) [45, 64–67] and the economic aspects [68].

The above-mentioned parameter of the disintegrator DSL-175 is demonstrated in Tables 2.1 and 2.2

Table 2.1 Velocity of collision and specific energy of treatment E_s material in DSL-175, as dependent on the velocity of rotation of rotors and the multiplicity of treatment

Rotation velocity of rotors, rpm	Velocity of collision, m/s	Specific energy of treatment E_s , kJ/kg by multiplicity of treatment			
		1	2	3	4
2000/2000	32	0.8	1.6	2.4	3.2
4000/4000	64	3.1	6.2	9.3	12.4
6000/6000	96	7.0	14.0	21.0	28.0
8000/8000	128	12.4	24.8	37.2	49.6
10000/10000	160	19.4	38.8	58.2	77.6
12000/12000	192	27.9	55.8	83.7	111.6

Table 2.2 The main characteristics of disintegrator milling system DSL-175

Parameter	Laboratory Disintegrator DSL-175
Power supply	3-phase 380 V with a frequency transformer
Drive	high-speed motor 12000 rpm, 200 Hz, 2x2.2kW
Speed control range	400 – 12000 rpm
Centrifugal classifier	the motor 0.33 kW, 380 V, 2800 rpm, the adjustment range 200–5600 1/min.
Rotor system	Two rotor system
Diameter of rotors	175 mm
Number of pins/blades roads	Up to 5
Rotation velocity of rotors	Up to 12000 rpm
Impact velocity	Up to 192 m/s
Possible operating system	Direct or separative
Specific energy of treatment E_s , (kJ/kg)	
direct mode	up to 28.0
separative mode	up to 2000
Input (maximum particle size)	2.5 mm
Milling environment	Air/argon

2.2 Design of classifier

The separation systems used in DS-series disintegrators are based on aerodynamic, inertial and centrifugal forces. A special inertial and centrifugal classifier with a closed air or gas system was developed [Paper I, III, V] (Figures 2.5a and b). These systems are autonomous and ecologically clean

owing to the use of kinetic energy of output material. The inertial system does not need any additional transportation devices or fans.

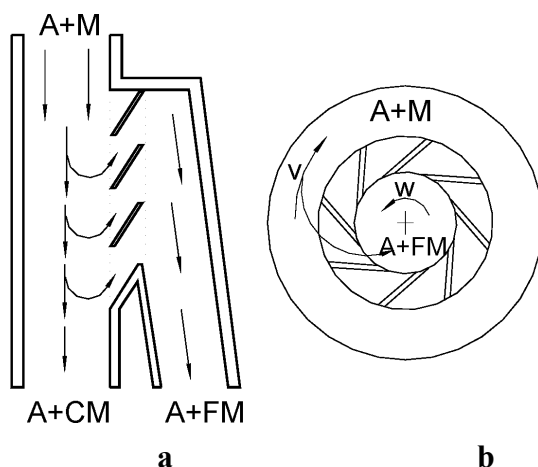


Figure 2.5 Principal schemes of a – inertial and b – centrifugal classifiers (*A* – air, *M* – materials, *CM* – coarse material, *FM* – fine material)

The theory of centrifugal separation was implemented and verified [69, 70] in several variants of centrifugal classifiers, providing a stable product with an average size of 1 to 20 μm (Table 2.3 and 2.4).

The particle size was controlled by granulometric analysis on the set of sieves and with a laser analyzer.

The main difference of the developed classifier is that inertial forces of separation are supplemented by the centrifugal component; instead of fixed separation grid a rotating grid was used.

Table 2.3 Parameters of centrifugal classifier

Parameter	Values
Power supply	3-phase 380 V with a frequency transformer
Drive	the motor 0.33 kW, 380 V, 2800 rpm
Specific energy of treatment E_s , kJ/kg	up to 2000

Table 2.4 Separation sensivity on centrifugal classifier

Density of materials, g/cm^3	Particles size, μm	Amount of fraction, %
$\rho \leq 2$	5–2	85–90
$2 \leq \rho \leq 7$	2–10	95
$\rho \geq 7$	1–5	98

Advantages of centrifugal classification

As an advantage of the new design the centrifugal classifier allows to:

- Significantly increase the airflow speed limit
- Gently adjust the airflow speed limit without changing parameters of the grinding machine
- Regulate air productivity Q during the separation
- Eliminate accidental slippage of coarse material particles due to counteraction of centrifugal forces generated by the rotating classifier

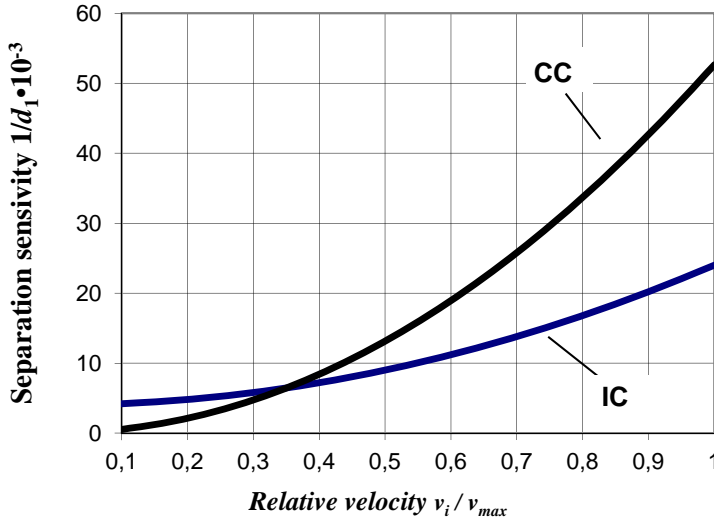


Figure 2.6 Dependence of separation effect on classifying parameters of (IC) inertial and (CC) centrifugal classifiers

Separation sensitivity is as a function of different parameters

$$1/d_1 \Rightarrow (F_{sep}) = f(Q, v_i, B, H),$$

where:

Q – separative air productivity, aspirated through the grid

v_i – current particle relative velocity

$$v_i = v + v_c,$$

v – air flow velocity in a disintegrator,

v_c – velocity of blades of CC

B, H – separation grid parameters

v_i / v_{max} – the ratio of the current relative speed of flow separation to the maximum possible.

2.3 Prediction of wear resistance of steels for grinding media

To evaluate the suitability of hardened steels as grinding media and to have wear curves $\varepsilon = f(H_a)$, wear rates of standard material – soft steel St37 (140–150 HV30) in abrasives in limestone (135–205 HV) and glass grit (550–600 HV), and wear rates of harder material steel Hardox 600 (580–635 HV30) in abrasives in glass grit and quartz sand (1100–1200 HV) were determined (Table 2.5).

Table 2.5 Chemical composition and hardness of the studied steels

Type of steel	Chemical composition, wt%	Hardness
St37	0.21–0.25 C; ≤ 0.055 P, S	140–150 HV30
Hardox 600	0.48 C; 0.7 Si; 1.0 Mn; 1.2 Cr; 2.5 Ni; 0.80 Mo	560–640 HBW*
Reference material C45 (normalized)	0.42–0.5 C; 0.5–0.8 Mn; ≤ 0.045 P and S	580–635 HV30
		230–260 HV30

*by specification

To construct curves $\varepsilon = f(H_a)$ for steels (soft and hard) for use as grinding items (mild steel St37 and hardened steel Hardox 600) sandstone as softer abrasive (140–205 HV), glass grit as medium abrasive (550–600 HV) and quartz sand as harder abrasive (1100–1200 HV) with similar particle size (0.1–0.3 mm) but different shape (Fig. 2.7) were used for tests.

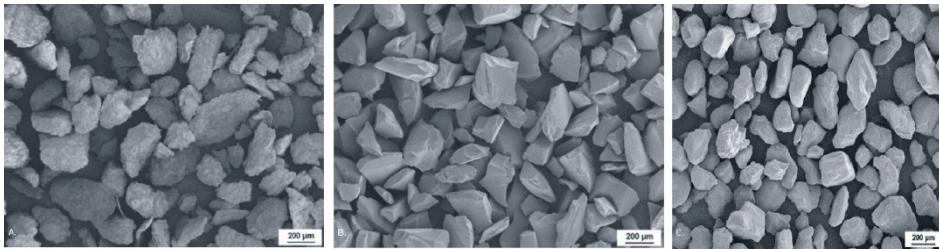


Figure 2.7 SEM images of abrasives: a – sand; b – glass grit; c – quartz sand

Experiment results are demonstrated in Table 2.6.

Table 2.6 Wear rates of studied steels in soft and hard abrasives

Steel	Hardness HV30	Wear rate L_g , mg/kg					
		Milled sandstone		Glass grit		Quartz sand	
		$\alpha = 30^\circ$	$\alpha = 90^\circ$	$\alpha = 30^\circ$	$\alpha = 90^\circ$	$\alpha = 30^\circ$	$\alpha = 90^\circ$
St37	140–150	248.4	141.9	587.2	437.7		
Hardox 600	580–635			323.4	312.8	376.9	438.4

Based on test results $\varepsilon-H_a$ – curves were constructed (Figure 2.8).

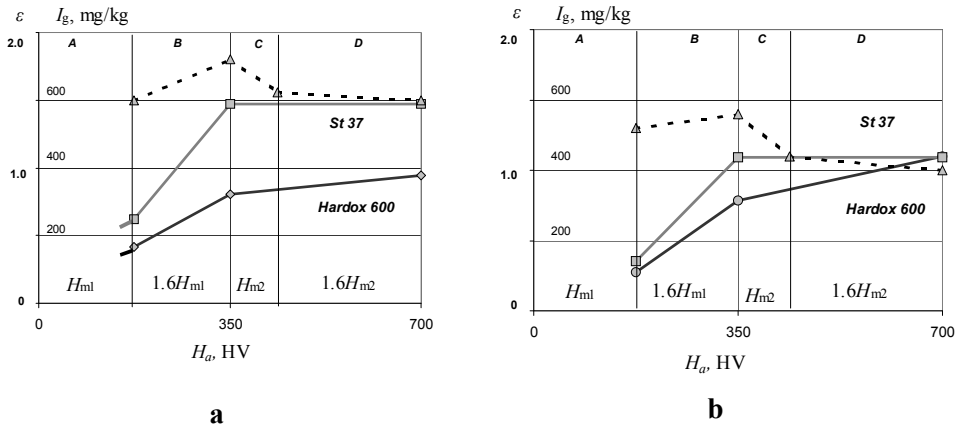


Figure 2.8 Wear rate of steel St37 (M_1) and Hardox 600 (M_2) of respective hardnesses H_{m1} and H_{m2} versus abrasive hardness H_a . Dash line: dependence of relative wear resistance of ε on H_a : a – impact angle 30° ; b – impact angle 90°

As indicated in Figure 2.8, four defined zones exist:

A – wear resistance is low;

B – wear resistance increases;

C – wear resistance decreases rapidly;

D – wear resistance of Hardox is low.

In interval B-C the use of Hardox is most favourable.

Comparative testing of soft and hardened steels as grinding items in disintegrator type crushing devices demonstrated that hardened steels are not prospective in these applications. With material cost increasing the effect is low – the increase of life span of milling elements is minimal.

That was confirmed by comparative testing of pins of different steels and different coatings [71, 72]. Relative wear resistance of steels and coatings in disintegrators by milling of materials with hardness about 1000HV and more is low.

3 TREATMENT OF DIFFERENT MATERIALS

Based on disintegrator milling technology, grindability of different groups of materials is studied:

- 1) Metallic materials: stainless steel and Ni- and Co- based alloys (examples of ductile material)
- 2) Ceramic materials: mineral ores (examples of brittle materials)
- 3) Composite materials: hardmetal (example of hard composite material), printed circuit boards (example of metallic-GFRP laminated plastic composite).

It can be assumed that materials grindability and properties of a ground product depend on brittleness–toughness properties of materials. If the size reduction of brittle materials takes place by direct fracture at collision, as a rule, ductile material cannot be fractured by collision. A theoretical model for size reduction of ductile materials, developed by us, is also proved in practice.

Metal powders of Cr-Ni - stainless steel AISI316, Ni-based and Co-based alloys with the particle size up to 1–5 μm were produced and used in disintegrator milling systems.

In experimental studies of different metallic materials the following disintegrator milling systems were used:

- 1) centrifugal-type precrusher for preliminary size reduction of initial material
- 2) experimental disintegrator DESI
- 3) laboratory multipurpose disintegrator milling system DSL-175

The main parameters of employed devices are demonstrated in Table 3.1. Characterisation of employed disintegrators

Table 3.1 Characterisation of employed disintegrators

Parameter	Laboratory disintegrator DSL-175	Experimental disintegrator DESI	Centrifugal-type precrusher DS-350
Rotor system	Two rotor system	Two rotor system	One/two rotor system
Diameter of rotors, mm	175	350	600
Number of pins/blades roads	5	3	3
Rotation velocity of rotors, rpm	Up to 12000	2880/5760	1440/2880
Impact velocity, m/s	Up to 192	95.5/191	90/180
Specific energy of treatment E_s , kJ/kg	Up to 28.0	2.9/11.7	1.8/3.6
Input (maximum particle size), mm	2.5	5	15
Used operating system	Direct or separative	Direct	Direct
Milling environment	Air/argon	Air	Air

3.1 Pretreatment of metallic materials

3.1.1 Production of metallic powders from steel chips

Stainless steel AISI 316 chips were treated in three steps (Paper III):

- preliminary treatment of continuous chips in disintegrator DS-350
- intermediate grinding in semi-industrial disintegrator DSL-115 by direct grinding system
- final fine grinding in laboratory disintegrator DSL-175 by separative grinding system.

The dependence of granularity on the specific energy of treatment is shown in Figure 3.1.

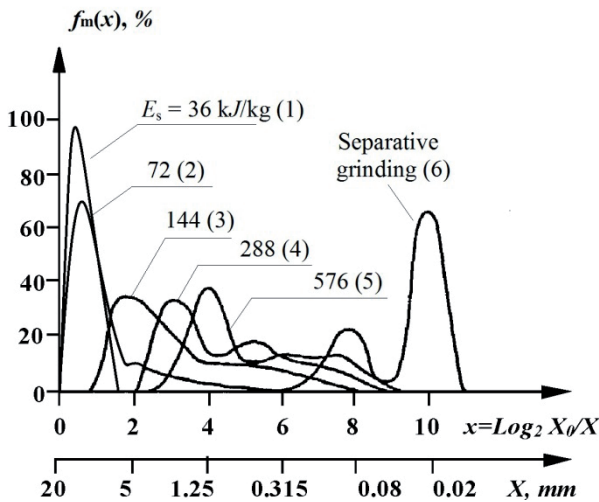


Figure 3.1 Dependence of granulometry of stainless steel AISI316 powders on the specific grinding energy E_s , kJ/kg ($X_0 = 20$ mm): 1,2–preliminary treatment of continuous chips up to particles size less than 5–10 mm; 3,4,5 –intermediate milling in direct grinding system (the average size of product was 100 μ m); 6 – final milling with inertial/centrifugal classifier in separative milling system

First, chips are plastically deformed and work hardened. As a result, their fracture resembles that of a brittle material (curves 1 and 2, DS-350). Next, disintegrator DSL-115 (curves 3, 4 and 5) was used.

Fine grinding was performed using DSL-175 in a separative grinding system (curve 6).

The particle shape of the powder milled by separative grinding at the intermediate stage (from circulation) is shown in Figure 3.2a – as a result of plastic deformation, the powder particles are spherical in form and at the final stage – lamellar with particle size of about 10–20 μ m (Figure 3.2b).

In Figures 3.1 and 3.2, disintegrator grinding results demonstrating changes in shape and granulometry of particles are indicated. Separately ground particles of fraction +160 –315 μm are spherical.

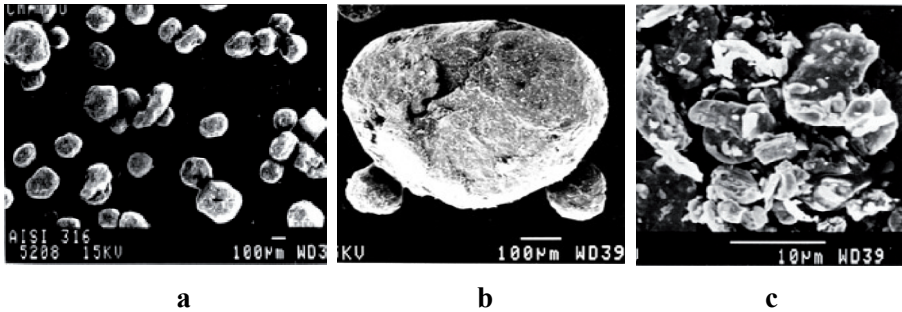


Figure 3.2 Shape of particles of stainless steel AISI 316 powders: a, b – powder +160–315 μm at the intermediate stage of separative grinding; c – final product of separative grinding

Figure 3.3 illustrates the grindability of different steel chips, depending on the specific grinding energy (low specific energy is achieved by direct multi-stage grinding, higher specific energy by using the separative grinding system).

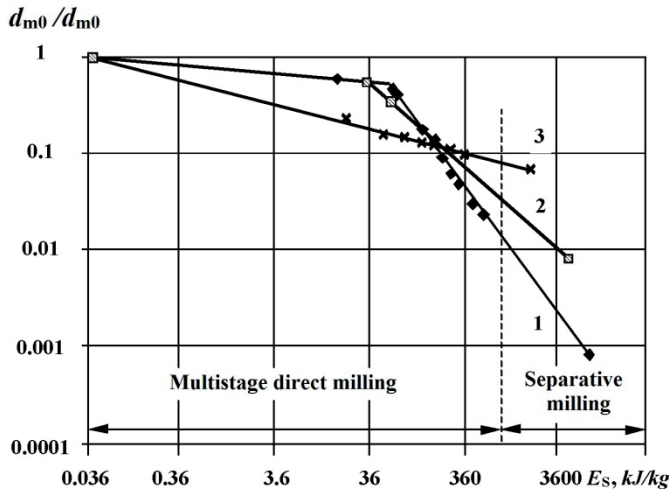


Figure 3.3 Dependence of the ratio of medium size d_m of the ground product to the initial size d_{m0} material on the specific grinding energy E_s : 1 –stainless steel AISI 316; 2 – ball-bearing steel 100Cr6; 3 – high speed steel HS 9-1-2-6

By low specific energy, as demonstrated in Figure 3.3, high speed steel (HSS) achieves better refining than stainless and ball bearing steels, explained by higher plasticity of the latter. At higher specific energy of grinding, after hardening the material, the rate of refining the ball bearing and stainless steel chips increases, being higher than in case of HSS. The intensity of grinding HSS chips depends linearly on the specific energy of grinding.

As a result of X-ray investigations of non-ground chips and of the ground product, the effect of work hardening of particles caused by impact grinding was observed. Regarding crystal lattice parameters, the difference was approximately from 5% to 10%.

3.1.2 Production of ultrafine Co- and Ni- based alloy powders

The following metal powders as initial materials were used:

- Ni-based powder Alloy 59 (MBC Metal Powders Ltd.)
- Co-based powder Anval Ultimet (Carpenter Powder Products Ltd.).

The chemical composition and the initial particle size of alloy powders used are demonstrated in Table 3.2.

Table 3.2 Selected metal powders and their composition

Powder type	Chemical composition, wt %	Initial particle size, μm
Alloy 59	23 Cr; 10 Mo; 1 Fe, Mn, Si; rest. Ni	45–150
Ultimet	26 Cr; 9 Ni; 5 Mo; 2 W; 0.8 Mn; 0.3 Si; 0.08 N; 0.06 C; rest. Co	–45

To produce ultrafine powders with particle size less than 5 μm , disintegrator milling system DSL-175 with the inertial and elaborated centrifugal classifiers was employed (Paper I). Powders were milled in a protective environment – argon.

Disintegrator milled ultrafine metallic powders were characterised by the following methods:

- specific surface area measurement
- particle size analysis
- oxygen content measurement

Figure 3.4 shows the particle shape of milled powders. Figure 3.5 and Table 3.3 present the particle size distribution and cumulative distribution functions (both in percentage by volume) determined by the laser particle size and image analysis.

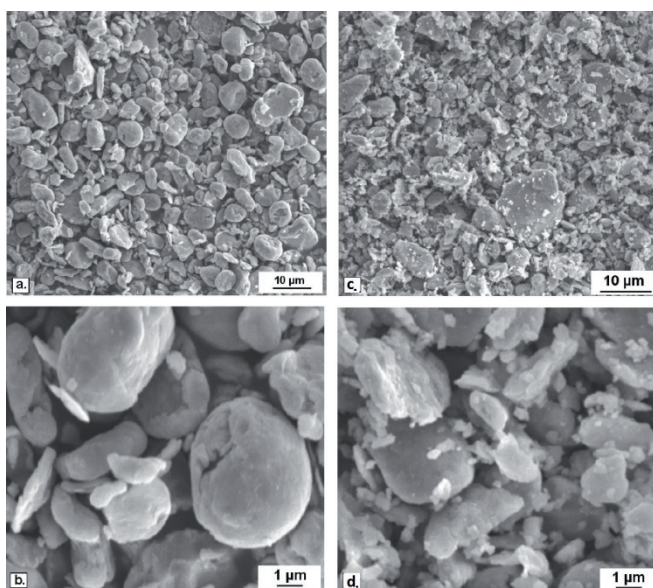


Figure 3.4 SEM images of milled ultrafine powders: a, b – Alloy; c, d – Ultimet

The results of granulometry studies of powders are demonstrated in Table 3.3.

Table 3.3 Results of powder particle size measurements

Powder type	Laser analysis, μm		Image analysis, μm	
	d_m	d_{\max}	d_m	d_{\max}
Alloy	2.77	6.57	1.89	5.42
Ultimet	2.58	8.20	1.74	7.23

As it follows from Figure 3.4, the disintegrator milling of ductile materials produces coarser spherical and finer plate-form particle micropowders. According to the results presented in Figure 3.5, the image and laser diffraction analyses show similar results. The studied particles had the same particle size distribution (especially cumulative) and the largest particles did not exceed 8–10 μm .

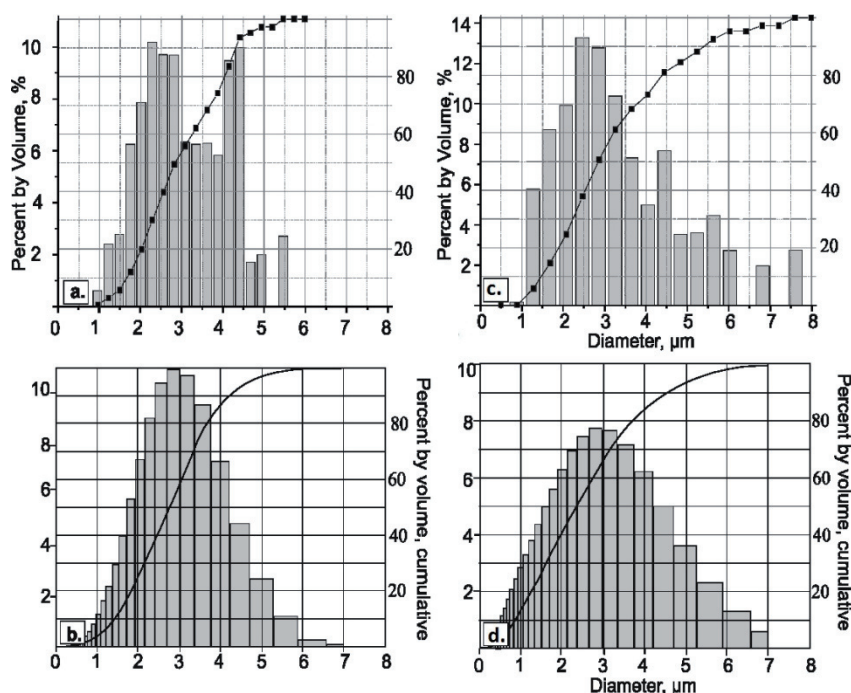


Figure 3.5 Particle size distribution (a, c, – laser analysis; b, d, – image analysis) of powder particles: a, b – Alloy; c, d – Ultimet

To ascertain the influence of milling and powder particle size reduction on the oxygen content in the final product, the oxygen content was measured by Leco analyser [73]. Regardless of milling in protective environment, i.e., argon, owing to a very high specific area of powder after milling, the oxygen content of the powder increased catastrophically both at milling and during its handling in the air. This is in direct correlation with the increase in the specific surface area of the powder (Table 3.4).

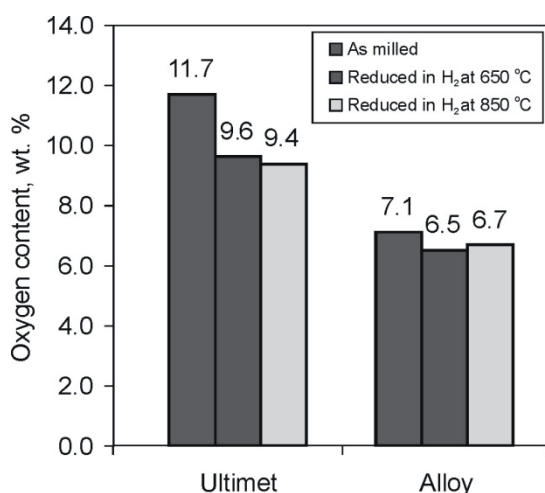
Table 3.4 Specific surface area and O_2 content of initial and milled powders

Powder type	Initial		After milling	
	Specific surface area, m^2/g	O_2 content, %	Specific surface area, m^2/g	O_2 content, %
Alloy	0.016	0.06	0.651 / 2.62	7.1
Ultimet	0.044	0.13	3.131 / 3.42	11.7

¹ BET method.

² Laser granulometry

To decrease the O_2 content, annealing of powder in hydrogen at temperatures 650 °C, 850 °C and 1000 °C was conducted. As it follows from Figure 3.6, decrease in O_2 content was only 5–20% (maximum for Alloy powder).



3.6 Results of oxygen measurements of milled powders

The particle shape was characterised by their elongation – the aspect ratio AS [72, 73]. Figure 3.7a indicates the particle aspect distribution of studied micropowders. Most of the powder particles had a relatively large elongation (mainly close to 2), which is normal in grinding of ductile materials by collision in the disintegrator mill. Alloy and Ultimet micropowder particles had practically the same shape parameter – the aspect AS distribution, while the Fukuda powder aspect was slightly smaller. Figure 3.7b demonstrates the dependence of aspect ratio AS on the mean diameter d_m of micropowder particles. As it follows from Figure 3.7b, $d_m = 2\text{--}3\text{ }\mu\text{m}$ size particles are elongated to a greater extent. At the same time, the aspect AS had the second smaller local maximum values between the size interval $d_m = 5\text{--}6\text{ }\mu\text{m}$.

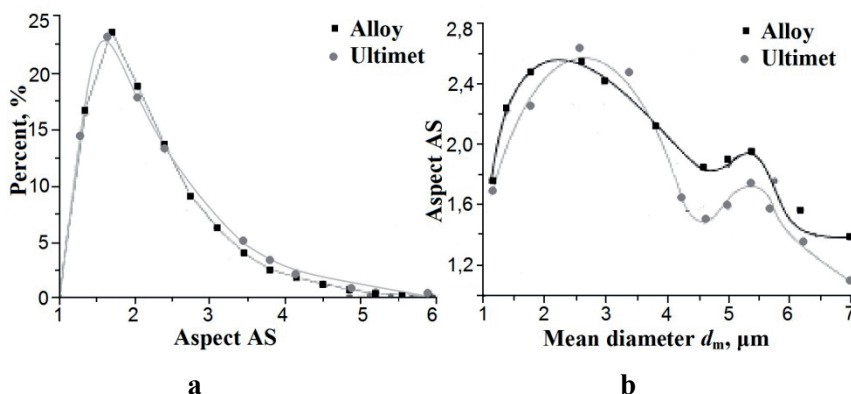


Figure 3.7 Particle size and morphology: a– shape factor – aspect AS distribution, and b – dependence of aspect AS on the particle size

It is probably caused by the nature of disintegrator milling of ductile materials. A rise in the elongation of larger particles was caused by particle deformation and by joining of smaller particles.

3.2 Grindability of mineral materials

To study the grindability of materials, different mineral materials (limestone, sandstone, basalt etc) were studied [Paper II].

Milling experiments to assess the grindability of different mineral materials (Table 3.5) were conducted in semi-industrial disintegrator DSL-137 with rotor diameter 600 mm and rotation velocity 1500 rpm. The parameter of grinding – specific treatment energy E_s was used to estimate grindability.

Table 3.5 Characterization of mineral materials to be milled

No and type of mineral materials	Initial particle size, mm	Hardness HV0.2
1. Limestone (Engis)	+6.3–10 and +10–14	135–205
2. Sandstone (Trooz)	+6.3–10 and +10–14	140–205/250–280*
3. Polphyry (Voutre)	+6.3–10	560–880
4. Basalt (Cerf)	+6.3–10 and +10–14	560–840

* Dark phase in sandstone

Table 3.6 Composition of selected mineral ores, wt%

No and type of ore	Quartz 2000 HV	Pyrite 1530 HV	Feldpars 1290 HV	Others
Gold ores				
Crown Mine (South Africa)	80	2.5	1.5	16
Waihi (Australia)	63	2.5	27	7,5
South Pipeline (USA)	51	-	8	41
KBGM (Australia)	30	1	35	24
Plutonic (Australia)	15	-	25	30 – Amphibole (946 HV)
Chromite				
CMI (South Africa)	1.1	-	4	82 – Chromite (1530 HV) 5.5 – Amphibole (946 HV) 7.4
Wonderkop (South Africa)	0.5	-	3	95 – Spinelle (725 HV) 1.5

Experiments to evaluate the suitability of hardened steels as grinding media in disintegrator were carried out and it was demonstrated that hardened steels are not prospective in these applications.

3.3 Pretreatment of composite materials

3.3.1 Production of hardmetal powders

To produce hardmetal powder, mechanical milling, one of the ways of retreatment of hardmetal wastes, was applied. The technology of producing hardmetal powder was composed of (Paper IV):

- preliminary thermo-cyclical treatment and mechanical size reduction of worn hardmetal parts in a centrifugal-type pre-crusher DS-350
- intermediate milling in disintegrator DESI
- final milling of pretreated particles by collision in the disintegrator milling system DSL-175

The preliminary size reduction of hardmetal parts in the disintegrator mill DS-350 and the following milling by DESI were conducted. Fine powder as a final product, with the particle size less than 500 μm , suitable for thermal spray and fusion, was one object of the study; coarse powder with particles more than 1 and less than 2.5 mm was taken as initial powder for subsequent final milling. As it follows from the metallographic studies, the particles were primarily equiaxed.

To produce a powder with particles less than 100 μm , final milling was conducted by the laboratory disintegrator milling system DSL-175. The particle size was determined by sieving analysis. The grindability curve of hardmetal powder with the initial maximum particle size of about 1.5 mm is demonstrated in Figure 3.8. As it follows from the metallographic studies, the particle shape of multi-milled powder was mainly isometric.

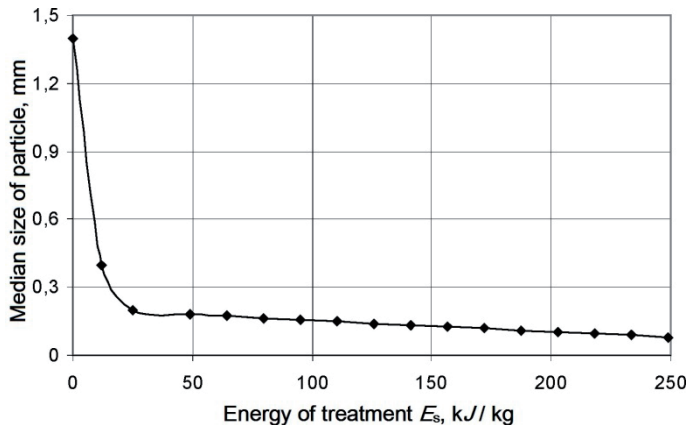


Figure 3.8 Dependence of the final product – hardmetal powder particle size on the specific energy of milling

Based on the study of grindability and the fracture mechanism of a hardmetal as an example of a brittle composite material, we can state that hardmetal milling takes place as a result of direct fracture. To study the size and shape

characteristics of powder particles depending on milling cycles in DSL-175, the 1x, 2x, 4x, 8x, 16x and 32x milled powder was considered.

To describe the particles size and shape (irregularity), the image analysis method was used. The angularity of powder particles was described by angularity parameter SPQ, developed by Stachowiak [74]. Table 3.7 demonstrates the results of granularity and morphology studies of disintegrator milled WC-Co hardmetal powders.

Table 3.7 Particle size and shape parameters of disintegrated WC-Co powder (for IP and SPQ calculation, only coarser fraction was used)

Particle size and shape parameters	Multiplicity of treatment					
	1x	2x	4x	8x	16x	32x
Mean diameter d_m , μm	257.5	83.4	36.6	9.1	2.5	2.0
Median diameter d_{50} , μm	561	209	144	88	57	30
Irregularity parameter IP	3.67	2.28	1.63	1.86	1.53	1.6
Angularity parameter SPQ	0.70	0.55	0.5	–	0.25	–

As it follows from Table 3.7 and Figure 3.8, the particle shape depends on the duration of milling: with increase in time, larger sized particle shape approaches spherical with a smooth surface.

Particle size and shape parameters of disintegrated WC–Co powder are given in Figure 3.9 (for IP and SPQ calculation, only coarser fraction was used).

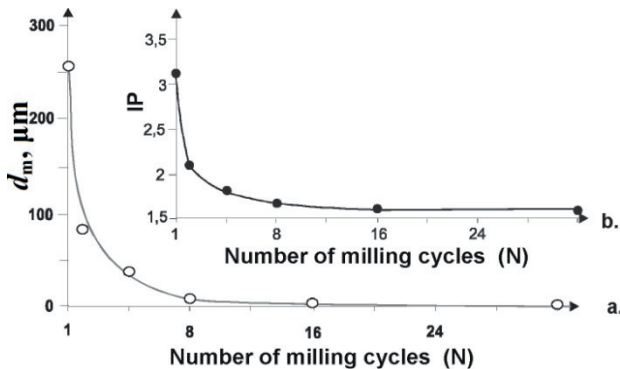


Figure 3.9 Dependence of a – particle mean diameter d_m , and b – particle shape parameter IP on the multiplicity of milling by image analysis

The SEM images of hardmetal powder particles after preliminary milling in DESI (Figure 3.10a) followed by eight times of treatment in DSL-175 (Figure 3.10b) demonstrate the observable difference in the particle shape, respectively.

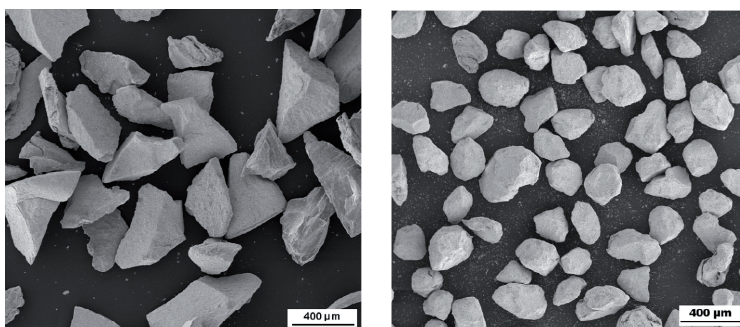


Figure 3.10 SEM images of investigated (WC-Co) hardmetal powders: a – milled in DESI and b – milled in DSL-175

3.3.2 Reprocessing of metallic-GFRP laminated plastic composite

Printed circuit boards (PCB) are an example of multi-component metallic-GFRP laminated plastic composite material (different metals, glass fibre, polymeric matrix etc).

The typical PCB consists of metals (wt%) < 30 copper ~16%, solder ~4%, iron, ferrites ~3%, nickel ~2%, silver 0.05%, gold 0.03%, palladium 0.01%, others (bismuth, antimony, tantalum, etc.) <0.01% [75, 76]. Significant quantities of nonmetallic materials (>70 wt%) in PCBs (thermoplastics, thermosets, glass fiber, ceramics) present an especially difficult challenge for recycling [77–79].

In addition to traditional mechanical direct contact milling methods (ball-milling, attritor milling, hammer milling, etc.), PCBs can be reprocessed by the collision method. The size reduction of PCBs as a function of the particle size of the specific energy of treatment was studied (Paper V).

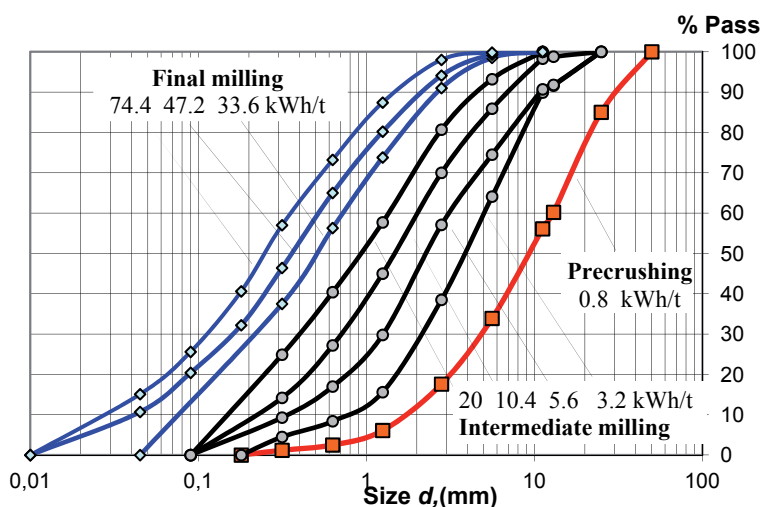


Figure 3.11 Dependence of the particle medium size of PCBs on the specific energy of treatment

The results of the preliminary size reduction, intermediate and final milling using different disintegrators are given in Figure 3.11.

As it follows from Figure 3.11, the medium particle size of the plastic component from a PCB after a 2-stage preliminary milling with specific energy of treatment $E_s=0.8$ kWh/t is about 5–10 mm, after 1–2 times of milling ($E_s=5.6$ kWh/t) about 1 mm. The subsequent intermediate milling ($E_s=15.2$ kWh/t) reduced the medium particle size to 0.45 mm. As the medium particle size and mass distribution were similar after milling with $E_s=15.2$ and 20 kWh/t, the new elaborated DS-serial disintegrator milling system for further size reduction was used. The next remarkable size reduction occurred after the milling with $E_s=47.2$ kWh/t, the medium particle size being 0.12mm.

Characterization of milled product was performed by two methods:

- sieve analysis (particle size more than 100 μm)
- laser diffraction analysis by Laser particle sizer Analysette 22 Compact (max particle size 300 μm)

The particles size and distribution of the fine material (70 wt%) obtained by multi-stage milling and with specific energy of treatment 74 kWh/t determined by laser granulometry is given on Figure 3.12.

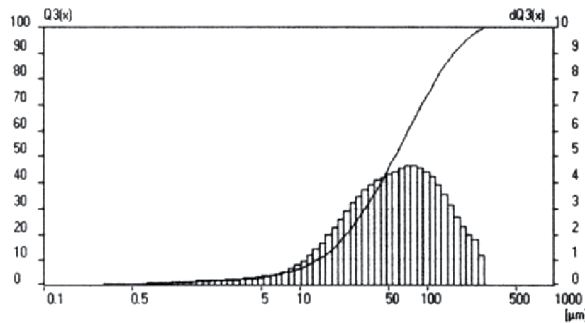


Figure 3.12 Results of laser granulometry of the milled PCB powder (0–0.3 mm)

The arithmetic mean diameter d_m of the particle was 74 μm .

The particles of milled ferrous components are given in Figure 3.13.

Multi-component metallic-GFRP laminated plastic composite material has a complex structure with brittle and ductile components. The mechanisms of the particle size reduction of the ductile and brittle materials are different.



Figure 3.13 Separated ferrous metals from the coarse fraction +1.25 – 2.5 mm

At a stage of preliminary crushing, large pieces of a composite are rapidly broken down into its component parts. The milling result is in a direct fracture. Then, each separated component is ground with own different speed.

Further each of these components is crushed with different speeds:

- slow size reduction of ductile metallic components as a result of fatigue fracture and
- fast size reduction of brittle non-metallic components as a result of direct fracture.

Such differences in mechanism and size reduction speeds allow classifying components by means of sieves, magnetic and air-inertial separation.

The powder particles from the PCB after the preliminary size reduction were mainly lamellar and they stayed lamellar after the multi-stage milling with specific energy of treatment 74 kWh/t.

3.4 Potential areas of application of produced metallic powders

The powders produced by disintegrator milling can be used for different applications.

Metal powders produced by disintegrator milling of metal chips can be used as a powdered material at shot peening as well as raw material in powder technology.

The coarse cast iron powder (from 0.3 mm to 0.6 mm) can be used as grit for surface treatment by grit blasting before spraying of coatings.

The hardmetal powders, manufactured through single and multiple milling processes, which resulted in powder particles with different shape (angular and round), were used for the production of composite powder coatings by the following thermal spray technologies [Paper IV]:

- flame spray and fusion of powder composite 25wt% (WC-Co) + 75wt% NiCrSiB self-fluxing powder [80]
- detonation gun spraying of the composite powder 85wt% (WC-Co) + 15wt% Co [81]
- high-velocity oxy-fuel spraying of the composite powder 85wt.% (WC-Co) + 15wt% Co [80]
- hardmetal powders sharp-edged in form can be used as abrasive material in abrasive tools.
- ultrafine superalloyed metal powders produced by disintegrator milling were used as a binder metal for the production of composite spray powders with higher corrosion resistance [Paper II].

CONCLUSIONS

1. The model of size reduction by collision of ductile and brittle materials is proposed. The fracture of particles at collision and refining the product to be ground can occur in one of the following ways:
 - direct fracture as a result of intensive stress waves originated from high velocity collisions (in case of brittle materials, such as cast iron and hardmetals, this mechanism is dominant)
 - low fatigue fracture as a result of numerous local plastic deformations owing to collisions is dominant for ductile materials, such as stainless steel
 - the shape of particles of brittle materials treated by collision approaches isometric form and that of ductile materials approaches spherical or sponge form. As a result, the bulk density and flowability of metal powder increases.
2. Owing to high velocities and high stresses during grinding, proposed models of size reduction were proved using designed and manufactured disintegrator.
3. Based on the analysis of existing milling methods and used disintegrators, modelling size reduction by collision and realising it through design and manufacturing of a new disintegrator milling system with centrifugal-type separation the following can be concluded:
 - Laboratory disintegrator milling systems were developed and kinetic parameters of the produced disintegrator for materials treatment was studied.
 - Specific energy of treatment as main parameter for characterization of milling process was proposed.
4. New principle of separation and a centrifugal classifier with high separative sensitivity, which is one order higher to compare with inertial classifier, was proposed that enables to reduce the size of metallic micropowders to below $5\mu\text{m}$.
5. Proposed models and a new disintegrator system were tested at milling of examples of different materials classes – brittle, ductile and composite materials
 - The results of disintegrator grinding of metal chips, used hardmetals and superalloy materials were presented.
 - Based on our theoretical model for size reduction due to fatigue of ductile materials by collision, a possibility of ultrafine powder production from nickel and cobalt based alloys was ascertained.

- Based on the grindability study of metal chips and used hardmetals, the feasibility of disintegrator milling technology for utilising industrial metal wastes was demonstrated.
- The prospectivity of using of disintegrator technology for reprocessing of PCB was shown. The best results of PCB waste reprocessing by disintegrators enabled a remarkable size reduction after two stages of preliminary crushing and four stages of intermediate milling. Larger metal particles and tinfoil stripes from condensators can be separated by sieving. The ferrous metallic components of coarse fractions can be separated with magnets.

Future plans

Following from latest papers, reports and patents [82–91] the main tendencies in disintegrator technology development are:

- Development of new configurations of a disintegrators and separation systems;
- Increasing of impact speed;
- Intensification of chemical processes taking place during the disintegration;
- Mixing of components and mechanical alloying;
- Processing of raw materials and utilization of dangerous wastes etc.

According to above mentioned the following activities are planned:

- Development of universal disintegrator to study grindability of different materials as well wears resistance of materials for grinding media.
- Development of promising selective disintegrator milling system in addition to direct and separative milling systems.
- Development of configuration for rotors, impact elements and operating chamber of disintegrators for precrushing large pieces of hard alloys to minimize extremely high wearing of these elements.
- Studying the parameters of high speed chemical reactions between air - liquid - material systems during milling, combining of cavitation - shock processing of viscous heavy oils to reduce length of molecules and increase the octane rating of fuels.

REFERENCES

1. Yokoyama, T., Inoue, Y. Chapter 10 Selection of Fine Grinding Mills. *Handbook of Powder Technology*, 2007, Vol. 12, 487-508.
2. Adetayo, A. The Chemistry of Powder Production. *Powder Technology*, 1997, Vol. 92, 3, 281.
3. Rhodes, M. Particle Size Reduction. *Introduction to Particle Technology*. John Wiley & Sons, Ltd, Chichester, UK. 2008.
4. Ilmar Kleis, I., Kulu, P. Solid Particle Erosion: Occurrence, Prediction and Control. Springer, 2008.
5. Hodakov G. S. Thin crushing of building materials. *M.: Building materials*, 1972, 239. (in russian)
6. Zerkleinerungsergebnisse bei der Einzelkornzerkleinerung mitverschiedenen Beanspruchungsarten / S. Baumgradt, B. Buss, P. May et al. –*Aufbereitungstechnik*, 1975, №9, 467-476.
7. Rumpf, H. Die einzelkornzerkleinerung als grundlage einer technischen zerkleinerung. –*Wissenschaft. Chemie-Ingenieur Technik*, 1965, Vol. 37, No. 3, pp.187–202.
8. Demidov, A.R. Ways of grinding and methods of evaluation of their efficiency / A.R. Demidov, SE Chirkov // *Elevator flour-and-large and compound feed rod*. M: MINTY Goskormzag USSR, 1969. (in russian)
9. Guyumdzhyan P. Development and research of hi-speed multistep impact-grinders: author's abstract of the dissertation of the candidate of Sciences. Ivanovo: ICTI, 1974. (in russian)
10. Demidov, A. Percussive-type mills. Overview / A.R. Demidov, SE Chirkov. *M: TSVIITE Ilegpischemash*. 1969. (in russian)
11. Kipnis, B.,M. (1983). Application UDA-technologies in the field of inorganic materials / Kipnis B.M., Vanaselya I.S., *Proc. USSR Acad. Sci. Khim. Sciences*. 1983, Vol. 6, 14, 11-15. (in russian)
12. Purga, A.,P. (1990). Some problems of physical and chemical bases of disintegrator technology. *Disintegrator Technology. Sat. articles and reports*. Tallinn: NGO «Disintegrator», 1990, Vol.1, 93-100. (in russian)
13. Lunge, G. Über Carr's Desintegrator. *Polytechnisches Journal*, Band 185, Nr. XL, 1867, 137–142.
14. Hint, I.A. Bases of production silicalcite items. *L: Gosstroizdat*, 1962. (in russian)
15. Tymanok, A.N. About the energy transferred to the processed material in multi-stage rotary mill. *Proc.TPI*. 1976, №393, 131-137. (in russian)
16. Primer, J. Untersuchungen zur Prallzerkleinerung von Einzelchen,

Dissertation. *Technische Hochschule Karlsruhe*, 1965.

17. Reiners, E. Der Mechanismus der Prallzerkleinerung beim geraden, zentralen Stoß und die Anwendung dieser Beanspruchungsart bei der Zerkleinerung, insbesondere bei der selektiven Zerkleinerung von spröden Stoffen. Dissertation. *Technische Hochschule Aachen. Forschungsberichte des Landes Nordrhein-Westfalen*, 1962, No 1059. Opladen, Technische Hochschule Aachen.
18. Lenkewitz, K.-H. Die Prallzerkleinerung körniger Massengüter Die Prallzerkleinerung körniger Massengüter durch einmalige Beanspruchung in einem Schlagrad bei unterschiedlichen Prallgeschwindigkeiten. *Fortschritt-Berichte der VDI-Zeitschriften*. 1970, 3, 36.
19. Drögemeier, R., Leschonski, K. Ultra fine grinding in a two stage rotor impact mill. *International Journal of Mineral Processing*, 1996, Vol. 44-45, pp.485-495
20. Tamm, B., Tymanok, A. Impact grinding and disintegrator. *Proc. Estonian Acad. Sci. Eng.*, 1996, Vol. 2, No. 2, 209–223.
21. Hunter, S., C. Energy absorbed by elastic waves during impact. *I. Mech. Phys. Solids* 5, 1957, 162-171.
22. Reed, J. Energy losses due to elastic wave propagation during an elastic impact. *J. Phys. D* 18, 1985, 2329-2337
23. Love, A., A. Treatise on the Mathematical Theory of Elasticity. *Cambridge University Press*, London, 1927, Chap. 8, pp. 184–203.
24. Crook, A. A study of some impacts between metal bodies by a piezoelectric method. *Proc. R. Soc. London*, Ser. A212, 1952, 377–390.
25. Goldsmith, W., and Lyman, P. T. The penetration of hard-steel spheres into plane metal surfaces. *Trans. ASME, J. Appl. Mech.* 27, 1960, 717–725.
26. Chang, C., Sun, C. T. Determining transverse impact force on a composite laminate by signal deconvolution. *Exp. Mech.* 29, 1989, 414–419.
27. Buttle, D. J., Scruby, C. B. Characterization of particle impact by quantitative acoustic emission. *Wear*, 1990, 137, pp. 63–90.
28. McLaskey G.C., Glaser S., D. Hertzian impact: experimental study of the force pulse and resulting stress waves. *J. Acoust. Soc. Am.* 128 (3): 2010, 1087-96.
29. Adams, G., Nosonovsky, M. Contact Modeling — Forces. *Tribology International*, 2000, Vol. 33, No. 5-6, 2000, 431-442.
30. Lamb, H. On the Propagation of Tremors over the Surface of an Elastic

- Solid. *Philosophical Transactions of the Royal Society of London A* 203, 1904, 1-42.
31. Pekeris, C. L. The Seismic Surface Pulse. *Proceedings of the National Academy of Sciences* 41, 1955, 469-480.
 32. Knopoff, L. Surface motions of a thick plate. *Journal of Applied Physics*, 29(4), 1958, 661-670
 33. Graff, K. Wave Motion in Elastic Solids, *Oxford University Press*, Mineola, NY, Chapters 5 and 6, (1975)
 34. Aki, K., Richards, P. Quantitative Seismology: Theory and Methods, *Freeman*, San Francisco, Chapter 4, (1980)
 35. McLaskey, G., Glaser, S. Impact of Small Steel Spheres Quantified by Stress Wave Measurement. Inaugural *International Conference of the Engineering Mechanics Institute*, Department of Civil Engineering, University of Minnesota, USA, (Eds. R. Ballarini, B. Guzina, and S. Wojtkiewicz), May, 2008, Vol. 1, p.m1101.
 36. McLaskey, G., Glaser, S. High-fidelity conical piezoelectric transducers and finite element models utilized to quantify elastic waves generated from ball collisions. M. Tomizuka, C. Yun, V. Giurgiutiu (Eds.), *Proc. SPIE*, 2009, Vol. 7292, 72920S-1 - 72920S-18.
 37. Tymanok, A., Kulu, P., Goljandin, D., Roštšin, S. Disintegrator as a machine for utilizing of metal chips to metal powder. *Proc. III ASM Intern. Conf. and Exhibition. The Recycling of Metals*, Barcelona, 1997, 513–522.
 38. Tymanok, A., Kulu, P. Treatment of different materials by disintegrator systems, *Proc. Estonian Acad. Sci. Eng.*, 1999, Vol. 5, No. 3, 222–242.
 39. Tymanok, A., Kulu, P., Goljandin, D. Metallic powders produced by mechanical methods, *Materials Science (Medžiagotyra)*, 1999, Vol. 2, No. 9, 3–7.
 40. Goljandin, D., Kulu, P., Peetsalu, P. Ultrafine metal powders produced by grinding from the industrial wastes, *Proc. TMS2002 Extraction and Processing Division Meeting on Recycling and Waste Treatment in Mineral and Metal Processing: Technical and Economical Aspects*, 2002, Vol. 1, pp.277–284.
 41. Peetsalu, P., Goljandin, D., Kulu, P., Mikli, V. and Käerdi, H. Micropowders produced by disintegrator milling, *Powder Metallurgy Progress*, 2003, Vol. 3, No. 2, 99–109.
 42. Tymanok, A., Kulu, P. and Goljandin, D. Technology and equipment for producing of spheroidized metallic powders. *Proc. Joint Nordic Conference in Powder Technology*, Oslo, 1999, 14.

43. Tymanok, A., Tamm, J. Development of the disintegrator-separator mill with the descending flow / Separative grinding with external separation. *Report state budgetary research IN 6010/1*, 1989. (in russian)
44. Patent invention: Laboratory Disintegrator System; Owner: Tallinn University of Technology; Authors: Alexei Tumanok, John Doe, George Sarandi; Priority: SU19833690204/29-33; Priority: 11/25/1983
45. Tymanok, A., Kulu, P., Mikli, V. Treatment of different materials by disintegrator systems, *Proc. Estonian Acad. Sci. Eng.*, 1999, Vol. 5, No. 3, 222–242.
46. Tadolder, J., Tamm, J. Peenpulbrite liikumise matemaatiline modelleerimine desintegraatorites ja inertsiaalklassifikaatorites: Aruanne 1994.a. tehtud tööst.
47. Tamm, J. About the aerodynamic testing and commissioning disintegrator systems with external air separator. *Abstracts of VIII all-Union seminar "Disintegrator technology"*, 1991, 1-3 October, 1. (19 - 20). Kiev: "Knowledge" Society of the Estonian SSR, 1991. (in russian)
48. Tymanok, A., Tamm, J. Study of milling of coal in the disintegrator in the separator. *Theses of the report of the tenth all-Union Symposium on mechano-emission and mechano-chemistry of solids*, 24-26 September 1986, 184 - 184. Rostov-on-don: "Knowledge" Society of the Estonian SSR, 1986. (in russian)
49. Tymanok, A., Tamm, J. Some energy aspects of the separation grinder by disintegrator. *Abstracts of the III workshop "UDA-technology"*, 4-6 September, 1984, 30 - 31. Tambov: Society "Knowledge" of the Estonian CCP (in russian)
50. Tamm, J., Tymanok, A. Change in particle size of the material in the disintegrator, depending on the energy processing. *Abstracts of the all-Union scientific-technical conference "Problems of fine grinding, classification and feeding"*, Ivanovo, 1982. (in russian)
51. Tamm, J. Separative refining fuel disintegrator: abstract of dissertation candidate of technical Sciences / *TPI. - Tallinn*, 1987. (in russian)
52. Tamm, B., Tymanok, A. Impact grinding and disintegrator. *Proc. Estonian Acad. Sci. Eng.*, 1986, Vol. 2, No. 2, 209–223.
53. Tymanok, A. About the specific energy of the collision and processing of the material in the disintegrator. Tallinn, 1981, 20. Deposited In VINITI 05.05.81, № 2957-81 Dep. (in russian)
54. Tymanok, A. About energy transmitted to the processed material in multi-stage rotary disintegrator // *Proceedings of the Tallinn Polytechnic Institute*, 1976, no. 393, 131-137. (in russian)
55. Tümanok, A., Tamm, J., Roes, A. Flow of air and particles mixture in a disintegrator. *Proceedings of the Estonian Academy of Sciences*.

- Physics. Mathematics*, 1994, 4, 280 – 292.
56. Tymanok, A. Estimation of the Rational Number of Grinding Elements and Kinetic Parameters of a Disintegrator. *Report IF.-D84. Tallinn Institute of Informatics*, 1984. (in russian)
 57. Tymanok, A., Kulu, P., Mikli, V. and Käerdi, H. Technology and equipment for production of hardmetal powders from used hardmetal. *Proc. 2nd International DAAAM Conference*, Tallinn, 2000, 197–200.
 58. Tymanok, A. On the motion of a particle in a multiple-row rotor mill. *Proc. of Tallinn Technical University*, 1973, 373, 37-47 (in russian).
 59. Tamm, J. and Tymanok, A. Interaction of Treated Material with the Plane Working Surface of a Disintegrator's Grinding Element. *Report 3E-D84. Tallinn Institute of Informatics*, 1983.
 60. Tymanok, A., Tamm, J., Suur U. Continuous model equations of the kinetics of grinding for crushing method by impact. *Proc. of the All-Union Regional Conference*, 1986. The technology of bulk materials - Himtehnika 86. (in russian)
 61. Tamm, J. and Tymanok, A. Interaction of Treated Material with the Plane Working Surface of a Disintegrator's Grinding Element. *Report 3E-D84. Tallinn Institute of Informatics*, 1983.
 62. Tamm, Jaan, Tadolder, Jüri. Modelling of fine material movement in a disintegrator. *Proc. OST-98 Symp. Machine Design. University of Oulu: Oulu University Press*, 1998, 135-141.
 63. Tymanok, A. Specific Energy of Impact Treating of the Material. Report 2957-81. Tallinn Technical University, 1981. *Deposited in the Institute of Technical Information (VINITI)*, Moscow—Ljubertsy (in russian).
 64. Tymanok, A., Tamm, J. Model of particle size of the material, crushed on the disintegrator // *Proc. all-Union meeting "Mechanochemistry of inorganic substances"*, Novosibirsk, 1982. (in russian)
 65. Tymanok, A., Tamm, J. On the mathematical modelling of particle size crushing product by the disintegrator / *Tallinn Polytechnic Institute. Dept. in RSTL ESSR №2E-D83*, 1983, 1 - 23. Acad. Sciences of the Estonian SSR, 1983. (in russian)
 66. Tymanok, A., Tamm, J. Rational choice of the empirical distribution law for the description of the product of grinding. - *News of SB as USSR. Series of Chemical Sciences. Series of chemical Sciences (8 - 11)*, 1983. Russian Academy of Sciences
 67. Fishman. E., Karev, I., Tymanok, A., Tamm, J. (1987). Modelling of grinding materials in the disintegrator. *Proceedings VNIIESM, Building*

- materials industry*, Series 10: The industry of sanitary equipment (2 - 7). Moscow: VNIIGPE, 1987. (in russian)
68. Stepanov, E., Golyandin, D., Abramov, M. The dependence of the average size of particles of quartz powder for the ceramic form of specific energy of grinding in disintegrator and type of fuel used in separation system. *Bulletin of the Rybinsk State Aviation Technological Academy Soloviev P.A.* 2011, 19(1), 193–198. (in russian)
 69. Kulu, P. *Wear Resistance of Powder Materials and Coatings*, Tallinn, Valgus Publishers, 1988.
 70. Peetsalu, P., Goljandin, D., Kulu, P., Mikli, V. and Käerdi, H. Micropowders produced by disintegrator milling, *Powder Metallurgy Progress*, 2003, Vol. 3, No. 2, 99–109.
 71. Kulu, P. Selection of powder coatings for extreme wear conditions, *Advanced Engineering Materials*, 2002, 4/6, pp. 392–397.
 72. Mikli, V., Kulu, P., Zimakov, S. and Käerdi, H. Characterization of metallic powders produced by mechanical milling, *Materials Science (Medžiagotyra)*, 1999, Vol. 2, No. 9, 19–21.
 73. Kulu, P., Mikli, V., Käerdi, H. and Bestercei, M. Characterization of disintegrator milled hardmetal powder', *Powder Metallurgy Progress*, 2003, Vol. 3, No. 1, 39–48.
 74. Stachowiak, G.W. Particle angularity and its relationship to abrasive and erosive wear', *Wear*, 2000, Vol. 241, 214–219.
 75. Zhang, S., Forssberg, E., Electronic scrap characterization for materials recycling, *Journal of Waste Management and Resource Recovery* 3, 1997, 157–167.
 76. M. Goosey, R. Kellner, Recycling technologies for the treatment of end of life printed circuit boards (PCB), *Circuit World* 29 (3) (2003), 33–37
 77. J. Guo, J.Y. Guo, B. Cao, Y. Tang and Z. Xu, Manufacturing process of reproduction plate by nonmetallic materials reclaimed from pulverized printed circuit boards, *Journal of Hazardous, Materials*, 163 (2009), 1019–1025.
 78. J.-M. Yoo, J. Jeong, K. Yoo, J. Lee and W. Kim, Enrichment of the metallic components from waste printed circuit boards by a mechanical separation process using a stamp mill, *Waste Manage.* 29, (2009), 1132–1137.
 79. *Electronic Waste Management: Design, Analysis and Application*, Eds. Ronald E. Hester, Roy M. Harrison, Royal Society of Chemistry, Cambridge CB4 0WF, UK, 2009.
 80. Zimakov, S., Pihl, T., Kulu, P., Antonov, M. and Mikli, V. Application of recycled hardmetal powder, *Proc. Estonian Acad. Sci. Eng.*, 2003,

Vol. 94, 304–316.

81. Kulu, P. and Zimakov, S. Wear resistance of thermal sprayed coatings on the base of recycled hardmetal, *Surface and Coatings Technology*, 2000, Vol. 130, 46–51.
82. Toneva, P., Epple, F., Breuer, M., Peukert, W., Wirth, K. Grinding in an air classifier mill — Part I: Characterisation of the one-phase flow. *Powder Technology*, 2011, Vol. 211, 1, 19–27.
83. Toneva, P., Peukert, W., Wirth, K. Grinding in an air classifier mill — Part II: Characterisation of the two-phase flow. *Powder Technology*, 2011, Vol. 211, 1, 28–37.
84. Voronov, V., Semikopenko, I., Penzev, P. Disintegrator with internal classification of the crushed material. *Bulletin of the BGTU Shukhov V.G.* 2011, 1, 75-77.
85. Maslovskaya, A. Grinding possess improvement and design of disintegrator with horizontal discs: author's abstract of the dissertation of the candidate of Sciences. Belgorod: 2013. (in russian)
86. Hase, I. Centrifugal impact milling of resins. *Production Engineering*. 2010, Vol. 4, 1, 1-8.
87. Palm, C. O. Method and apparatus for the preparation of finely divided calcium hydroxide: WO2012080565, 2012.
88. Becker, A., Becker, C. Pre-grinding mill or pre-disintegrator: WO 2012104495 A1, 2012.
89. Bunetsky, V., Remenyak, S. Grinding work member and centrifugal disintegrator based thereon: WO2013085478, 2013.
90. Kleshakov, V. Mikrovortex disintegrator: WO2012148311, 2012.
91. Kulikov, A. Processing line for grinding materials in particular waste tires: WO 2007111526, 2007.

ACKNOWLEDGEMENTS

First of all, I wish to express my gratitude to my supervisors Prof. Priit Kulu of the Department of Materials Engineering of TUT and Prof. Jaan Kers, Department of Polymer Materials of TUT, for continuous support, encouragement and advice.

I would like to thank my colleagues at the Department of Materials Engineering of TUT, especially Priidu Peetsalu, Riho Tarbe, Andrei Surženkov, Heikki Sarjas for their versatile co-operation, help and support in our teamwork.

I would like to thank Valdek Mikli of Materials Research Centre for his help with materials characterisation.

Writing this thesis would not have been possible without the support from the Estonian Ministry of Education and Science for financing the targeted project SF0140091s08 "Hard coatings and surface engineering" (2008-2013)

Finally, I want to express my special gratitude to project "Doctoral School of Energy and Geotechnology II" for the opportunity to continue my studies in doctoral studies.

ABSTRACT

Mills of intensive action with high load speed, such as vibration, jet, disintegrators and other types are widely used by industries to produce finely dispersed powders. Out of all these machines, the most perspective devices are mills of the percussive type.

In comparison with other mills, disintegrators have a number of advantages: they are compact, allow milling materials with very wide hardness range, allow varying the specific energy for processing the materials being milled, have a relatively low specific energy consumption and very wide range of productivity, etc.

Traditionally, disintegrators are used for the processing of brittle materials. However, given that:

- stresses, arising in the impact area, by order of magnitude are higher than the strength of the material, and
- an extremely short time in the treatment zone

essentially allow the use of disintegrators for the treatment of ductile materials.

The aim of the present work is to develop a new laboratory disintegrator milling system for production of ultrafine powders for hard to grind ductile materials with determined granularity and studying of grindability of different materials (brittle and ductile, metallic and non-metallic, composites).

In the paper were considered the theoretical aspects of the formation of small particles when they hit the work surface of the grinding element, and calculated were the necessary conditions for the separation of fine particles from the work area.

During the work, the following results were achieved:

1. Calculated were the required parameters of the occurrence and separation of fine particles
2. The model of size reduction by collision of ductile and brittle materials was developed.
3. The fracture mechanism of particles at collision was described.
4. New principle of separation and a centrifugal classifier with high separative sensitivity, which is one order higher, to compare with inertial classifier, was proposed, which enables to reduce the size of metallic micropowders to below 5 μ m.
5. Based on the analysis of existing milling methods and the used disintegrators, modeling size reduction by collision and proposed centrifugal-type separation, using the laboratory disintegrator milling systems, were developed and kinetic parameters of the produced disintegrator for materials treatment was studied.

6. Proposed models and a new disintegrator system were tested during milling of examples of different material classes – brittle, ductile and composite materials
 - The results of disintegrator grinding of metal chips, used on hard metals and super alloy materials, were presented.
 - Based on our theoretical model for size reduction due to fatigue of ductile materials by collision, a possibility of ultrafine powder production from nickel and cobalt based alloys was ascertained.
 - Based on the grindability study of metal chips and used hard metals, the feasibility of disintegrator milling technology for utilizing industrial metal wastes was demonstrated.

Keywords: disintegrator, disintegrator milling and separation, recycling, hardmetal powders, grindability, granularity, morphology, separation.

KOKKUVÕTE

Kõrgenergeetiliste ja kõrge laadimiskiirusega jahvatusveskid nagu vibroveskid, jugaveskid, desintegraatorid jt. on laialt kasutuses tööstuses peente pulbriliste materjalide tootmiseks. Kõige perspektiivsemad seadmed neist on suure kiirusega löögil põhinevad veskid – desintegraatorid.

Võrreldes teiste veskitega omavad desintegraatorid mitmeid eeliseid: nad on kompaktsed, nad lubavad purustada materjali väga laia kõvaduse vahemikuga, nad lubavad varieerida purustatavate materjalide töötlemise erienergiat ja nad on suhteliselt madala jahvatuse erienergiaga ning nad on laias tootlikkuse vahemikus.

Tavapäraselt kasutatakse desintegraatoreid habraste materjalide töötlemiseks. Kuid asjaolud, et pinged, mis tekivad löögi piirkonnas, on suurusjärgu võrra suuremad kui materjali tugevus ning erakordselt lühike töötlemise piirkonnas viibimise aeg lubavad desintegraatoreid põhimõtteliselt kasutada ka sitkete materjalide töötlemiseks.

Käesoleva töö eesmärk on töötada välja uus laboratoorne desintegraator-jahvatussüsteem raskelt purustatavate ja ka sitkete materjalide töötlemiseks etteantud osiselise koostisega erinevate materjalide (habras ning sitke, metalne ning mittemetalne, komposiitne) jahvatamiseks.

Töö esimene peatükk käsitleb nii löökjahvatuse teooriat, osakese mõõtmete vähenemist kui ka peenosise eemaldamist jahvatusprotsessist. Vaatluse all on osakese mõõtmete vähenemine habraste materjalide otsepurunemise teel kui ka plastsete metalsete materjalide osakeste tekke mehhanism läbi madalatsüklilise väsimuse. Samuti vaadeldakse peenosise eemaldamist jahvatusseadmest nii inertsiaal- kui ka tsentrifugaalpõhimõtet kasutades.

Teine peatükk on pühendatud universaalse laboratoorse desintegraatorjahvatus-süsteemi loomisele, mis sisaldab nii desintegraatori konstruktsiooni kui ka tsentrifugaalklassifikaatorit seadmele. On toodud välja DS-seeria desintegraatorite konstrueerimise põhimõtted ja kasutuse võimalused. On võrreldud separatsiooniks projekteeritud tsentrifugaalklassifikaatori tundlikkust inertsiaalklassifikaatori omaga. Esimene võimaldab stabiilset jahvatusprodukti osisega 1 kuni 20 µm eraldamist.

Töö kolmandas peatükis tuuakse erinevate materjalide desintegraatorjahvatatavuse uurimise tulemused. On uuritud järgmisi materjaligruppe:

- metalsed materjalid (korrosioonikindla terase laast, Ni- ja Co-sulamite pulbrid kui sitkete materjalide esindajad)
- keraamilised materjalid (mineraalsed maagid kui habraste materjalide esindajad)
- komposiitmaterjalid (kõvasulam kui keraamilis-metalse komposiidi ja trükkplaadid kui metall-klaaskiudarmeeritud laminaadi esindajad)

On toodud jahvatusprodukti osiselise koostise jaotus, osakeste keskmise suuruse sõltuvus jahvatuse erienergiast – jahvatuskõverad kui ka osakeste kuju (korrosioonikindel teras ja kõvasulam) sõltuvus jahvatustsüklite arvust.

Töös vaadeldakse löökpurustamise teoreetilisi aspekte ülipeente osakestega pulbrite saamiseks, on arvutatud tekkitud peente osakeste töötsoonist eraldamiseks vajalikud eeldused.

Töö käigus on saavutatud järgmised tulemused:

1. On arvutatud välja peente osakeste tekkimise ja separeerimise vajalikud parameetrid.
2. On arendatud edasi peenendamise mudelit.
3. On kirjeldatud purunemise mehhanisme osakeste pötkel.
4. On pakutud välja uus separatsiooni põhimõte ning tsentrifugaalklassifikaatori konstruktsioon, kus inertsiaalklassifikaatoriga võrreldes on 2–3 korda kõrgem separatsioonitundlikkus. See võimaldab vähendada saadava metalse mikropulbri suurust alla 5 µm.
5. Olemasolevate purustamismeetodite ja kasutuses olevate desintegraatorite analüüsi põhjal on arendatud ja töötatud välja laboratoorne desintegraator-jahvatussüsteem, mis võimaldab vähendada osakeste suurust pötkemeetodil ning eraldada tsentrifugaalseparatsiooni kasutades vajalike parameetritega jahvatusprodukti.
6. Pakutud mudeleid ning uut desintegraatorjahvatussüsteemi testiti erinevate materjaligruppide esindajate proovide purustamisel (haprad mitte-metalsed, sitked metalsed ning komposiitmaterjalid).

On tõestatud võimalus ülipeente pulbrite tootmiseks Ni- ja Co-baasil sulamitest, toetudes teoreetilisele mudelile osakeste suuruse vähendamiseks ja tsentrifugaalseparatsioonipõhimõttele ja selle tundlikkusele.

On demonstreeritud kasutatud kõvasulami ja lamineeritud metallplastist PCB plaatide jahvatamise võimalusi desintegraatoritehnoloogiat kasutades ning tööstusjäätmete ümbertöötlemise teostavust ja otstarbekust.

Töö uudsus seisneb järgnevas:

1. Desintegraatoris ja separaatoris osakeste liikumise kiiruse arvutusvalemis, trajektoori määramises töökambris ja jahvatus- ja separatsiooni elementide arvu, geomeetria jt. parameetrite määramises.
2. Jahvatuse erienergia efektiivsuse määramises.
3. Etteantud osiselise koostise ja osakeste kujuga ülipeente ja sfäärilise kujuga pulbrite saamises plastsetest metallidest.

Praktiline tähtsus seisneb uudse desintegraatorjahvatussüsteemi loomises ja valmistamises.

Võttesõnad: desintegraator, desintegraatorjahvatus, separatsioon, Ni- ja Co-sulamid, kõvasulamid, laminaatkomposiidid, peenpulber, jahvatatavus, taaskasutus, morfoloogia.

PUBLICATIONS

Publication I

Zimakov, S.; Goljandin, D.; Peetsalu, P.; Kulu, P. (2007). Metallic powders produced by the disintegrator technology. *International Journal of Materials and Product Technology*, 28(3/4), 226 - 251.

DOI: <http://10.1504/IJMPT.2007.013081>

Metallic powders produced by the disintegrator technology

Sergei Zimakov*, Dmitri Goljandin,
Priidu Peetsalu and Priit Kulu

Department of Materials Engineering,
Tallinn University of Technology,
Ehitajate tee 5, Tallinn 19086, Estonia

E-mail: sergei.zimakov@ttu.ee E-mail: goljandin@email.ee
E-mail: priidup@ttu.ee E-mail: priit.kulu@ttu.ee

*Corresponding author

Abstract: The paper deals with the peculiarities of disintegrator milling, the development of disintegrator milling systems and the grindability of different metallic materials. In the first part of the paper the size reduction by collision is under consideration. A theoretical model for the size reduction of ductile materials by collision is proposed. The second part of the paper is focused on the development of disintegrators for processing of materials, which differs significantly from the other grinding equipment. The third part of the paper is focused on the disintegrator milling technology used for mechanical treatment of different metallic materials.

Keywords: disintegrator; disintegrator milling and separation; recycling of metals; metal powders; grindability; granularity; morphology.

Reference to this paper should be made as follows: Zimakov, S., Goljandin, D., Peetsalu, P. and Kulu, P. (xxxx) 'Metallic powders produced by the disintegrator technology', *Int. J. Materials and Product Technology*, Vol. 28, Nos. 3/4, pp.226–251.

Biographical notes: Dr. Sergei Zimakov (born November 25, 1975) graduated from Tallinn University of Technology in 1997 with a Diploma of Mechanical Engineering. He defended his MScEng in Tallinn University of Technology in 1999 and PhD in 2004. Since 2004 the Senior Researcher at the Department of Materials Engineering of TUT. Main research areas: surface engineering and wear resistant powder coatings. He has published publications in materials science journals and conference proceedings.

Dmitri Goljandin (born March 23, 1973) is PhD Student of Tallinn University of Technology at the faculty of Mechanical Engineering. He defended his MScEng in Tallinn University of Technology in 2002. His research interests are in the field of grinding and impact milling mechanics (grinding by disintegrators, separation and classification of a product, development of milling systems with centrifugal classifier-separator for producing ultrafine metal powders). He has published papers in conference proceedings and materials science journals.

Priidu Peetsalu (born March 31, 1976) is PhD student of Tallinn University of Technology at the faculty of Mechanical Engineering. He received his MScEng in Materials Engineering from Tallinn University of Technology. His research interests are in the field of ultrafine metal powders (composition, metallography, image analysis). He has published papers in conference proceedings and materials science journals.

Professor Priit Kulu (born February 13, 1945) graduated from Tallinn University of Technology (TUT) in 1968 with a Diploma of Mechanical Engineering. Received his PhD Eng from the Institute of Materials Science of Ukrainian Academy of Sciences and DSc in powder metallurgy and coatings from the Association of Powder Metallurgy of Byelorussia. Since 1983 professor of materials science at the Department of metals Processing of TUT, from 1991 professor of materials science and Head of the Department of Materials Engineering of TUT. From 2005 Dean of Faculty of Mechanical Engineering of TUT. Main research areas: surface engineering and wear resistant powder coatings; has published over 150 publications in this field.

1 Introduction

In contemporary industry, the demand and prices of raw materials are increasing. Thus, economy of the resources and recycling of materials are topical issues. Circulation of metals assumes the formation of metal scrap (metallurgical, industrial and old) and waste metal. However, the utilisation of the industrial scrap (formed during the manufacturing process), in particular, the use of metal chips in the metallurgical process, is irrational (Taptik et al., 1994).

Metal powders as the initial material for powder metallurgy are produced by different technologies (Philips, 1990). The most used one is the atomising of melted metal. An alternative technology for producing metal powder is the milling of metal chips.

One of the methods for production of metal powder is grinding by collision. This method has some advantages (Tymanok et al., 1997b):

- nothing will be lost in the chemical composition of the alloy
- the quality of the material will increase as the microstructure of the material improves owing to the intensive impact stresses and mechanical activation
- the retreatment of chips solves two problems: recycling of chips and producing raw material for powder metallurgy.

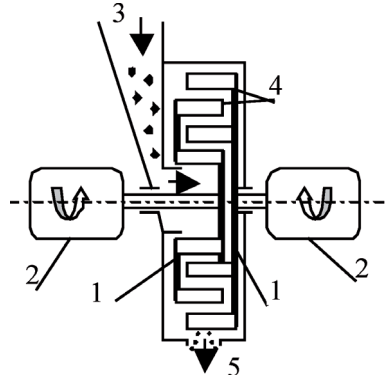
Disintegrators can be effectively used for the treatment of industrial metallic wastes, especially for different kinds of chips (Tymanok et al., 1997b). Besides milling, owing to high intensity collisions, the ground material will be mechanically activated. By disintegration, the grinding of mineral materials, e.g., the mixture of quicklime, quartz sand and water, the raw materials of silicalcite, activates the materials and strengthens the final product (Tamm and Tymanok, 1996). Disintegrator milling is also characterised by the selectivity of the process.

The highest selectivity rate of grinding is observed at treatment by collision, for example, selective grinding of slag and slimes enables separation of valuable components.

2 Grinding by collision

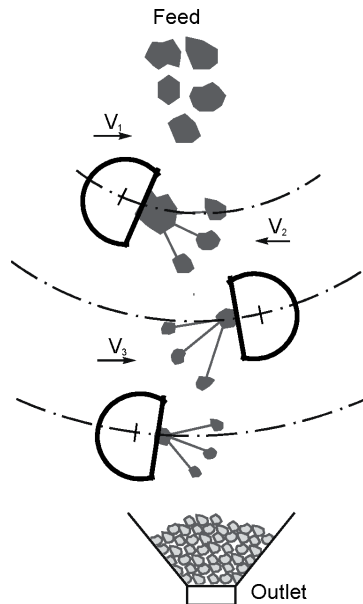
The disintegrator is a grinding mill consisting of two rotors rotating in the opposite direction that treats material by collision. The principal scheme of disintegrator equipment is shown in Figure 2.

Figure 2 Principal scheme of the disintegrator: 1 – rotors; 2 – electric drives; 3 – material supply; 4 – grinding elements; 5 – output



These rotors are equipped with one or more concentric rings (Figure 3), with a row of grinding bodies on each ring. The grinding bodies are effective as targets for the colliding particles and as accelerators for the next collision.

Figure 3 Principal scheme of disintegrator rotors equipped with grinding bodies



2.1 Stresses on collision

The stresses generated in the particle at collision have not been measured experimentally till today. They cannot be calculated exactly, but it is possible to estimate them by two extreme models: either according to the quasistatic *Hertz model* applied to a spherical particle or according to the *Wave model* where the particle with a plane side hits the target exactly with the same side (Rumpf, 1965). According to the *Hertz model*, the both colliding particles are spheres. The stresses σ_H of collision for the general case

$$\sigma_H = 0.279 A^{-3/5} \times B^{1/5} \times C^{4/5} \times v^{2/5}, \quad (1)$$

where

$$\begin{aligned} A &= R_1 \times R_2 / (R_1 \times R_2), \\ B &= \rho_1 \times R_1^3 \times \rho_2 \times R_2^3 / (\rho_1 \times R_1^3 + \rho_2 \times R_2^3), \\ C &= (1 - \mu_1^2) / E_1 + (1 - \mu_2^2) / E_2 \end{aligned}$$

and

v : Velocity of collision.

R_1, R_2 : Radius of the colliding bodies.

ρ_1, ρ_2 : Densities of the colliding bodies.

E_1, E_2 : Young's module.

μ_1, μ_2 : Poisson's coefficient.

In case a spherical particle collides with a plane surface, the stresses can be calculated by equation (1) provided $R_2 \rightarrow \infty$.

$$\sigma_H = 0.279 \rho_1^{2/5} \times C^{-4/5} \times v^{2/5}. \quad (2)$$

The stresses are independent from the radius of the particle although in formula (1) the stress depends on the radius through A but the dependence is weak.

According to the *Wave model*, it is supposed that the particles collide mainly with their plane surfaces. Then the stress waves begin to propagate in both particles to the opposite directions from the contact surface. Using the law of the momentum of motion for the stressed parts of particles, one can derive the formula of *Wave model* stresses in the contact surfaces:

$$\sigma_w = \rho_1 \times c_1 \times \rho_2 \times c_2 / (\rho_1 \times c_1 + \rho_2 \times c_2) \quad (3)$$

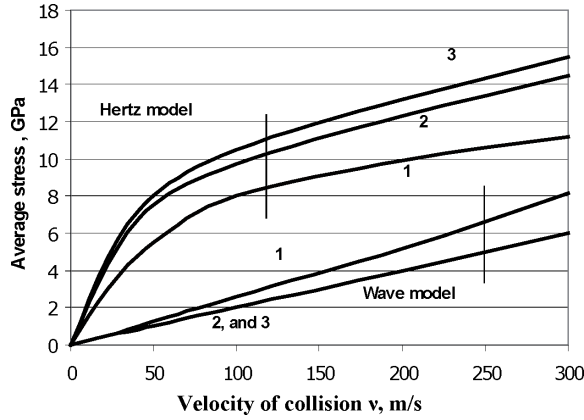
where c_1 and c_2 are the velocities of the elastic waves

$$c_i = E_i / \rho_i, \quad i = 1, 2. \quad (4)$$

Since real particles differ from ideal spheres and they do not collide precisely with plane surfaces, the *Hertz model* and *Wave model* ought to be observed as boundary cases, and the actual real stresses are between these limit values (Figure 4).

Figure 4 shows the change of the stresses in a steel particle with diameter 2 mm depending on the collision velocity and the target (grinding element). Three grinding elements were tested: a WC-6Co hardmetal plate, an AISI316 steel plate and a steel particle of the same size.

Figure 4 Dependence of maximum of average stress on velocity of collision of AISI316 steel particle ($d = 2$ mm) to: 1 – hardmetal WC-6Co plate; 2 – plate of same steel; 3 – same equal another particle



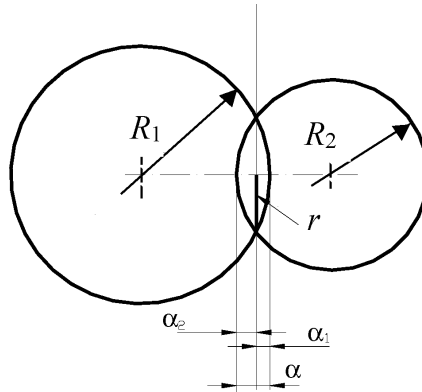
2.2 Collision of particle with another particle or plate

Initial metal chips of ductile materials are loose and the metal is partially work hardened. At collision, at the initial stage of milling, its behaviour is nearly similar to ductile material. With reduction of size, the chip's particles approach an isometric and even spherical form. At the last stage, the particles produced by collision with the size of 1–3 mm have a spherical form. In the process of producing powder from metal chips the principal part of energy is used up to the last stage of reducing spherical particles to powder. On the basis of quasistatic *Hertz model*, the stresses given by formulas (1–3) were derived. At collision, the particles deform (Figure 5). Their contact area is a circle with the radius r_k . From quasistatic consideration of collision, the approach of the centres of particles can be derived

$$\alpha = 1.729 A^{1/5} \times B^{2/5} \times C^{2/5} \times v^{4/5} \quad (5)$$

where the marks are the same as equation (2).

Figure 5 Collision of two spherical particle: α – approach of the centers, α_1 , α_2 – approach of each particle r_k – contact area radius



In case the particle collides with a plate, the formula (equation (5)) takes the form

$$\alpha = 1.729 \rho^{1/5} \times C^{2/5} \times R_1 v^{4/5}. \quad (6)$$

The approach of the particle is proportional to the particle's radius. The radius of the contact area is derived and can be expressed by formulas corresponding to both the general case and the plate case

$$r_k = 1.86 \rho_1^{2/5} \times C^{1/5} \times R_1 v^{2/5}. \quad (7)$$

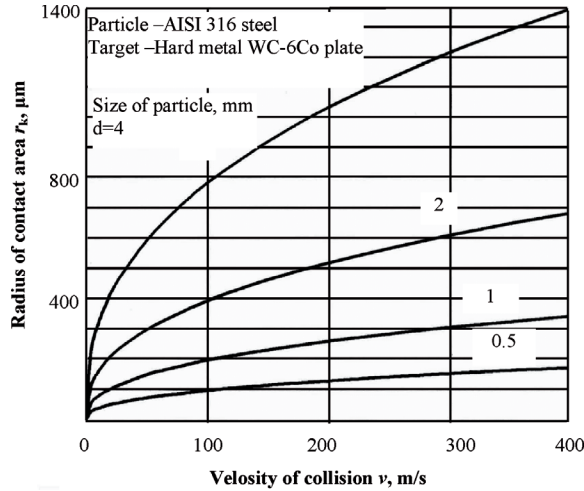
It is notable that both approach α_1 and radius r_k are proportional to the size of particle.

Maximum stress σ_m and average stress σ_{av} can be expressed as follows

$$\sigma_{\max} = \frac{3}{2} \times \sigma_{av} \text{ and } \sigma_{av} = \frac{F}{\pi r^2}. \quad (8)$$

The material is plastically deformed in a certain area smaller than the contact area. As at collision the order of stresses is high, we can suppose that the radius of plastic deformation area is equal to the contact area (Figure 6).

Figure 6 Dependence of radius of contact area between AISI316 particle and hard metal WC-6Co plate on velocity of collision and size of particle d



2.3 Size reduction model

The size reduction of ductile metal particles goes by low-cycle fatigue fracture. When the particle of radius $R_i < R$ is loaded with an enormous number of collisions, then at each loading a small plastic deformation area will arise (Tymanok et al., 1997a). After a certain number n_i of loadings, the surface of the particles will be completely covered with plastic deformations.

$$n_1 = \frac{4\pi R^2}{\pi r_k^2} = \left(\frac{2R}{r_k} \right)^2 = 1.15 \rho_1^{-2/5} C^{-2/5} v^{-4/5}. \quad (9)$$

We can mention that n_1 depends on collision velocity, elastic properties of materials and thickness of particles, but not on the radius R of particle. By repeating such series many times (a great number of cycles) the area will be deformed again and again. As a result of repeated collision loading and fatigue breaking of the surface of particles, small pieces with the size of δ will be detached. After a certain number n_2 of loading series a layer with thickness δ will be separated. The size of particles is reduced by 2δ . A simple differential equation can be written.

$$\frac{dR}{d\delta} = -\frac{n}{n_1 n_2}. \quad (10)$$

The solution of the equation, where R_0 is the initial radius of the particle, takes the form

$$R = R_0 - \frac{n\delta}{n_1 n_2}. \quad (11)$$

The particle will be ‘ground’ when the radius R approaches the boundary size to be separated in the classifier by separative grinding. If the boundary size is equal to δ , it gives a necessary number of collision loadings for grinding the particle of size $2R_0$.

$$n = n_1 n_2 \left(\frac{R_0}{\delta} - 1 \right) \text{ or } n \cong n_1 n_2 \times (R_0 / \delta). \quad (12)$$

The depth of plastic deformation is of the same order as the approach $\alpha_1 = \alpha$. The separated size of δ is smaller but of the same order of size as α . It is supposed that

$$\delta = \alpha / k \quad (13)$$

where $k = 2 - 8$.

Actually, grinding AISI316 steel particles of size $d = 2-2.5$ mm at the velocity $v = 150$ m/s the approach $\alpha = 80$ μm , the ground particles in the product are of the order $\delta = 20$ μm and $k = 4$ (Tymanok et al., 1997a, 1997b). On the other hand, AISI 316 steel particles with the above described size will be fully ground by separative grinding with approximately $n = 30.000 \dots 40.000$ collision loadings. From equation (10) number n_2 of loading for fatigue fracture can be found. In our cases, from equations (9) and (12)

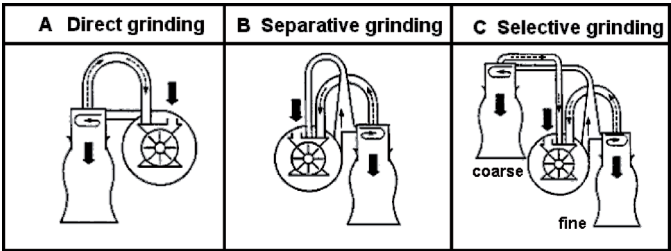
$$n_1 = 17 \text{ and } n_2 = n\delta / (n_1 R_0) = 17.6 - 18.8. \quad (14)$$

It follows from this that by impact on the same place of the surface the particle of AISI 316 steel must be loaded $n_2 \cong 20$ times before fatigue breaking takes place. That is low-cycle fatigue breaking, which occurs owing to the high rate of intensity of stresses at high velocity of collision. As the stresses at collision depend weakly on the size of particle, n_1 does not depend on the size of particle, then in the first approximation n_2 will not depend on the size of particle. It depends on properties of materials and velocity of collision.

3 Development of disintegrator systems for materials treatment

On the basis of theoretical investigations, the corresponding mills, the DS- series disintegrator, have been designed and developed at TUT (Tymanok et al., 1996, 1999, 1999b). They are operating in a system of direct, separative (closed), selective or selective–separative grinding (Figure 7).

Figure 7 Different modes of disintegrator grinding of materials



In the DS-series disintegrator systems, the ground material ejected from the rotors carries significant kinetic energy that can be used for further transportation of the material. This is taken into account in disintegrators of direct grinding (for transportation of the material into the bunker or into the classifier for separative or selective grinding).

The separation systems used in the DS-series disintegrators are based on aerodynamic and centrifugal forces. A special inertial and centrifugal classifier with a closed air or gas system has been developed. These systems are autonomous and ecologically clean owing to the use of the kinetic energy of the output material. The system does not need any additional devices of transportation or fans (Figures 8 and 9).

Figure 8 Principal schemes of (a) inertial and (b) centrifugal classifiers (A – air, M – materials, CM – coarse material, FM – fine material)

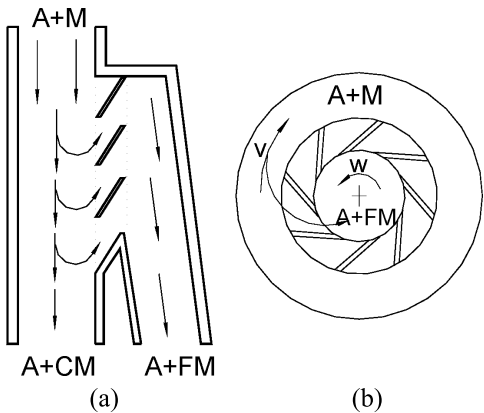
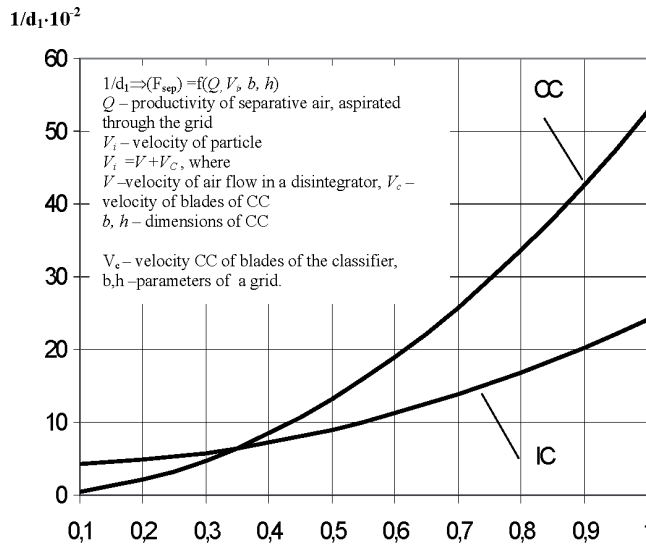


Figure 9 Dependence of separation effect on classifying parameters of (IC) inertial and (CC) centrifugal classifiers



The DS-series disintegrators include small laboratory multipurpose disintegrator systems DSL-160, DSL-175, with the capacity of some kilograms per hour, semi-industrial and industrial disintegrators, for example, DSL-115 with several hundred kilograms per hour and DSA-600 at some t/h (Tymanok et al., 1997b, 1999b, 2000).

The DS-series disintegrators and disintegrator systems have been designed on the basis of the following principles:

- modular design
- convenience of operating and service
- possibility to use an autonomous and ecologically clean closed gas system
- possibility to realise direct, separative, selective and selective–separative grinding modes with simplicity of switching from one mode to another
- elastic support of motors with a possibility to use automatic balancing of the rotor system
- high level of safety.

The DS-series disintegrator is foreseen for definite technologies and aims. Therefore, rotors, classifiers and other auxiliary devices ought to be designed according to the demands. With small modifications, the DS-series disintegrators can be adjusted for solving different problem, such as:

- maximum output of certain size of the ground material
- maximum volume density of the ground product
- high level of activation of materials
- mixing, homogenisation and alloying of materials.

At high abrasivity of materials to be treated, the grinding media is subjected to intensive wear. Rotors with a special configuration of working blades are designed. Thus, portions of materials fall periodically on the working surface, covering it with a thick layer of the treated material. This layer is formed from the fine and coarse particles of materials, and it protects the working surface against wear.

For the production of micrometrical powders, a special multipurpose disintegrator milling system – the disintegrator DSL-175 with a combined inertial–centrifugal classifier – was developed (Goljandin et al., 2002).

The main kinetic parameter in materials treatment is the specific energy of treatment both regarding the grinding effect (grindability) and the economic aspects. The above-mentioned parameter of the disintegrators DSL-175 and DSL-115 is shown in Tables 2 and 3.

Table 2 Velocity of collision and specific energy of treatment E_s material in DSL-175, as dependent on the velocity of rotation of rotors and the multiplicity of treatment

Rotation velocity of rotors (rpm)	Velocity of collision (m/s)	Specific energy of treatment E_s (kJ/kg) by multiplicity of treatment			
		1	2	3	4
2000/2000	32	0.8	1.6	2.4	3.2
4000/4000	64	3.1	6.2	9.3	12.4
6000/6000	96	7.0	14.0	21.0	28.0
8000/8000	128	12.4	24.8	37.2	49.6
10000/8000	142	15.2	30.4	42.6	60.8
10000/9000	151	17.3	34.6	51.9	69.2
10000/10000	160	19.4	38.8	58.2	77.6

Table 3 Treatment parameters of the disintegrator DSL-115

Direct grinding			Separative grinding			Selective grinding		
Rotors, number of rows	Total productivity (kg/h)	Specific energy E_s (kJ/kg)	Max size of product (μm)	Productivity (t/h)	Specific energy E_s (kJ/kg)	Rotors, number of rows	Total productivity (kg/h)	Specific energy E_s (kJ/kg)
2	1000	14.0	100	0.1	180	2	1000	14.0
3	900	21.2				3	900	21.2
4	700	27.0	250	0.25	72	4	700	27.0
5	500	31.7				5	500	31.7

Milling of different materials by disintegrator systems requires the feed materials with parts of sizes from 2.5 mm to 10–20 mm (which depends on the disintegrator type and design). For these purposes, a special machine – a centrifugal accelerator for preliminary size reduction of materials parts by impact is designed. The centrifugal type pre-crusher DS-350 is presented in Figure 10 and the main kinetic parameters (velocity and specific energy of treatment) of the device are given in Table 4.

Figure 10 Schematic representation of centrifugal pre-crusher DS-350: (1-2) mono-rotor system, (1-2-3) duplex-rotor system (CF – central feed, SF – side feed)

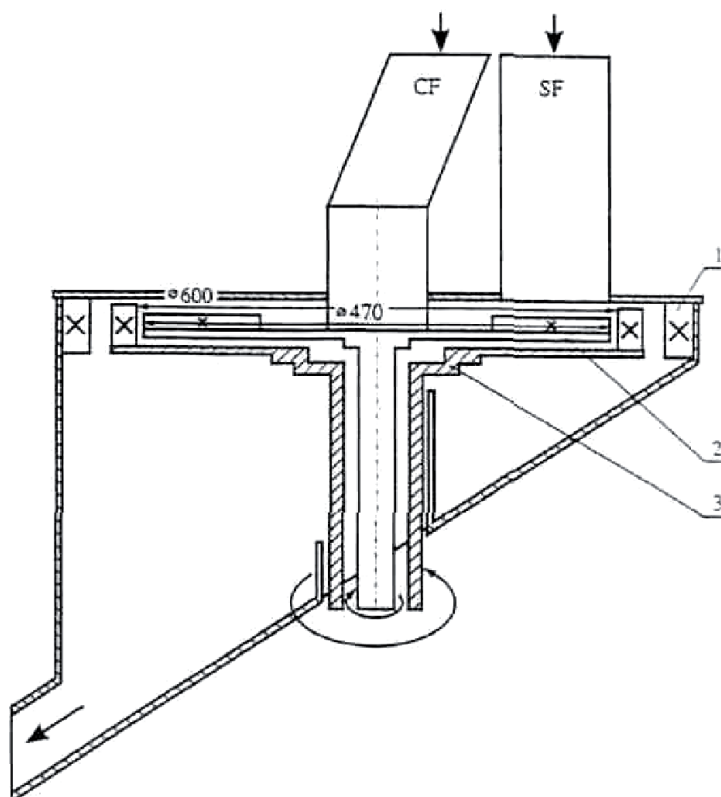


Table 4 Maximum velocity of impact and specific energy of treatment E_s of material in DS-350

Type of system	Maximum velocity of impact (m/s)	Specific energy of treatment E_s (kJ/kg)	
		Central feed (CF)	Side feed (SF)
Mono-rotor (MR) system	45	1.01	1.33
Two-rotor (DR) system	75	3.82	4.15

In the experimental studies of different metallic materials the following disintegrator milling systems were used:

- the laboratory multipurpose disintegrator milling system DSL-175
- the experimental disintegrator DESI
- for the preliminary size reduction of initial material, the centrifugal-type pre-crusher DS-350.

The main parameters of the devices used are given in Table 5.

Table 5 Characterisation of the disintegrators used

<i>Parameter</i>	<i>Laboratory disintegrator DSL-175</i>	<i>Experimental disintegrator DESI</i>	<i>Centrifugal-type mill DS-350</i>
Rotor system	Two rotor system	Two rotor system	One/two rotor system
Diameter of rotors (mm)	175	350	600
Number of pins/blades roads	5	3	3
Rotation velocity of rotors (rpm)	Up to 12000	2880/5760	1440/2880
Impact velocity (m/s)	Up to 192	95.5/191	90/180
Specific energy of treatment E_s (kJ/kg)	Up to 28.0	2.9/11.7	1.8/3.6
Input (maximum particle size) (mm)	2.5	5	15
Possible operating system	Direct or separative	Direct	Direct
Milling environment	Air/argon	Air	Air
Classifying system	Inertial or centrifugal	–	–

4 Grindability studies of different metallic materials

Based on the disintegrator milling technology, the disintegrator milling of different metallic materials was studied:

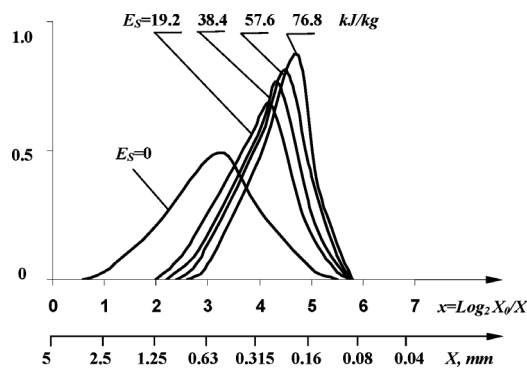
- cast iron (example of brittle material)
- stainless steel, Ni- and Co-based alloys (example of ductile material)
- hardmetal (example of composite material).

It can be assumed that materials grindability and the properties of the ground product depend on the brittleness–toughness properties of the materials. If the size reduction of brittle materials takes place by the direct fracture at collision, as a rule, ductile material cannot be fractured by collision. A theoretical model for size reduction of ductile materials, developed by us, is also proved in practice. Metal powders of stainless steel AISI316, Ni-based and Co-based alloys with the particle size up to 1–5 μm were produced by collision treatment in the disintegrator milling system DSL-175.

4.1 Milling of cast iron chips

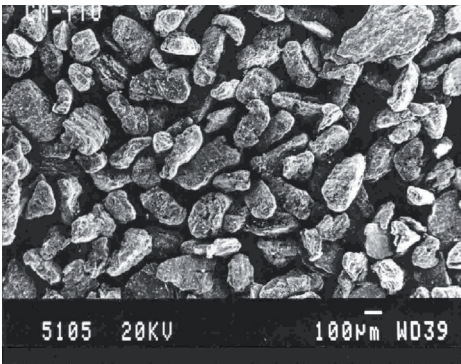
Cast iron chips with the initial particle size from 1 mm to 20 mm were ground by direct milling (Tymanok et al., 1999, 1999a, 1999c). As shown in Figure 11, the granulometry of ground cast iron GG15 depends on the specific energy of grinding. By treatment with low specific energy, the particle size reduction depends on the direct fracturing of initial chips as the number of impacts (cycles) is low.

Figure 11 Dependence of the granulometry of the cast iron GG15 powders on the specific grinding energy E_s kJ/kg ($X_0 = 5$ mm)



Multi-stage grinding produces a new finer fraction after each grinding. This fine product is the result of the direct fracturing of particles. Figure 12 illustrates the shape of the cast iron powder ground at optimal parameters. It can be seen that the particle shape is mainly isometric.

Figure 12 Shape of the particles of the ground cast iron GG15 powder



The results of the granulometry and morphology studies of the produced cast iron powder of fraction from 160 μm to 315 μm are given in Table 6. As it follows from Table 6 and Figure 12, the powder particles are isometric in form, the granularity of main fraction of the ground powder is narrow (70% of fraction from 60 μm to 180 μm).

Table 6 Main characteristics of the ground cast iron with granularity from 160 μm to 315 μm

Method*	Granularity		Morphology			
	Main fraction (70%) (μm)	d_m (μm)	Aspect AS		Roundness RN	
			Main	Mean	Main	Mean
PPP	+180–245	220	1.25–2.05	1.8	1.45–1.85	1.7
CSP	+145–190	165	1.3–2.3	2.05	2.35–4.2	3.95

*PPP: projections of powder particles.

CSP: cross-section polish.

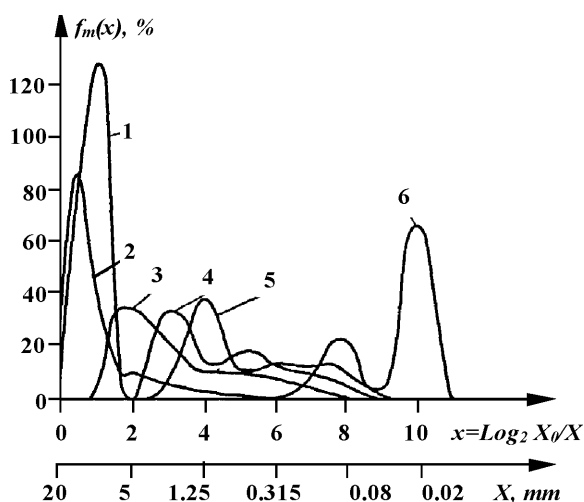
4.2 Production of stainless steel powder from chips

Stainless steel AISI 316 chips were treated in three steps (Tymanok et al., 1997a, 1997b, 1999, 1999a):

- preliminary treatment of continuous chips in the disintegrator DS-350
- intermediate grinding in the semi-industrial disintegrator DSL-115 by direct grinding system
- final fine grinding in the laboratory disintegrator DSL-175 by separative grinding system.

The dependence of the granularity on the specific energy of treatment is shown in Figure 13.

Figure 13 Dependence of the granulometry of stainless steel AISI316 powders on the specific grinding energy E_s , kJ/kg ($X_0 = 20$ mm)



First, chips are plastically deformed and work hardened. As a result, their fracture resembles that of a brittle material (curves 1 and 2, DS-350). Next, the disintegrator DSL-115 (curves 3, 4 and 5) was used.

Fine grinding was performed using DSL-175 in a separative grinding system (curve 6).

The particle shape of the powder milled by separative grinding at the intermediate stage (from circulation) is shown in Figure 14(a) – as the result of plastic deformation, the powder particles are spherical in form and at the final stage – lamellar with the particle size of about 10–20 μm (Figure 14(b)).

As it is seen in Figures 13 and 14, the disintegrator grinding results in the changes of the shape and granulometry of the particles. Separately ground particles of fraction +160–315 μm are spherical. The main characteristics (size and shape of the particles) of the stainless steel powder are presented in Table 7.

Figure 14 Shape of the particles of stainless steel AISI 316 powders: (a) powder +160–315 μm at the intermediate stage of separative grinding; (b) final product of separative grinding

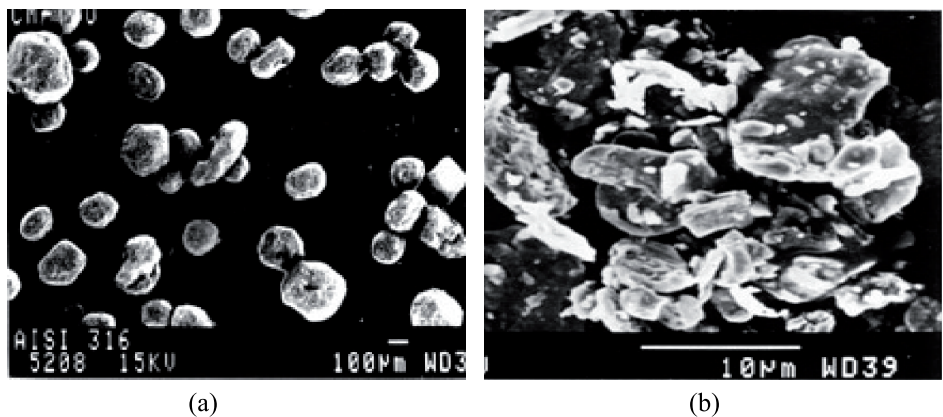


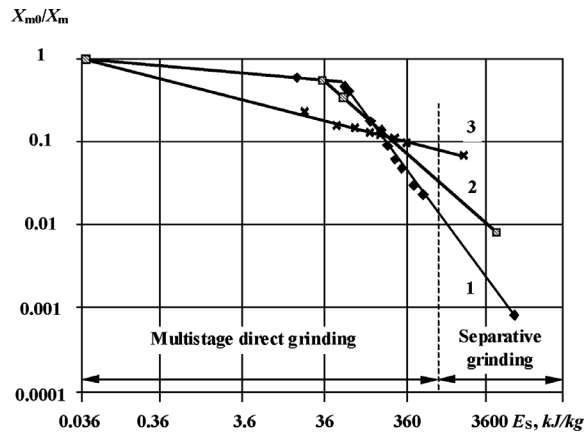
Table 7 Main characteristics of the ground stainless steel powder with granularity from 160 μm to 315 μm

Method*	Granularity		Morphology			
	Main fraction (70%) (μm)	d_m (μm)	Aspect AS		Roundness RN	
			Main	Mean	Main	Mean
PPP	+160–230	200	1–1.2	1.25	1.15–1.3	1.25
CSP	+180–260	220	1.1–1.4	1.35	1.35–1.8	1.7

*PPP: projections of powder particles.
CSP: cross-section polish.

Figure 15 illustrates the grindability of different steel chips, depending on the specific grinding energy (low specific energy is achieved by direct multi-stage grinding, higher specific energy by using the separative grinding system).

Figure 15 Dependence of the ratio of the medium size d_m of the ground product to the initial size d_{m0} material on the specific grinding energy E_s ; 1 -stainless steel AISI 316; 2 – ball-bearing steel 100Cr6; 3 – high speed steel HS 9-1-2-6



By low specific energy, as shown in Figure 15, High Speed Steel (HSS) achieves better refining than stainless and ball bearing steels, explained by higher plasticity of the latter. At higher specific energy of grinding, after the work hardening of the material, the rate of refining of the ball bearing and stainless steel chips increases, being higher than for the HSS. The intensity of grinding of the HSS chips depends linearly on the specific energy of grinding.

As a result of the X-ray investigations of the non-ground chips and of the ground product, the effect of work hardening of the particles caused by impact grinding was observed. Regarding crystal lattice parameters, the difference was approximately from 5% to 10%.

4.3 Production of ultrafine superalloy powders

The following metal powders as initial materials were used:

- Ni-based powder Alloy 59 (MBC Metal Powders Ltd.)
- Cr–Ni alloy powder Fukuda SX717 (Fukuda Metal Foil & Powder Co. Ltd.)
- Co-based powder Anval Ultimet (Carpenter Powder Products Ltd.).

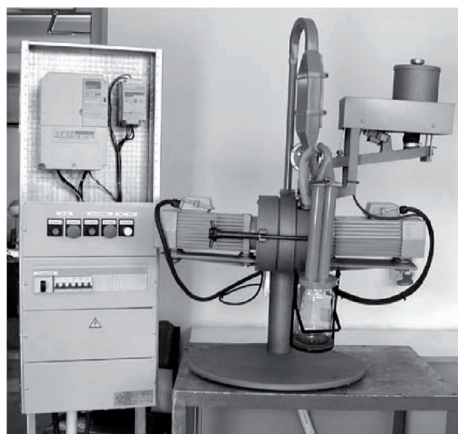
The chemical composition and the initial particle size of alloy powders used are given in Table 8.

Table 8 Selected metal powders and their composition

<i>Powder type</i>	<i>Chemical composition (wt. %)</i>	<i>Initial particle size (μm)</i>
Alloy	Ni- 23Cr-10Mo-1Fe-Mn-Si	45–150
Fukuda	Cr-42Ni-2.5Mo-1.0Si-0.5B	53–150
Ultimet	Co-26Cr-9Ni-5Mo-2W-0.8Mn-0.3Si-0.08N-0.06C	–45

To produce ultrafine powders with the particle size less than 5 μm, the disintegrator milling system DSL-175 with the inertial and centrifugal classifiers was used (Figure 16) (Kulu et al., 2002a). Powders were milled in a protective environment – argon.

Figure 16 Laboratory disintegrator milling system DSL-175 with the air classifier



Disintegrator milled ultrafine metallic powders were characterised by the following methods (Peetsalu et al., 2003):

- specific surface area measurement
- particle size analysis
- oxygen content measurement.

Figure 17 shows the particle shape of the milled powders. Figure 18 and Table 9 present the particle size distribution and cumulative distribution functions (both in percentage by volume) determined by the laser particle size and image analysis. The results of granulometry studies of powders are given in Table 9.

Figure 17 SEM images of milled ultrafine powders: a, b – Alloy; c, d – Fukuda; e, f – Ultimet

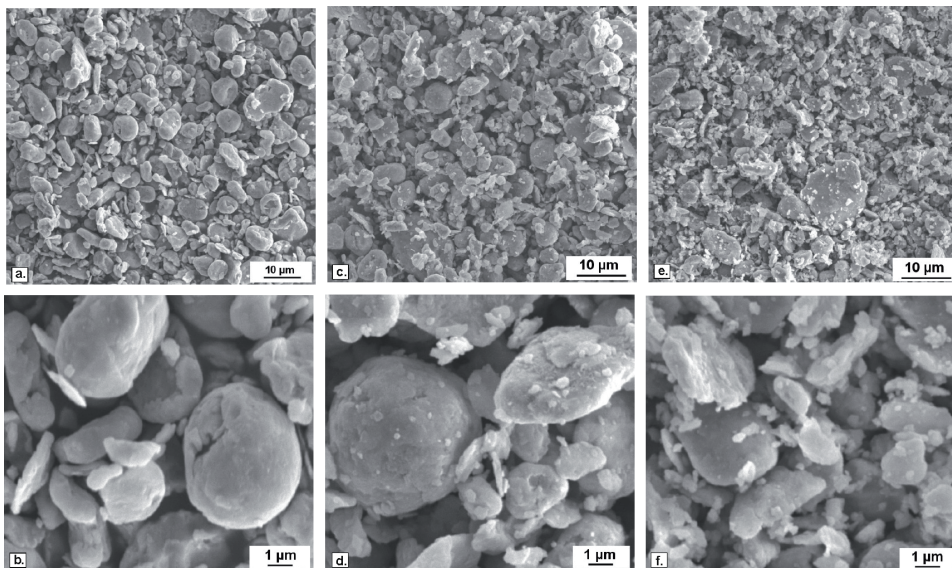
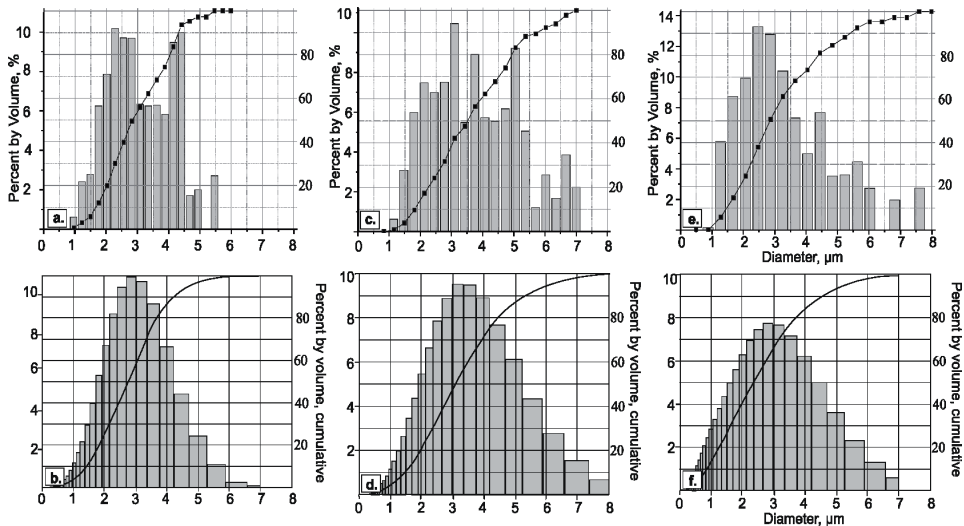


Table 9 Results of powder particle size measurements

<i>Powder type</i>	<i>Laser analysis (µm)</i>		<i>Image analysis (µm)</i>	
	d_m	d_{max}	d_m	d_{max}
Alloy	2.77	6.57	1.89	5.42
Fukuda	3.26	9.16	2.12	6.81
Ultimet	2.58	8.20	1.74	7.23

As it follows from Figure 17, the disintegrator milling of ductile materials produces coarser spherical and finer plate-form particle micropowders. According to the results presented in Figure 18, the image and laser diffraction analyses show similar results. The particles studied had the same particle size distribution (especially cumulative) and the largest particles did not exceed 8–10 µm.

Figure 18 Particle size distribution (a, c, e – laser analysis; b, d, f – image analysis) of powder particles: a, b – Alloy; c, d – Fukuda; e, f – Ultimet

To ascertain the influence of milling and powder particle size reduction on the oxygen content in the final product, the oxygen content was measured by the Leco analyser (Peetsalu et al., 2003). Regardless of milling in the protective environment, i.e., argon, owing to a very high specific area of the powder after milling, the oxygen content of the powder increased catastrophically both at milling and during its handling in the air. This is in direct correlation with the increase in the specific surface area of the powder (Table 10).

Table 10 Specific surface area and O₂ content of initial and milled powders

Powder type	Initial		After milling	
	Specific surface area (m ² /g)	O ₂ content (%)	Specific surface area (m ² /g)	O ₂ content (%)
Alloy	0.016	0.06	0.65 ¹ /2.6 ²	7.1
Fukuda	0.016	0.01	2.87 ¹ /2.4 ²	10.1
Ultimet	0.044	0.13	3.13 ¹ /3.4 ²	11.7

¹BET method.

²Laser granulometry.

To decrease the O₂ content, the annealing of powder in hydrogen at temperatures 650°C, 850°C and 1000°C were conducted. As it follows from Figure 19, the decrease in O₂ content was only 5–20% (maximum for Alloy powder).

The particle shape was characterised by their elongation – the aspect ratio *AS* (Mikli et al., 1999). Figure 20(a) shows the particle aspect distribution of the micropowders studied. Most of the powder particles had a relatively large elongation (mainly close to 2), which is normal in grinding of ductile materials by collision in the disintegrator mill. Alloy and Ultimet micropowder particles had practically the same shape parameter – the aspect *AS* distribution, while the Fukuda powder aspect was

slightly smaller. Figure 20(b) demonstrates the dependence of the aspect ratio AS on the mean diameter d_m of micropowder particles. As it follows from Figure 20(b), $d_m = 2\text{--}3\text{ }\mu\text{m}$ size particles are elongated to a greater extent. At the same time, the aspect AS had the second smaller local maximum values between the size interval $d_m = 5\text{--}6\text{ }\mu\text{m}$. It is probably caused by the nature of disintegrator milling of ductile materials. A rise in the elongation of larger particles was caused by particle deformation and by joining of smaller particles.

Figure 19 Results of oxygen measurements of milled powders

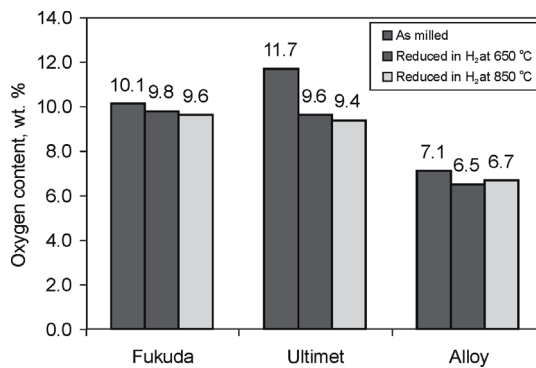
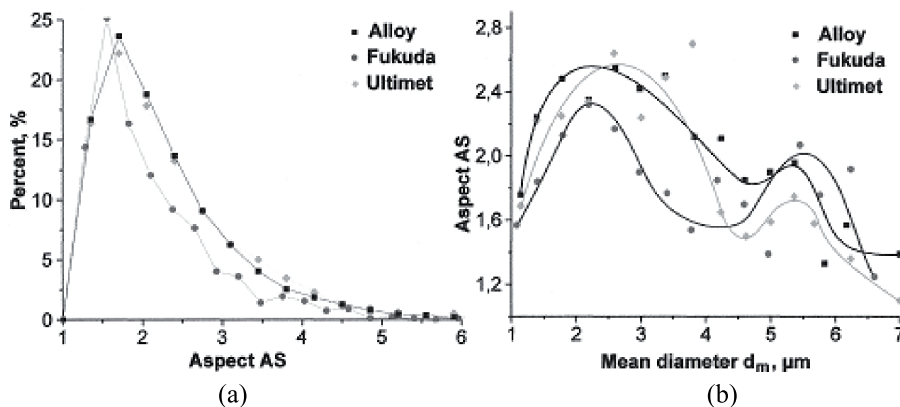


Figure 20 Particle shape factor – aspect AS distribution (a) and dependence of the aspect on the particle size (b)



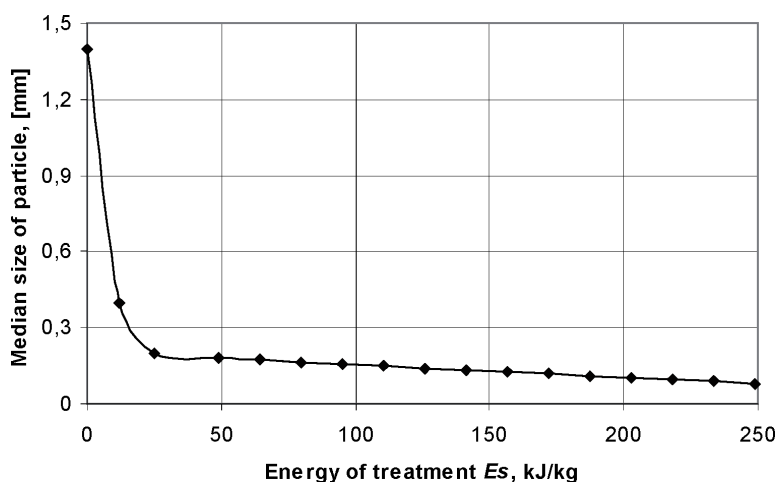
4.4 Retreatment of used hardmetal

To produce hardmetal powder, mechanical milling, one of the ways of retreatment of hardmetal wastes, was used. The technology of producing hardmetal powder was composed of (Kulu et al., 2002b, 2003):

- preliminary thermo-cyclical treatment and mechanical size reduction of worn hardmetal parts in a centrifugal-type pre-crusher DS-350
- intermediate milling in disintegrator DESI
- final milling of pretreated particles by collision in the disintegrator milling system DSL-175.

The preliminary size reduction of hardmetal parts in the disintegrator mill DS-350 and the following milling by DESI were carried out. Fine powder as a final product, with the particle size less than 500 μm , suitable for thermal spray and fusion, was one object of the study; coarse powder with particles more than 1 and less than 2.5 mm was taken as initial powder for subsequent final milling. As it follows from the metallographic studies, the particles were primarily equiaxed. To produce a powder with particles less than 100 μm , final milling was carried out by the laboratory disintegrator milling system DSL-175. The particle size was determined by the sieving analysis. The grindability curve of hardmetal powder with the initial maximum particle size of about 1.5 mm is shown in Figure 21. As it follows from the metallographic studies, the particle shape of multi-milled powder was mainly isometric.

Figure 21 Dependence of the final product – hardmetal powder particle size on the specific energy of milling



Based on the study of grindability and the fracture mechanism of a hardmetal as an example of a brittle composite material, we can state that hardmetal milling takes place as a result of direct fracture. To study the size and shape characteristics of powder particles depending on milling cycles in DSL-175, the 1x, 2x, 4x, 8x, 16x and 32x milled powder was considered.

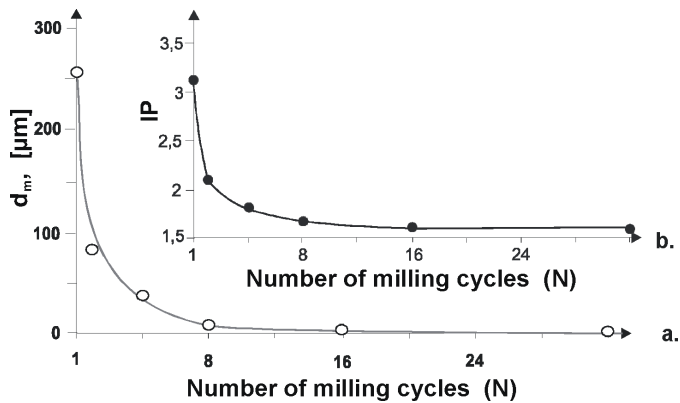
To describe the particles size and shape (irregularity), the image analysis method was used. The angularity of powder particles was described by angularity parameter SPQ, developed by Stachowiak (2000). Table 11 shows the results of granularity and morphology studies of disintegrator milled WC-Co hardmetal powders.

As it follows from Table 11 and Figure 22, the particle shape depends on the duration of milling: with an increase in time, larger sized particle shape approaches spherical with a smooth surface.

Table 11 Particle size and shape parameters of disintegrated WC-Co powder (for *IP* and *SPQ* calculation, only coarser fraction was used)

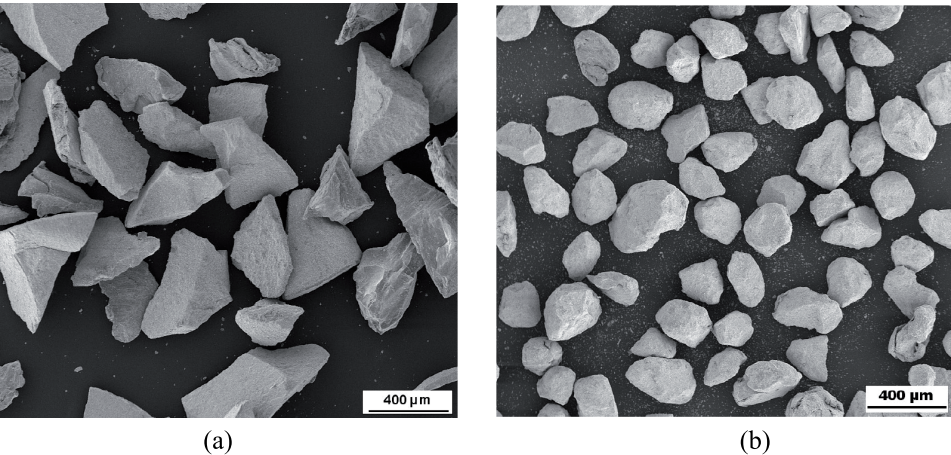
Particle size and shape parameters	Multiplicity of treatment					
	1x	2x	4x	8x	16x	32x
Mean diameter d_m (μm)	257.5	83.4	36.6	9.1	2.5	2.0
Median diameter d_{50} (μm)	561	209	144	88	57	30
Irregularity parameter <i>IP</i>	3.67	2.28	1.63	1.86	1.53	1.6
Angularity parameter <i>SPQ</i>	0.70	0.55	0.5	–	0.25	–

Figure 22 Dependence of (a) particle mean diameter d_m and (b) particle shape parameter *IP* on the multiplicity of milling by image analysis



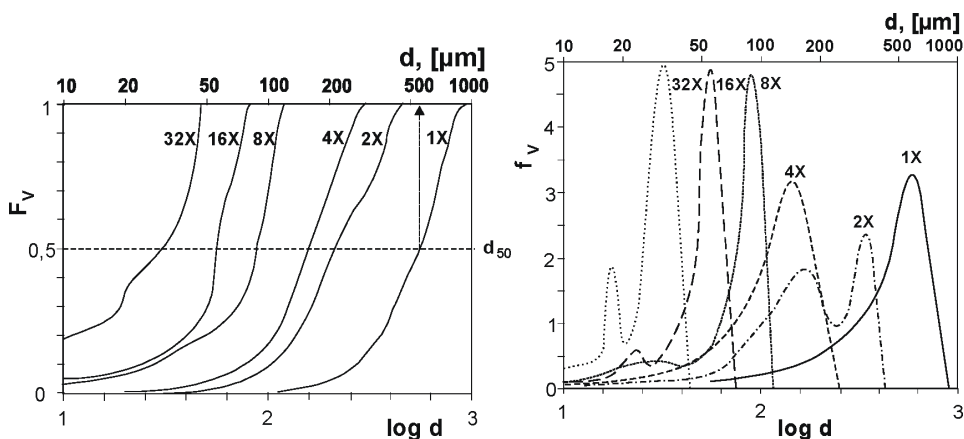
The SEM images of hardmetal powder particles after preliminary milling in DESI (Figure 23(a)) followed by eight times treatment in DSL-175 (Figure 23(b)) show the observable difference in the particle shape, respectively.

Figure 23 SEM images of investigated (WC-Co) hardmetal powders: (a) milled in DESI and (b) milled in DSL-175



To describe the granularity of hardmetal powder, the cumulative volume distribution function F_V and the volume density function f_V were calculated as well (Mikli et al., 2001, 2002). Figure 24(a) presents the cumulative distribution function F_V obtained by image analysis. An increase in the number of milling cycles causes the F_V curve shift to the left (in the direction of smaller particles). At the same time, the left side of the curve shifts up. It means that the currently used system did not distinguish smaller particles and F_V could be used as an indicator of the accuracy of the analysis. For instance, in the case of 32x milled powder, 20% of particles are smaller than $d = 10 \mu\text{m}$ ($\log d = 1$, Figure 24(a)). The median diameter d_{50} calculated from the experimental cumulative distribution functions (Figure 24(a)) is presented in Table 11. As it is seen from the image analysis data in Table 11, d_m is two to three times smaller than d_{50} owing to the different nature of descriptors (d_m — linear descriptor; d_{50} — volume descriptor). The probability density function f_V of the particle volume is calculated using the data obtained from the image analysis. The results are shown in Figure 24(b). The f_V curve of 2x milled powder has two maximum (at ca $150 \mu\text{m}$ and $350 \mu\text{m}$).

Figure 24 Cumulative distribution functions of particles volume F_V (a) and the probability density function of particles volume f_V of image analysis at different multiplicity of milling



5 Application of produced metallic powders

The powders produced by disintegrator milling can be used for different applications.

Metal powders produced by disintegrator milling of metal chips can be used as a powdered material at shot peening as well as a raw material in powder technology.

The coarse cast iron powder (from 0.3 mm to 0.6 mm) can be used as a grit for surface treatment by grit blasting before spraying of coatings.

The hardmetal powders, manufactured through single and multiple milling processes, which resulted in powder particles with different shape (angular and round), were used for the production of composite powder coatings by the following thermal spray technologies:

- flame spray and fusion of powder composite 25wt.%(WC-Co) + 75wt.%NiCrSiB self-fluxing powder (Zimakov et al., 2003)
- detonation gun spraying of the composite powder 85wt.%(WC-Co) + 15wt.%Co (Kulu and Zimakov, 2000)
- high-velocity oxy-fuel spraying of the composite powder 85wt.%(WC-Co) + 15wt.%Co (Zimakov et al., 2003).

The hardmetal powders sharp-edged in form can be used as abrasive material in abrasive tools.

The ultrafine superalloyed metal powders produced by disintegrator milling were used as a binder metal for the production of composite spray powders with higher corrosion resistance (Kulu et al., 2002b).

6 Conclusions

- Different disintegrator systems have been developed and kinetic parameters of the frequently used disintegrators for materials treatment have been studied. The results of disintegrator grinding of metal chips, used hardmetals and superalloy materials have been presented.
- The developed disintegrator milling system with a centrifugal classifier of high separative sensitivity enables to reduce the size of metallic micropowders to below 5 μm .
- Based on our theoretical model for size reduction of ductile materials by collision, a possibility of ultrafine powder production from nickel and cobalt – based alloys was ascertained.
- Based on the grindability study of metal chips and used hardmetals, the feasibility of disintegrator milling technology for utilising industrial metal wastes has been shown.
- The fracture of particles at collision and refining of the product to be ground can occur in one of the ways:
 - direct fracture as the result of intensive stress waves originated from high velocity collisions (in case of brittle materials, such as cast iron and hardmetals, this mechanism is dominant)
 - low fatigue fracture as a result of numerous local plastic deformations owing to collisions is dominant for ductile materials, such as stainless steel.
- The shape of the particles of brittle materials treated by collision approaches the isometric form and that of ductile materials approaches the spherical or sponge form. As a result, the bulk density and flowability of metal powder increases.
- Owing to high velocities and high stresses during grinding, an additional effect of mechanical activation of the ground material is observed, which influences the end product in two ways, deteriorating the compactedness of powders and activating the diffusion in the technological processes.

References

- Goljandin, D., Kulu, P. and Peetsalu, P. (2002) 'Ultrafine metal powders produced by grinding from the industrial wastes', *Proc. TMS2002 Extraction and Processing Division Meeting on Recycling and Waste Treatment in Mineral and Metal Processing: Technical and Economical Aspects*, Vol. 1, pp.277–284.
- Kulu, P. and Zimakov, S. (2000) 'Wear resistance of thermal sprayed coatings on the base of recycled hardmetal', *Surface and Coatings Technology*, Vol. 130, pp.46–51.
- Kulu, P., Käerdi, H. and Mikli, V. (2002a) 'Retreatment of used hardmetals', *Proc. TMS'2002, Recycling and Waste Treatment in Mineral Processing: Technical and Economic Aspects*, Lulea, pp.139–146.
- Kulu, P., Mikli, V., Käerdi, H. and Besterce, M. (2003) 'Characterization of disintegrator milled hardmetal powder', *Powder Metallurgy Progress*, Vol. 3, No. 1, pp.39–48.
- Kulu, P., Zimakov, S., Goljandin, D. and Peetsalu, P. (2002b) 'Novel thermal spray powders for corrosion and wear resistant coatings', *Materials Science (Medžiagotyra)*, Vol. 8, No. 4, pp.409–412.
- Mikli, V., Kulu, P. and Käerdi, H. (2001) 'Application of image analysis methods to characterize the impact-milled WC-Co powder particles', *Image Analysis Stereology*, Vol. 20, pp.199–204.
- Mikli, V., Kulu, P. and Käerdi, H. (2002) 'Angularity of the disintegrated ground hardmetal powder particles', *Materials Science (Medžiagotyra)*, Vol. 8, No. 4, pp.430–433.
- Mikli, V., Kulu, P., Zimakov, S. and Käerdi, H. (1999) 'Characterization of metallic powders produced by mechanical milling', *Materials Science (Medžiagotyra)*, Vol. 2, No. 9, pp.19–21.
- Peetsalu, P., Goljandin, D., Kulu, P., Mikli, V. and Käerdi, H. (2003) 'Micropowders produced by disintegrator milling', *Powder Metallurgy Progress*, Vol. 3, No. 2, pp.99–109.
- Philips, T.A. (1990) 'Recycling of Iron. Steel and Superalloys', *ASM Handbook*, Vol. 1, pp.1023–1033.
- Primer, J. (1965) *Untersuchungen zur Prallzerkleinerung von Einzelchen*, Dissertation. Technische Hochschule Karlsruhe.
- Rumpf, H. (1965) 'Die einzelkornzerkleinerung als grundlage einer technischen zerkleinerung', *Wissenschaft. Chemie-Ingenieur Technik*, Vol. 37, No. 3, pp.187–202.
- Stachowiak, G.W. (2000) 'Particle angularity and its relationship to abrasive and erosive wear', *Wear*, Vol. 241, pp.214–219.
- Tamm, B. and Tymanok, A. (1996) 'Impact grinding and disintegrator', *Proc. Estonian Acad. Sci. Eng.*, Vol. 2, No. 2, pp.209–223.
- Taptik, Y., Aydin, S. and Arslan, C. (1994) 'Metal recycling activities and its economics in developing countries. A case study', *Proc. 1994 Conference on the Recycling of Metals*, Amsterdam, pp.183–190.
- Tymanok et al. (1999) 'Metallic powders produced by mechanical methods', *Materials Science (Medžiagotyra)*, Vol. 2, No. 9, pp.3–7.
- Tymanok, A. and Kulu, P. (1999) 'Treatment of different materials by disintegrator systems', *Proc. Estonian Acad. Sci. Eng.*, Vol. 5, No. 3, pp.222–242.
- Tymanok, A., Kulu, P. and Goljandin, D. (1999a) 'Metal powders produced by disintegrator milling from the industrial wastes', *Proc. 4th ASM International Conference and Exhibition on the Recycling of Metals*, Vienna, pp.309–318.
- Tymanok, A., Kulu, P. and Goljandin, D. (1999b) 'Metallic powders produced by mechanical methods', *Materials Science (Medžiagotyra)*, Vol. 2, No. 9, pp.3–7.
- Tymanok, A., Kulu, P. and Goljandin, D. (1999c) 'Technology and equipment for producing of spheroidized metallic powders', *Proc. Joint Nordic Conference in Powder Technology*, Oslo, p.14.

- Tymanok, A., Kulu, P., Goljandin, D, Roštšin, S. (1997a) ‘Theoretical model for grinding by collision ductile metal chips into metal powder’, *Proc. 1st Intern. DAAAM Conf. on Industrial Engineering. Actual Activities*, Tallinn, pp.130–132.
- Tymanok, A., Kulu, P., Goljandin, D, Roštšin, S. (1997b) ‘Disintegrator as a machine for utilizing of metal chips to metal powder’, *Proc. III ASM Intern. Conf. and Exhibition. The Recycling of Metals*, Barcelona, pp.513–522.
- Tymanok, A., Kulu, P., Mikli, V. and Käerdi, H. (2000) ‘Technology and equipment for production of hardmetal powders from used hardmetal’, *Proc. 2nd International DAAAM Conference*, Tallinn, pp.197–200.
- Zimakov, S., Pihl, T., Kulu, P., Antonov, M. and Mikli, V. (2003) ‘Application of recycled hardmetal powder’, *Proc. Estonian Acad. Sci. Eng.*, Vol. 94, pp.304–316.
- Zimakov, S., Tarbe, R. and Kulu, P. (2002) ‘Thermally sprayed WC-Co hardmetal based coatings’, *Materials Science (Medžiagotyra)*, Vol. 8, No. 4, pp.409–412.

Publication II

Goljandin, D.; Kulu, P.; Käerdi, H.; Bruwier, A. (2005). Disintegrator as device for milling of mineral ores. *Materials Science (Medžiagotyra)*, 11(4), 398 - 402.
DOI: <http://dx.doi.org/10.5755/j01.ms.18.1.1348>

Disintegrator as Device for Milling of Mineral Ores

Dmitri GOLJANDIN^{1*}, Priit KULU¹, Helmo KÄERDI², Alex BRUWIER³

¹Department of Materials Engineering, Tallinn University of Technology, Ehitajate tee 5, 19086 Tallinn, Estonia

²Department of Mathematics, Estonian National Public Service Academy, Kase 61, 12012 Tallinn, Estonia

³Slegten S.A., Belgium

Received 08 June 2005; accepted 07 July 2005

One of the predominant technologies in mining, in the production of minerals, and in materials treatment is grinding and the ball mills mainly used. Grinding by collision is more effective method for refining of brittle material and one of the few machines for material grinding by collision is disintegrator. This type of grinding implemented in twin-rotored machines is characterized with high productivity but at the same time with the heightened demands to the grinding media – to the materials of grinding elements and linings. The aims of this investigation were (1) to study the grindability of different mineral materials using milling by collision in disintegrator and (2) evaluate the erosion wear resistance of steels as grinding media for mineral materials milling. Grindability of different mineral materials (limestone, sandstone, basalt, gold ores, chromite etc) was studied. The abrasivity of materials was found and relative erosion wear resistance of steel Hardox 600 in the stream of above mentioned materials as abrasives was determined.

Keywords: mineral ores, grindability, disintegrator milling, abrasive erosion, wear resistance of steels.

1. INTRODUCTION

One of the predominant technologies in mining, in the production of minerals, and in materials treatment is grinding. Due to the increasing scales of mining operations the large diameter ball mills are introduced. Much of the research was directed towards modifying existing materials and selected variations of high manganese steel [1]. Because of its ability to withstand the severe impact conditions such as those experienced in the large ball mills, the high manganese steel became the focus of many of the early investigations [2]. In such kind of comminution machines as ball mills, a particle remains between the two grinding bodies (balls) and is broken by shifting. The maximum generated stresses σ that occur in particle are locally equal or exceed the strength of the material [3].

Grinding by collision is a more effective method for refining of brittle material. One of the few machines for material grinding by collision is a disintegrator [4]. The value of the stresses generated in a material to be ground exceeds the strength of the material about ten times and the particles fall into pieces [3].

This type of grinding implemented in twin-rotored machines is characterized by high productivity, but at the same time with the heightened demands to the grinding media – to the materials of grinding elements and linings due to the high impact velocities and abrasivity of materials to be treated [5]. As it was shown in [6, 7], by treatment of very hard composite material as tungsten carbide based hardmetal contamination of ground product – ultrafine hardmetal powder with iron from grinding media was surprisingly high (up to 15 %). From this point of view, both the grindability of the materials in a disintegrator and the wear performance of grinding media are very important.

To predict the suitability of concrete materials and to find relative erosion resistance of them erosion theory has also been developed [8]. It is needed when the lifespan of some part is to be increased by replacing the material not used yet in similar conditions. So-called S-curves law and a diagram for evaluation of the “hardness value” were produced, depending on material type and the hardening method. To construct the curves in the axes $\varepsilon - H_m$ the data needed are wear rates of standard and studied materials against abrasive that is softer or equal than standard or studied materials and against abrasive that is those’s 1.6 times harder than it [8].

The aims of this investigation were (1) to study the grindability of different mineral materials using milling by collision in a disintegrator and (2) to predict the relative erosion wear resistance of steels as grinding media for mineral materials milling under conditions similar those to industry.

2. EXPERIMENTAL MATERIALS AND METHODS

To study the grindability of materials, different mineral materials (limestone, sandstone, basalt etc) were under study.

Milling experiments to assess the grindability of different mineral materials (Table 1) were conducted in semi-industrial disintegrator DSL-137 with rotor diameter 600 mm and rotation velocity 1500 rpm. The parameter of grinding – specific treatment energy E_s was used to estimate grindability [9].

For the abrasivity study of above mentioned mineral materials and different gold ores, the centrifugal accelerator CAK-4 was used. The velocity of abrasive particles was 80 m/s and impact angles – 30°, 60° and 90°. Milled mineral materials with particle size less 1 mm were used as abrasives. The types of mineral materials, gold ores and chromites as abrasives are given in Table 1 and Table 2.

*Corresponding author. Tel.: +372-620-3357; fax.: + 372-620-3196.
E-mail address: goljandin@email.ee (D. Goljandin)

Table 1. Characterization of mineral materials to be milled

No and type of mineral materials	Initial particle size, mm	Hardness HV0.2
1. Limestone (Engis)	+6.3-10 and +10-14	135 – 205
2. Sandstone (Trooz)	+6.3-10 and +10-14	140 – 205/250 – 280*
3. Polphyry (Voutre)	+6.3-10	560 – 880
4. Basalt (Cerf)	+6.3-10 and +10-14	560 – 840

*Dark phase in sandstone.

Table 2. Composition of selected mineral ores, wt%

No and type of ore	Quartz 2000 HV	Pyrite 1530 HV	Feldpars 1290 HV	Others
<i>Gold ores</i>				
5. Crown Mine (South Africa)	80	2.5	1.5	16
6. Waihi (Australia)	63	2.5	27	7.5
7. South Pipeline (USA)	51	–	8	41
8. KBGM (Australia)	30	1	35	24
9. Plutonic (Australia)	15	–	25	30 – Amphibole (946 HV) 30
<i>Chromite</i>				
10. CMI (South Africa)	1.1	–	4	82 – Chromite (1530 HV) 5.5 – Amphibole (946 HV) 7.4
11. Wonderkop (South Africa)	0.5	–	3	95 – Spinelle (725 HV) 1.5

Table 3. Chemical composition and hardness of the studied steels

Type of steel	Chemical composition, wt%	Hardness
St37	0.21 – 0.25 C; ≤0.055 P, S	140 – 150 HV30
Hardox 600	0.48 C; 0.70 Si; 1.00 Mn; 1.20 Cr; 2.50 Ni; 0.80 Mo	560 – 640 HBW*
Reference material C45	0.42 – 0.50 C; 0.50 – 0.80 Mn; ≤0.045 P and S	580 – 635 HV30
(normalized)		230 – 260 HV30

*by specification.

Wear tests to assess the erosion behaviour of the grinding media – steels St 37 and Hardox 600 were conducted in wear tester CAK-4 at the impact velocity $v = 80$ m/s and impact angles 30° and 90° . The selected abrasives (sandstone, glass and quartz) with particle size 0.1 – 0.3 mm were used. The chemical composition and hardness of steels is given in Table 3. Microhardness by Micromet 2001 of mineral materials and abrasives (Table 1) and Vickers hardness of studied steels (Table 3) were determined. Steel of 45 % C was adapted as a reference material.

The coefficient of abrasivity A of materials used in abrasive wear tests was determined by steel St37 (normalized, 140 – 150 HV).

$$A = I_g^{\text{mineral ore}} / I_g^{\text{quartz sand}}, \quad (1)$$

where I_g is the wear rate by weight, mg/kg

The wear resistance of the grinding media mostly influenced by the hardest components in the mixture and calculated/reduced hardness H' values of mineral materials (gold ores and chromites) were used in estimation of wear resistance.

$$H' = H_1 \cdot V_1 + H_2 \cdot V_2 + H_3 \cdot V_3 + \dots + H_n \cdot V_n = \sum_{i=1}^n H_i \cdot V_i, \quad (2)$$

where $H_1 \dots H_n$ are the hardness of the components of abrasive, $V_1 \dots V_n$ are the relative weight amounts of components in the mixture.

To construct curves $\varepsilon = f(H_a)$ for steels (soft and hard) used as the grinding media (mild steel St37 and hardened steel Hardox 600) sandstone as softer abrasive (140 – 205 HV), glass grit as medium abrasive (550 – 600 HV) and quartz sand as harder abrasive (1100 – 1200 HV) with similar particle size (0.1 – 0.3 mm) but different shape (Fig. 1) were used for tests.

3. RESULTS AND DISCUSSIONS

3.1. Grindability and abrasivity of mineral materials and ores

The results of grindability studies of mineral materials are given in Fig. 2.

As shown in Fig. 2, a sandstone and porphyry showed better grindability, the materials with higher hardness showed a decrease in the mean particle size after one step milling about 20 %, after twin milling about 50 % and more. The size reduction of limestone and basalt after first millings was less.

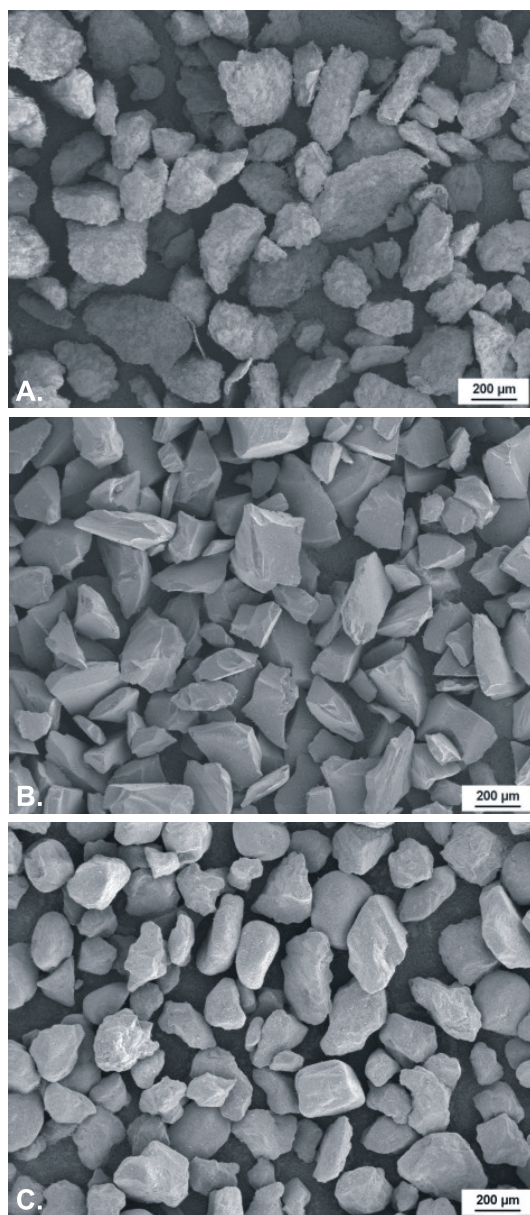


Fig. 1. SEM images of abrasives: A – sandstone; B – glass grit; C – quartz sand

At the same time results after multiple milling did not differ (limestone and porphyry after fifth milling).

Based on the abrasive wear studies the abrasivity of materials was found. It was demonstrated that no direct correlation between the hardness and abrasivity of materials to be tested exists (Table 4).

3.2. Wear resistance of the grinding media in mineral abrasives

The results of erosion tests of steel St37 with abrasives – ground mineral materials particles at impact velocity

80 m/s and impact angles 30°, 60° and 90° similar to industrial conditions are given in Fig. 3 and Fig. 4.

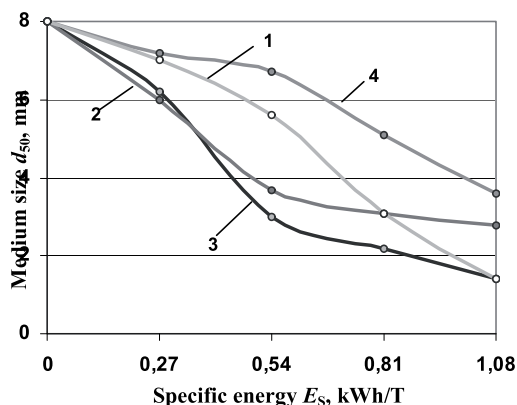


Fig. 2. Grindability curves of minerals: 1 – limestone; 2 – sandstone; 3 – porphyry; 4 – basalt

Table 4. Hardness and abrasivity of the studied mineral ores

Used abrasives and their No	Hardness	Coefficient of abrasivity A
Limestone (No. 1)	135 – 205*	0.30 – 0.36
Sandstone (No. 2)	140 – 205*	0.71 – 0.64
Porphyry (No. 3)	560 – 880*	0.59 – 0.48
Basalt (No. 4)	560 – 840*	0.43 – 0.33
<i>Cold ore</i>		
Crown Mine (No. 5)	1658**	1.00 – 0.94
Waihi (No. 6)	1647**	0.64 – 0.56
South Pipeline (No. 7)	1123**	0.51 – 0.41
KBGM (No. 8)	1067**	0.59 – 0.52
Plutonic (No. 9)	906**	0.46 – 0.32
<i>Chromite</i>		
CMI (No. 10)	1380	1.20 – 1.15
Wonderkop (No. 11)	775	0.85 – 0.75

*Vickers hardness measured with Micromet 2001 at the load 2 N (HV0.2).

**Calculated by Eq (2). The components with hardness ≥ 700 HV in the mixture were taken into consideration.

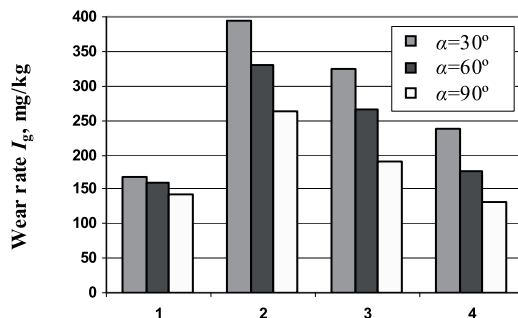


Fig. 3. Wear rate of steel St37 at different impact angles and in abrasives: 1 – limestone; 2 – sandstone; 3 – porphyry; 4 – basalt

As shown in Fig. 3, the wear rate by the studied four abrasives is not in correlation with the hardness of materials to be tested.

Higher wear rate by relatively soft sandstone can be explained by the existence of a harder component in the material and by the shape of abrasives particles – the particles of sandstone were more angular as compared with polphyry or basalt.

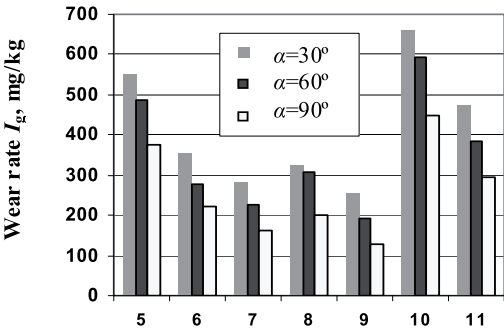


Fig. 4. Wear rate of steel St37 at different impact angles and in gold ore abrasives: 5 – Crown Mine; 6 – Waihi; 7 –South Pipeline; 8 – KBGM; 9 – Plutonic; 10 – CMI; 11 – Wonderkop

As shown in Fig. 4, the wear rate of steel St 37 in the stream of different abrasives is in good correlation with their hardness. With the increase of hardness, the wear rate is decreasing.

The influence of impact angle on wear rate by all abrasives studied was even – with the increase of the impact angle, the wear rate is decreasing. It is similar to steels as plastic materials. As compared with limestone, the wear resistance of sandstone is about 2.3 and 1.9 times higher at 30° and 90° respectively.

The wear rate and relative wear resistance in different mineral ores with hardness from 775 HV up to 1647 HV depends first on the composition of ores, on the amount of the hardest component – quartz (2000 HV) in mixture (see Table 2).

The wear rate is the highest by chromite (82 % in mixture is component with hardness 1530 HV), followed by gold ore – Crown Mine (main component – 80 % is quartz with hardness 2000 HV).

3.3. Prediction of relative erosion resistance of the grinding media

To evaluate the suitability of hardened steels as the grinding media and to have the wear curves $\varepsilon=f(H_a)$, the wear rates of standard material – soft steel St37 (140 – 150 HV30) in abrasives – in limestone (135 – 205 HV) and

Table 5. Wear rates of studied steels in soft and hard abrasives

Steel	HV30	Wear rate I_g , mg/kg					
		Milled sandstone		Glass grit		Quartz sand	
		$\alpha=30^\circ$	$\alpha=90^\circ$	$\alpha=30^\circ$	$\alpha=90^\circ$	$\alpha=30^\circ$	$\alpha=90^\circ$
St37	140 – 150	248.4	141.9	587.2	437.7		
Hardox 600	580 – 635			323.4	312.8	376.9	438.4

glass grit (550 – 600 HV) and wear rates of harder material – steel Hardox 600 (580 – 635 HV30) in abrasives – in glass grit and quartz sand (1100 – 1200 HV) were determined. The results of experiments are given in Table 5.

On the base of test results the $\varepsilon-H_a$ curves were constructed (Fig. 5).

As shown in Fig. 5, four defined zones exist: A – wear resistance is low; B – wear resistance increases; C – wear resistance decreases rapidly; D – wear resistance of Hardox is low. In interval B – C the use of Hardox is most favourable.

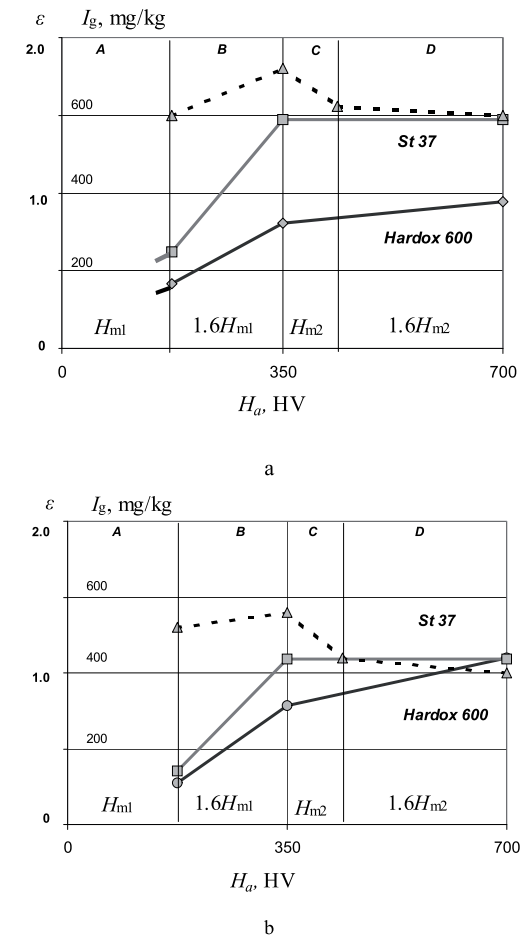


Fig. 5. Wear rate of steel St37 (M_1) and Hardox 600 (M_2) of respective hardness H_{m1} and H_{m2} versus abrasive hardness H_a . The dash line: dependence of relative wear resistance of ε on H_a : a – impact angle 30°; b – impact angle 90°

The comparative testing of soft and hardened steels as the grinding media in disintegrator type crushing devices demonstrated that hardened steels are not prospective in these application. With the material cost increasing the effect is low – the increase of life span of milling elements is minimal. It was confirmed by comparative testing of pins from different steels and different coatings [10, 11]. Relative wear resistance of steels and coatings in disintegrators by the milling of materials with hardness about 1000 HV and more is low.

4. CONCLUSIONS

1. The grindability of different mineral materials using milling by collision in disintegrator was studied and the influence of particle size reduction on specific energy of treatment was clarified.
2. The abrasivity of the milled minerals was found. It was demonstrated that there does not exist direct correlation between hardness and abrasivity of materials to be treated.
3. The experiments to evaluate the suitability of the hardened steels as the grinding media in disintegrator was carried out and it was demonstrated that hardened steels are not prospective in these application.

Acknowledgements

The authors are grateful to Slegten S. A. and Dr. Alex Bruwier for the support to this research.

REFERENCES

1. **Cherje, T. W., Simbi, D. J., Navara, E.,** Relationship between Microstructure, Hardness, Impact Toughness and Wear Performance of Selected Grinding Media for Mineral Ore Milling Operations *J. Materials and Design* 25 2004: pp. 11 – 18.
2. **Benjamin, D.,** Properties and Selection: Stainless Steels, Tool Materials and Special Purpose Metals. Metals Handbook, 9th edition, Vol. 3, ASM, p. 576.
3. **Tamm, B., Tymanok, A.** Impact Grinding and Disintegrators *Proc. Estonian Acad. Sci. Eng.* 2/2 1996: pp. 209 – 223.
4. **Tümanok, A., Kulu, P.** Treatment of Different Materials by Disintegrator Systems *Proc. Estonian Acad. Sci. Eng.* 5/3, 1999: pp. 222 – 242.
5. **Uuemõis, H., Piil, M.** Selection and Evaluation of Materials for Impact Crushers *Proc. of Tall. Univ. of Techn.* 478 1979: pp. 31 – 36 (in Russian).
6. **Kulu, P., Käerdi, H., Mikli, V.** Retreatment of Used Hardmetals *Proc. TMS 2002 Recycling and Waste Treatment in Mineral and Metal Processing: Technical and Economic Aspects* Sweden Vol. 1 2002: pp. 139 – 146.
7. **Zimakov, S., Pihl, T., Kulu, P., Antonov, M., Mikli, V.,** Applications of Recycled Hardmetal Powder *Proc. Estonian Acad. Sci. Eng.* 9/4 2003: pp. 304 – 316.
8. **Kleis, I., Uuemõis, H.** *Untersuchung des strahlverschleissmechanismus von Metallen Zeitschrift für Werkstofftechnik* Heft 7 1974: s. 381 – 389.
9. **Goljandin, D., Kulu, P., Peetsalu, P.** Ultrafine Metal Powder Produced by Grinding from the Industrial Wastes *Proc. TMS 2002 Recycling and Waste Treatment in Mineral and Metal Processing: Technical and Economic Aspects*, Sweden Vol. 1 2002: pp. 277 – 284.
10. **Kulu, P.** Wear Resistance of Powder Materials and Coatings, Tallinn, Valgus Publishers, 1988: 119 p. (in Russian).
11. **Kulu, P.** Selection of Powder Coatings for Extreme Wear Conditions *Advanced Engineering Materials* 4/6 2002: pp. 392 – 397.
12. **Kulu, P.** The Principles of Creation of Erosion Wear Resistant Powder Materials and Coatings *Doctoral Thesis*, Tallinn, 1989 (in Russian).

Publication III

Käerdi, H.; Goljandin, D.; Kulu, P.; Sarjas, H.; Mikli, V. (2013).
Characterization of Mechanically Milled Cermet Powders Produced by
Disintegrator Technology. Hussainova, I. (Toim.). *Key Engineering Materials
and Tribology (148 - 153)*. Trans Tech Publications Ltd.
DOI: [10.4028/www.scientific.net/KEM.527.148](https://doi.org/10.4028/www.scientific.net/KEM.527.148)

Characterization of Mechanically Milled Cermet Powders Produced by Disintegrator Technology

Helmo Käerdi^{1, a}, Dmitri Goljandin^{2, b}, Priit Kulu^{2, c}, Heikki Sarjas^{2, d},
Valdek Mikli^{3, e}

¹ Chair of Engineering and Mathematics, Estonian Academy of Security Sciences, Kase 61, 12012 Tallinn, Estonia

² Department of Materials Engineering, Tallinn University of Technology, Ehitajate tee 5, 19086 Tallinn, Estonia

³ Centre for Materials Research, Tallinn University of Technology, Ehitajate tee 5, 19086 Tallinn, Estonia

^ahelmo.kaerdi@sisekaitse.ee (corresponding author), ^bdmitri.goljandin@ttu.ee, ^cpriit.kulu@ttu.ee, ^dheikki.sarjas@ttu.ee, ^evaldek.mikli@ttu.ee

Keywords: cermet, powder, grindability, angularity, morphology.

Abstract. The current paper deals with characterization of TiC-NiMo cermet powders produced by mechanical milling technology. TiC-based cermets scrap was processed by semi-industrial and laboratory disintegrator milling system. Chemical composition, shape and size of produced powders were analyzed. To estimate the properties of recycled cermet powders the sieving analysis, and angularity studies were conducted. The grindability was estimated using specific energy parameter (E_s). Considering that viewpoint, the study is focused on angularity studies as the shape of spray powder has considerable influence on spraying efficiency, the quality and reliability of the coating. To describe the angularity of milled powders, spike parameter – quadratic fit (SPQ) was used and experiments for determination of SPQ sensitivity and precision to characterize particles angularity were performed. Uncertainty of measurements demonstrated trustworthiness of results. The standard deviation of SPQ regardless of milling cycles is on the same order. For use of produced powders as reinforcements in sprayed coatings the technological parameters of powders were studied. Perspective future use of powders as reinforcements in composite coatings as well as abrasives in tooling were demonstrated.

Introduction

Thermal spray technologies are mainly used in areas where wear resistance as well as high temperature solutions are required [1,2]. However, high cost of feedstock materials [3], especially carbides, limits the use of Plasma Transferred Arc (PTA) and High Velocity Oxygen Fuel (HVOF) technologies in cost sensitive areas. At the same time, our natural resources are decreasing and recycling of materials becomes more important in order to save resources and still be competitive in the market. Therefore, the need for developing cheaper powder production methods and using of secondary materials is topical. However, there are not many low cost effective recycling technologies to produce powders from secondary materials [4]. Disintegrator technology is one of possible methods [5].

Today PTA welding and HVOF spraying have high demands for feedstock materials especially for particle morphology [6]. In order to assure efficient spraying and get good quality coating, particles should be homogenous, spherical and free of undesirable impurities.

The aim of this work was to investigate the processing of TiC-based cermet scrap and suitability of produced powders as a feedstock material for thermal spray. Disintegrator milling of TiC-NiMo cermet was conducted with grindability, particle size distribution and angularity analysis.

Experimental

Preliminary crushing of the used experimental armor plates was performed under a press-crusher up to particles size less than 5.6 mm. Final multi-step milling was carried out with centrifugal-type disintegrator.

Milling of materials by collision occurs as a result of fracture in a treated material. By particle collision to a wall (target, grinding body) from the point of contact, an intensive wave of pressure begins to propagate [7]. Values of stresses are higher than material strength. The material processing parameters in a disintegrator differ essentially from traditional milling methods and equipment (jaw crusher, mortar, hand-mill, quern, vibro-, and ballmill). TiC-NiMo cermet powder was produced by semi-industrial disintegrator DS-350. All together 16 milling cycles were performed and test samples for further particle size and morphology study was separated. Principal scheme of milling equipment – centrifugal-type disintegrator mill DS-350 is demonstrated in Fig. 1.

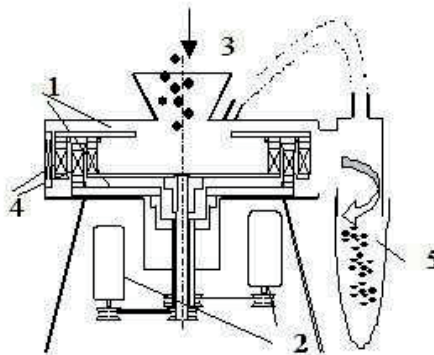


Fig. 1 Schematic representation of two-rotor disintegrator DS-350: 1 – rotors; 2 – electric drives; 3 – feed supply; 4 – grinding elements; 5 – output.

The main kinetic parameter in materials processing using disintegrator milling systems is the specific energy of treatment regarding the grinding effect and the economic aspect of the process. For grindability evaluation specific treatment energy E_s (kWh/ton) was used. Particle size by sieving was determined and size distribution was analyzed.

For angularity study of milled powders, spike parameter – quadratic fit (SPQ) [9,10] was described and experiments for determination of SPQ sensitivity and precision to characterize particles angularity were performed. In current study the trend of SPQ depending on milling cycles (1, 2, 3, 4, 5 and 16 times respectively) was under investigation. Images used for calculating SPQ were taken by SEM Zeiss EVO MA-15 and processed with Omnimet Image Analyser 22. The SPQ parameter takes into account only those spikes that protrude outside the circle centred on the particle's centroid and have an average radius. One of the advantages of SPQ is that it considers only the boundary protrusions that are likely to come in contact with the opposing surface [10]. The sides of the outside spike are represented by fitting quadratic polynomials. Differentiating the polynomials yields the apex angle Θ and the spike value $SV = \cos(\Theta/2)$. $SPQ = SV_{\text{mean}}$ are calculated as the mean SV over the all outside spikes.

Results and discussion

Grindability, as function of particles size d on the specific energy of treatment E_s was studied [8]. The results were documented after 1st, 2nd, 3rd, 4th, 5th and 16th cycle of treatment. It can be noticed that after the one – two milling cycles, the efficiency of milling decreases – particle size reduction stabilizes (Fig. 2). Apart from that, the assumption is that after reaching the “critical size” (100–150 μm), particles do not break into pieces anymore and are mainly rounded further on.

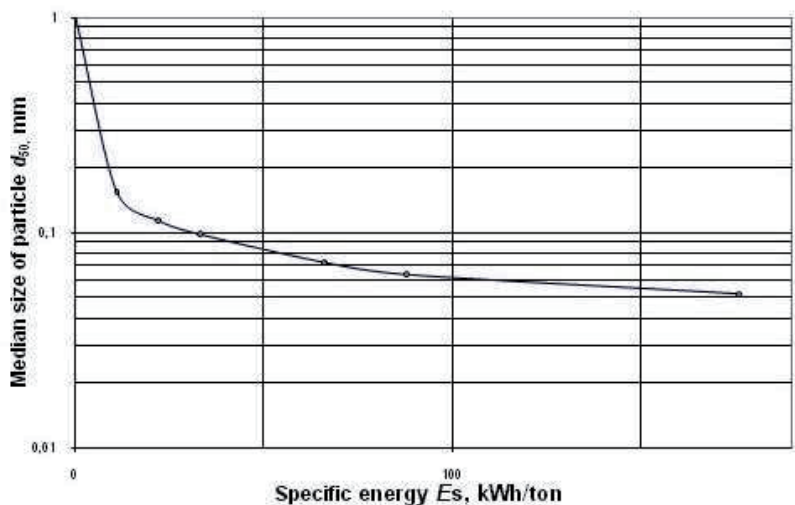


Fig. 2 Grindability curve – median particle size dependence on the specific energy E_s of TiC-NiMo powder.

Chemical composition analyses indicate that TiC-NiMo powders mainly consist of TiC carbide and Ni-Mo binder matrix (Table 1). Only a small amount of excessive iron was detected; to compare with WC-Co hardmetal powder, the iron content is about 3 times less, but comparable with Cr_3C_2 -Ni powders [11].

Table 1 Chemical composition of TiC-NiMo cermet powder

Type of powder	Composition, [wt %]				
	Carbide	Ni	Mo	Fe	W
TiC-NiMo	TiC-72.0	8.9	7.4	3.7	6

In Table 2, the results and calculations of angularity studies are shown. It can be noticed that all measurements expanded uncertainty with confidence level 0.95, has relatively the same value which constitutes 7–18% from total value of SPQ. Similarities between SPQ_{mean} and $\text{SPQ}_{\text{median}}$ indicate stability between measurements variational series.

Table 2 TiC-NiMo cermet powder particles angularity parameter at different milling cycles

Parameter	Number of milling cycles, N					
	1	2	3	4	5	16
$\text{SPQ}_{\text{mean}}^1$	0.619 ± 0.042	0.526 ± 0.056	0.416 ± 0.039	0.316 ± 0.047	0.366 ± 0.048	0.179 ± 0.032
$\text{SPQ}_{\text{median}}^2$	0.619	0.549	0.384	0.293	0.366	0.152
SD^3	0.145	0.192	0.134	0.156	0.154	0.101
n^4	46	46	46	43	39	39

¹ SPQ_{mean} – the mean value of the SPQ data set
² $\text{SPQ}_{\text{median}}$ – the median value of the SPQ data set
³ SD – standard deviation of SPQ data set
⁴ n – number of studied particles (data set size)

On Figure 3, dependence on SPQ_{mean} from milling cycles and uncertainties of measurements of TiC-NiMo powder particles is shown. Data are approximated by logarithmic trendline $\text{SPQ} = -0.162\ln(N) + 0.6079$. The coefficient of determination is $R^2 = 0.946$. It can be noticed that the angularity parameter change mechanism is linear on the first 3–4 milling cycles. After 16 milling cycles the SPQ_{mean} has decreased from 0.619 to 0.179 and particles are nearly spherical.

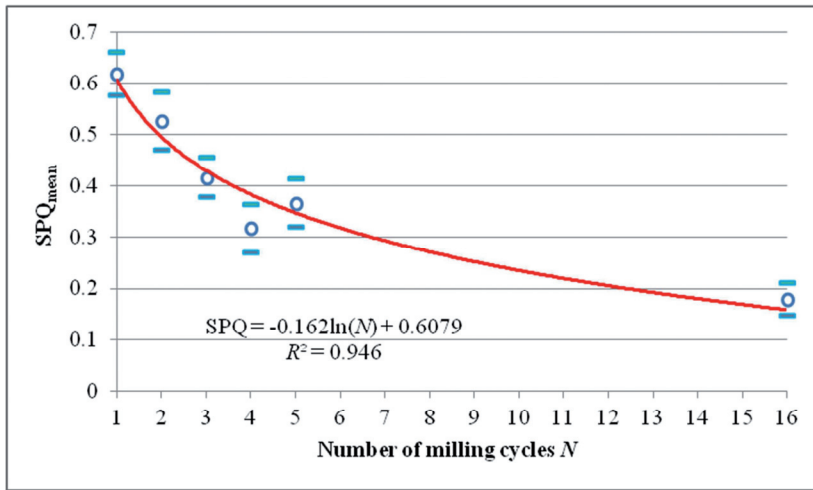
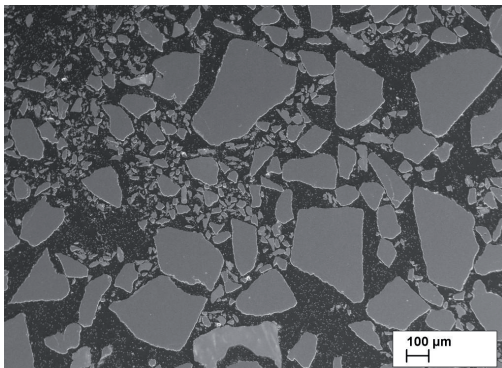
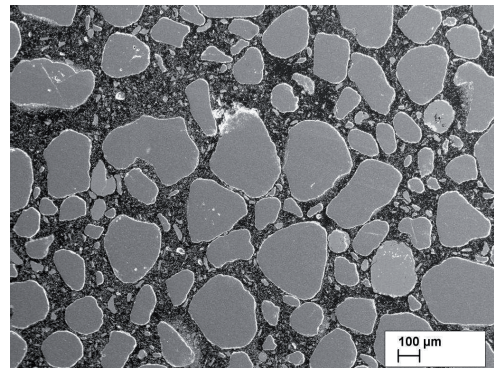


Fig. 3 Angularity parameter SPQ_{mean} dependence of TiC-NiMo powder particles on milling cycles.

Image analysis of powders confirmed the assumption made after milling – particles do not break into pieces, but are rounded during milling (Fig. 4a and b). After 16 milling cycles the shape of particles is nearly spherical.



(a)



(b)

Fig. 4 SEM images of TiC-NiMo powder particles after: a – 3 milling cycles, b – 16 milling cycles.

Close look-up of TiC-NiMo powder particles with some iron impurities (Fig. 5a) shows only few cracks in them, compared to Cr_2C_3 -Ni cermet powder particles (Fig. 5b), which are full of defects. This indicates to higher ductility of raw material used in experiment. Moreover, the possibility of deformation during high velocity spraying later is lower due to the absence of inter cracks compared to Cr_2C_3 -Ni powders and in comparison on spraying of composite powders, consisting of WC-Co hard particles [11].

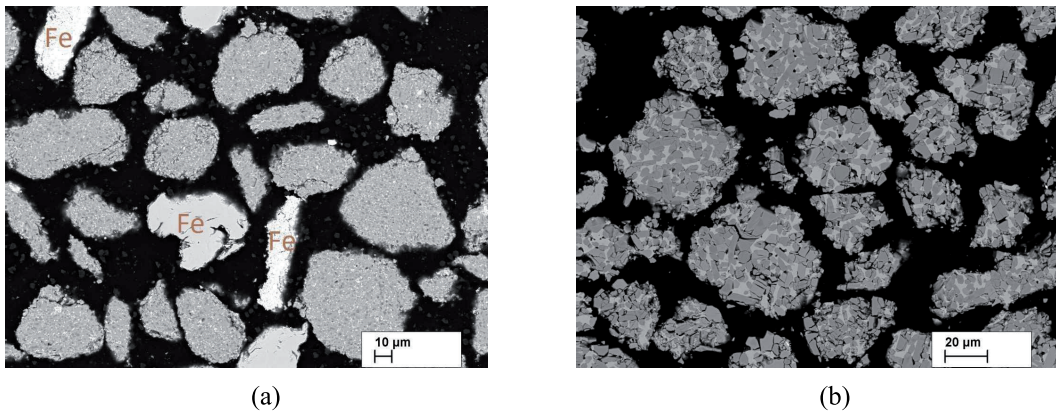


Fig. 5 Structure of powder particles with fraction of +50-35 µm after milling: a – TiC-NiMo, b – Cr₂C₃-Ni [11].

Conclusions

Experiments concerning the production of cermet powder from used TiC-based cermet parts using mechanical method – disintegrator technology is prospective. The following conclusions can be drawn from the study:

1. Grindability study of TiC-NiMo cermets demonstrated that they break into pieces during the first-second milling cycle only, later, rounding of particles takes place. Angularity parameter SPQ of TiC-NiMo powder particles reduces during the first 3–4 milling cycles almost linearly.
2. With 16 milling cycles near spherical shape of particles was achieved being positive in the point of following high velocity thermal spray.
3. Contamination of TiC-NiMo cermet powder produced in disintegrator with grinding media – mainly with iron is minimal. Grain defectivity of used powder particles is low.

Acknowledgement

The authors would like to express their gratitude to Sten Vinogradov from Tallinn University of Technology in his participation in powder milling. This research was supported by the Estonian Ministry of Education and Research (target-financed project SF 01400091s08).

References

- [1] D.J. Branagan, M.C. Marshall, B.E. Meacham, High toughness high hardness iron Based PTA Weld Materials. Materials Science and Engineering. A428, (2006) 116–123.
- [2] K.W.D. Hart, D.H. Harper, M.J. Gill, G.R. Heath, Case studies in wear resistance using HVOF, PTAW and spray fusion surfacing. Thermal Spray Surface Engineering via applied research, ASM International, Materials Park, (2000) 1117–1125.
- [3] K.O. Legg, B. Sartwell, Alternatives to functional hexavalent chromium coatings: HVOF thermal spray, Rowan Technology Group (2004).
- [4] T. Kojima, T. Shimizu, R. Sasai, H. Itoh, Recycling process of WC-Co cermets by hydrothermal treatment. Journal of Materials Science 40 (2005) 5167–5172.
- [5] P. Kulu, H. Käerdi, V. Mikli, The grindability of hardmetals, Proc. TMS 2002 Recycling and Waste Treatment in Mineral and Metal Processing: Technical and Economic Aspects. 1 (2002) 139–146.
- [6] Handbook of Thermal Spray Technology, ed., J.R. Davis, ASM International, 2004.

-
- [7] A. Tümanok, P. Kulu, Treatment of different materials by disintegrator systems, Proc. Estonian Acad. Sci. Eng. 5/3 (1999) 222–242.
 - [8] D. Goljandin, P. Kulu, P. Peetsalu, Ultrafine metal powder produced by grinding from the industrial wastes, Proc. TMS 2002 Recycling and Waste Treatment in Mineral and Metal Processing: Technical and Economic Aspects. 1 (2002) 277–284.
 - [9] G.B. Stachowiak, G.W. Stachowiak, J.M. Brandt, Ball-cratering abrasion tests with large abrasive particles, Elsevier. Tribology International. 39 (2006) 1–11.
 - [10] V. Mikli, P. Kulu, H. Käerdi and M. Besterçi, Angularity of the disintegrated ground hardmetal powder particles, Materials Science (Medžiagotyra). 8/4 (2002) 430–433.
 - [11] D. Goljandin, H. Sarjas, P. Kulu, H. Käerdi, V. Mikli, Metal-matrix hardmetal/cermet reinforced composite powders for thermal spray. Materials Science (Medžiagotyra). 18/1 (2012) 84–89.

Publication IV

Goljandin, D.; Sarjas, H.; Kulu, P.; Käerdi, H.; Mikli, V. (2012). Metal-Matrix Hardmetal/Cermet Reinforced Composite Powders for Thermal Spray.

Materials Science (Medžiagotyra), 18(1), 84 - 89.

DOI: <http://dx.doi.org/10.5755/j01.ms.18.1.1348>

Metal-Matrix Hardmetal/Cermet Reinforced Composite Powders for Thermal Spray

Dmitri GOLJANDIN^{1*}, Heikki SARJAS¹, Priit KULU¹, Helmo KÄERDI², Valdek MIKLI³

¹ Department of Materials Engineering, Tallinn University of Technology, Ehitajate tee 5, 19086 Tallinn, Estonia

² Chair of Engineering and Mathematics, Estonian Academy of Security Sciences, Kase 61, 12012 Tallinn, Estonia

³ Centre for Materials Research, Tallinn University of Technology, Ehitajate tee 5, 19086 Tallinn, Estonia

crossref <http://dx.doi.org/10.5755/j01.ms.18.1.1348>

Received 07 June 2011; accepted 05 September 2011

Recycling of materials is becoming increasingly important as industry response to public demands, that resources must be preserved and environment protected. To produce materials competitive in cost with primary product, secondary producers have to pursue new technologies and other innovations. For these purposes different recycling technologies for composite materials (oxidation, milling, remelting etc) are widely used. The current paper studies hardmetal/cermet powders produced by mechanical milling technology. The following composite materials were studied: Cr_3C_2 -Ni cermets and WC-Co hardmetal. Different disintegrator milling systems for production of powders with determined size and shape were used. Chemical composition of produced powders was analysed. To estimate the properties of recycled hardmetal/cermet powders, sieving analysis, laser granulometry and angularity study were conducted. To describe the angularity of milled powders, spike parameter–quadric fit (SPQ) was used and experiments for determination of SPQ sensitivity and precision to characterize particles angularity were performed. Images used for calculating SPQ were taken by SEM processed with Omnimet Image Analyser 22. The graphs of grindability and angularity were composed. Composite powders based on Fe- and Ni-self-fluxing alloys for thermal spray (plasma and HVOF) were produced. Technological properties of powders and properties of thermal sprayed coatings from studied powders were investigated. The properties of spray powders reinforced with recycled hardmetal and cermet particles as alternatives for cost-sensitive applications were demonstrated.

Keywords: grindability, angularity, recycling, hardmetal/cermet powders, morphology.

1. INTRODUCTION

Product lifetime is the main concern in the field of material engineering. High Velocity Oxygen Fuel (HVOF) spray coatings show significant reliability even in harsh conditions [1]. Recently, attention has been focused on reduced consumptions of existing resources and materials recycling due to increasing cost of primary materials during the last decade [2, 3].

From that point of view, recycling of materials is becoming more important in order to preserve natural resources, on the other hand industrial needs have to be considered. Thermal spray powders may involve considerable amount of all spraying process expenses.

However, utilization of industrial hardmetal scrap in metallurgical processes is often irrational [4]. One of the effective methods for producing those materials is grinding by collision [5]. Disintegrator technology allows to produce different hard and brittle materials.

One of the main limitations of using thermal spray coatings is the high cost of feedstock materials. Today use of iron based self-fluxing alloys is relatively limited compared with more expensive nickel, chromium or tungsten alloys. Hence, utilizing cheap iron based alloys reinforced with recycled hardmetal particles could be a rational alternative.

For producing high-quality powders and coatings, the shape and size of particles in production process must be

well controlled. Usually, spherical and homogenous powders with high flowability are preferred. The size of powder articles can be determined by image or sieving analyses. Another important parameter is morphology [6, 7] that can be characterized by description or quasi-quantitatively.

In this paper Disintegrator milling of Cr_3C_2 -Ni, WC-Co hardmetals was conducted with grindability, granulometry and angularity analysis. Composite powders based on iron and nickel based alloy reinforced with hardmetal/cermet particles were studied, powder granularity and technological properties were estimated before and after mixing.

2. EXPERIMENTAL

For material grinding by collision the disintegrators were used [8]. Refining of materials occurs as a result of fracture in a treated material. By particle collision to a wall (target, grinding body) from the point of contact, an intensive wave of pressure begins to propagate. Values of stresses are higher than material strength. The material processing parameters in a disintegrator differ essentially from traditional milling methods and equipment (jaw crusher, mortar, hand-mill, quern, vibro-, and ballmill). Recycled Cr_3C_2 -Ni and WC-Co powders were produced by experimental multi-functional disintegrators. Principal schemes of milling equipment – centrifugal-type disintegrator mill DSL-350 (a) and laboratory disintegrator milling system DSL-175 (b) are shown in Fig. 1.

*Corresponding author. Tel.: + 372-6203357; fax.: + 372-6203196.
E-mail address: goljandin@email.ee (D. Goljandin)

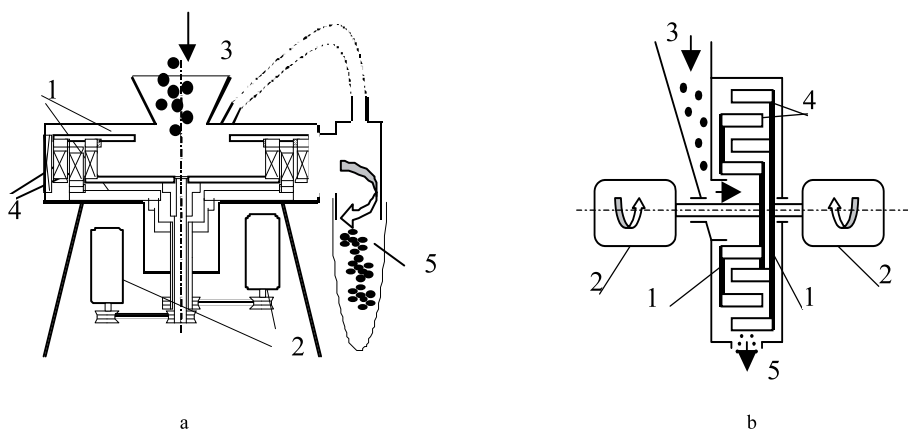


Fig. 1. Schematic representation of preliminary size reduction centrifugal-type mill DSL-350 (a) and vertical laboratory milling disintegrator DSL-175. Equipment (b): 1 – rotors; 2 – electric drives; 3 – material supply; 4 – grinding elements; 5 – output

The main kinetic parameter in materials processing using disintegrator milling systems is the specific energy of treatment regarding the grinding effect and the economic aspect of the process. Grindability, as function of particles size d on the specific energy of treatment E_S was studied in [9].

Determination of particle size distribution was carried out on vibratory sieve shaker Analysette 3 PRO for materials with particle size 12.5 mm – 0.025 mm and with a laser diffraction particle size Analysette 22 for powders finer than 300 μm was used.

For describing the angularity of milled powders, spike parameter – quadratic fit (SPQ) was described and experiments for determination of SPQ sensitivity and precision to characterise particles angularity were performed. Images used for calculating SPQ were taken by SEM Zeiss EVO MA-15 and processed with Omnimet Image Analyser 22. The parameter SPQ considers only those spikes that are outside the circle with equal particle centred over the particle centroid [10, 11]. The sides of the outside spike are represented by fitting quadratic polynomials. Differentiating the polynomials yields the apex angle θ and the spike value $SV = \cos(\theta/2)$. $SPQ = SV_{\text{mean}}$ are calculated as the mean SV over the all outside spikes.

Prior to spraying the composite powders were analysed to determine the cumulative particles distribution of composite powders and shape by SEM.

Table 1. Particle size and chemical composition of commercially produced powder

Type of powder	Particle size	Chemical composition, wt %					
		Ni	Fe	B	C	Si	Cr
FeCrSiB	–45+10	6	bal	3.4	2.1	2.7	13.7
iCrSiB	–53+15	bal	2.5	1.6	0.25	3.5	7.5
WC-CoCr	–45+15	WC – 86			Co – 10		4

In the current study composite spray powders consisting of 60 vol% of Fe-based self-fluxing alloy and 40 vol% of recycled hardmetal particles ($\text{Cr}_3\text{C}_2\text{-Ni}$;

WC-Co) were used. The properties of Fe-based self-fluxing alloy and other commercially produced powders used in comparative test are shown in Table 1. The technological properties (flowability and tap density) were determined. FeCrSiB and NiCrSiB powders were produced by Hoganas and had trade marks 6A and 1640-02 respectively. WC-CoCr 86/10/4 is a trademark of Tafa/Paxair.

From technological properties flowability of powders was studied. Hall flowmeter test was performed to determine the flowability of studied composite powders and to compare them with different commercially produced thermal spray powders. Flowability was calculated as time of 50 g of spray powder flowing through 2.5 mm hole in funnel according to standard EVS-EN ISO 4490:2008.

3. RESULTS AND DISCUSSION

Process of production of hard phase materials consisted of three steps:

- Preliminary crushing of the initial plate material (20×10×4) mm under a press-crusher up to particles size less than 5.6 mm;
- Intermediate direct multi-stage milling of the pre-crushed material down to 1.4 mm by the centrifugal-type disintegrator-mill DSL-350;
- Final multi-stage milling with particles size smaller than 50 μm was conducted with laboratory disintegrator system DSL-175.

The parameter of grinding – specific treatment energy E_S was used to estimate grindability. The results of the intermediate direct multi-stage milling of the pre-crushed material parts by the centrifugal-type disintegrator mill DSL-350 are shown in Fig. 2.

Fine powder as the final product, with particle size less than 50 μm , suits for thermal spray. Particle size of initial powder for subsequent milling was up to 1.4 mm. The grindability curves, acquired with laboratory disintegrator system DSL-175 of fine-milled powders are shown in Fig. 3. Due to higher brittleness of $\text{Cr}_3\text{C}_2\text{-Ni}$ based cermet

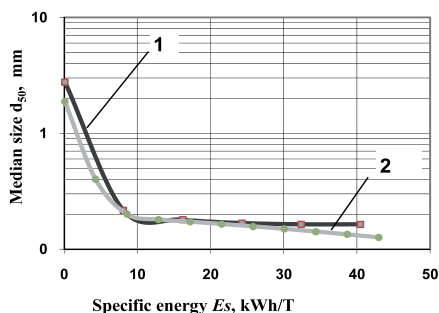


Fig. 2. Dependence of the hardmetal powder particle median size_{d50} on the specific energy of intermediate direct multi-stage milling. Grindability curves of materials: 1 – ($\text{Cr}_3\text{C}_2\text{-Ni}$); 2 – (WC-Co)

main size reduction takes place during the first 3–4 millings.

Particle shape depends on the duration of milling with increase in time. With longer milling time particles sphericity also increases (Fig. 4, a and b). At the same time, the angularity of fine particles, mainly the product of direct fracture, does not always decrease essentially.

Particles of $\text{Cr}_3\text{C}_2\text{-Ni}$ are more spherical and similar to each other than WC-Co . This can be explained by higher

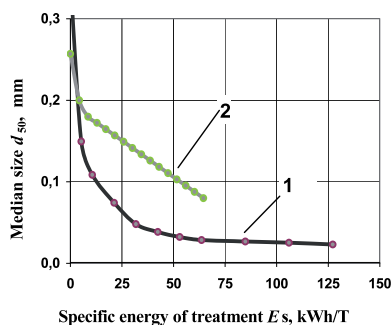
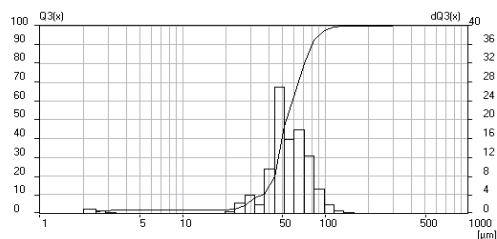


Fig. 3. Dependence of the median particle size_{d50} on the specific energy of final multi-stage milling. Grindability curves of materials: 1 – ($\text{Cr}_3\text{C}_2\text{-Ni}$); 2 – (WC-Co)

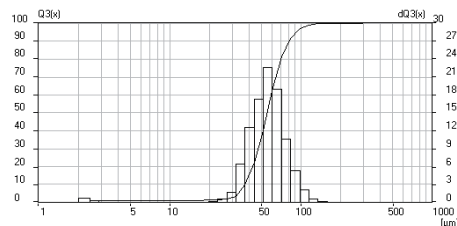
brittleness of WC-Co . Fig. 5, a and b, shows the particle size distribution of a ground product.

Chemical analysis of the recycled hardmetal powders for thermal spray by EDS showed that about 75 % of powders are carbides (WC-Co ; $\text{Cr}_3\text{C}_2\text{-Ni}$) (Table 2). Relatively high amount of iron in WC-Co powder has came from milling process (Table 2).

Powder particles in structure are typical of hardmetals: Co and Ni-based metal matrix (Fig. 5, a and b). Carbides grain size is mainly in range of $20\text{ }\mu\text{m} - 50\text{ }\mu\text{m}$.

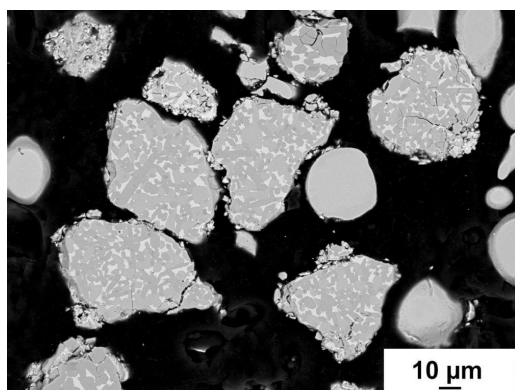


a

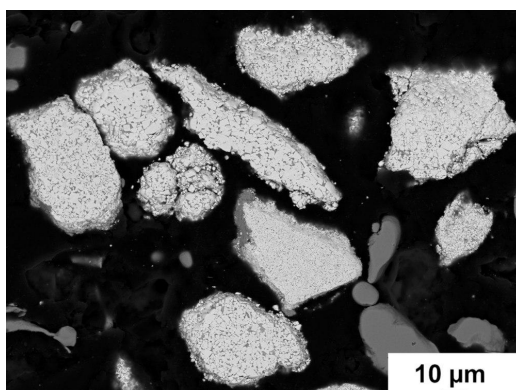


b

Fig. 4. Particle size distribution histograms and cumulative distribution functions a – ($\text{Cr}_3\text{C}_2\text{-Ni}$), b – (WC-Co)



a



b

Fig. 5. Morphology of ground product after final milling by laboratory disintegrator system DSL-17: a – ($\text{Cr}_3\text{C}_2\text{-Ni}$); b – (WC-Co)

Table 2. Chemical composition and particle size of recycled hardmetal/cermet powders

Type of Powder	Composition, wt %					Screen size, μm
	carbide	Co	Ni	Fe	W	
WC-Co	WC- 75.6	11,5		12,9		+20–50
Cr ₃ C ₂ -Ni	Cr ₃ C ₂ -78		14	3,1	2,5	+20–50

In Fig. 6 (a and b), the data of angularity studies are shown, where n is number of particles, ε expanded uncertainty of measurement [12] with confidence level 0.95 and s standard deviation of SPQ. Values of $\text{SPQ} = \text{SV}_{\text{mean}}$ and $\text{SV}_{\text{median}}$ are approximately the same.

The proximity of arithmetic mean and median shows relatively stable behaviour of measurements. The results (Fig. 6) show that angularity of recycled materials acts differently with decrease of particle size: SPQ of WC-Co is stable, while the SPQ of Cr₃C₂-Ni increases. For WC-Co the standard deviation of SPQ is practically the same in all particle sizes. For Cr₃C₂-Ni powders, the standard deviation of SPQ differs twice when particle size varies. However, the divergence of measurements is not significantly different. The confidence of measurements, which is described by expanded uncertainty ε and is on the order of 5 percent of the SPQ and can be considered at least satisfactory.

Flowability was tested on iron based self-fluxing alloy powders containing 40 vol% of recycled WC-Co and Cr₃C₂-Ni as reinforcement (Table 3).

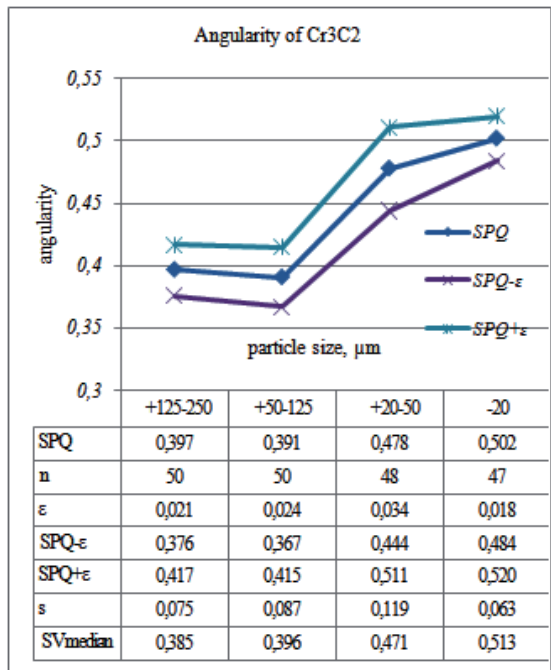
Table 3. Flowability of different spray powders

Composition of powder	Time, s	Flow, g/h
WC-CoCr	22.3	2.3
NiCrSiB	14.8	3.4
FeCrSiB	X	X
FeCrSiB+WC-Co	35.9	1.4
FeCrSiB +Cr ₃ C ₂ -Ni	38	1.3

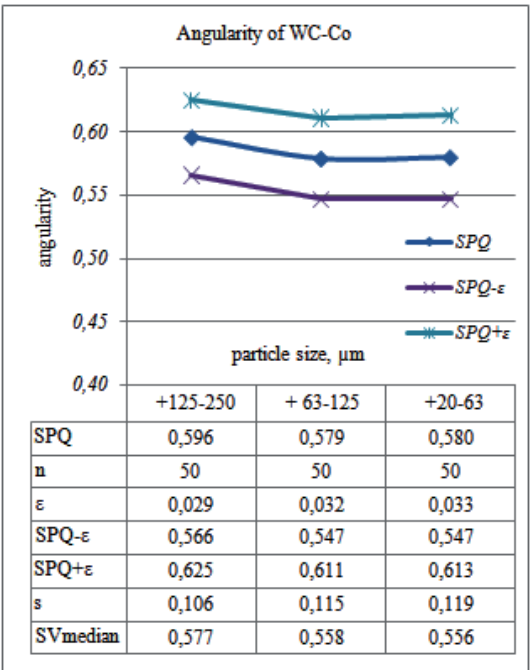
The results show that studied composite powders have significantly lower flowability than commercially produced (NiCrSiB and WC-CoCr) powders while tests with FeCrSiB self fluxing alloy were unsuccessful probably due to high occurrence of high magnetic forces in process.

SEM images of composite powders shown in Fig. 7 containing 40 vol% of hardmetal/cermet and 60 vol% of self-fluxing alloys were studied prior to spraying via granulometry and SEM once again to estimate the size and distribution of powders (Fig. 8, a–d). All particle size probability density function charts have one sharp maximum (mode) indicating homogenous distribution of powders size.

Powders based on Ni self-fluxing show slightly sharper maxima and narrower distribution than expected based on data in Table 1 and Table 2. Morphology study of those powders also demonstrated that there is more dust in iron based self-fluxing alloy based powders than Ni based self-fluxing alloy. SEM analysis also showed and

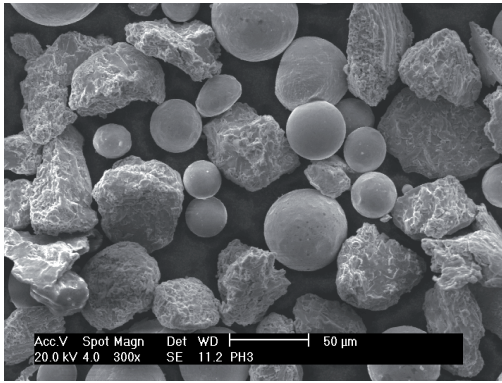


a

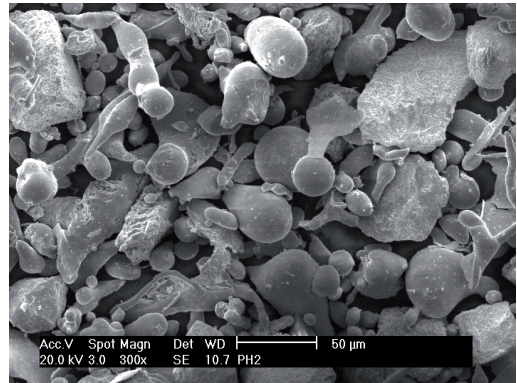


b

Fig. 6. Angularity integrals of milled powders a – (Cr₃C₂-Ni); b – (WC-Co)

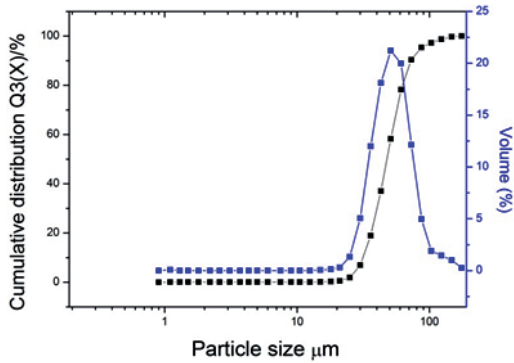


a

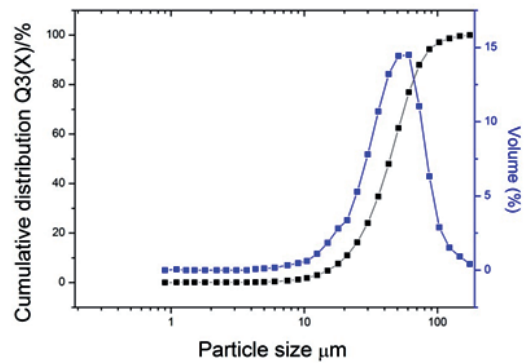


b

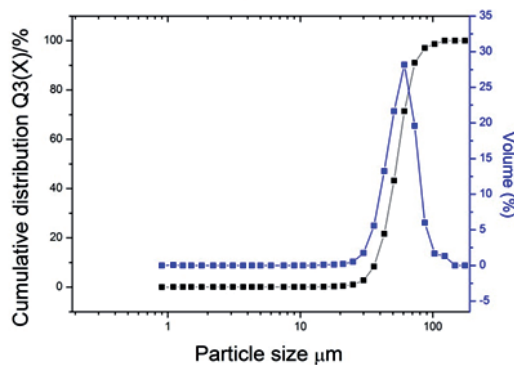
Fig. 7. Morphology of spray powders a – (WC-Co)-FeCrSiB, b – (Cr₃C₂-Ni)+NiCrSiB



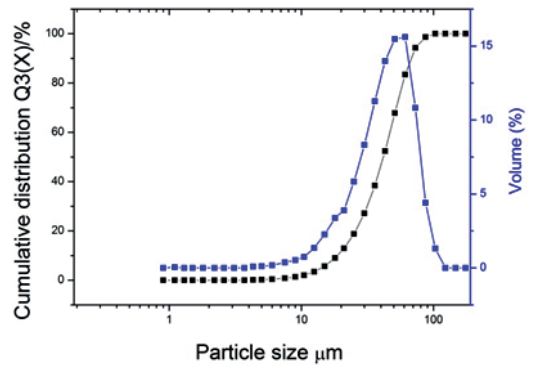
a



b



c



d

Fig. 8. Spray powders particle size probability density functions and cumulative distribution functions a – (WC-Co)+NiCrSiB, b – (WC-Co) FeCrSiB, c – (Cr₃C₂-Ni)+NiCrSiB, d – (Cr₃C₂-Ni)+FeCrSiB

confirmed that the angularity of WC-Co particles is higher than the ones of Cr₃C₂-Ni, which can be seen on Fig. 7, a and b.

According to the results of the study composite powders have significantly lower flowability due to more

angular shape of hardphase particles than commercially produced (NiCrSiB and WC-CoCr) powders while tests with FeCrSiB self fluxing alloy were unsuccessful probably to due high occurrence of high magnetic forces in process.

4. CONCLUSIONS

1. The grindability of hardmetal/cermet using milling by collision in disintegrator was studied and the influence of particle size reduction on specific energy of treatment was clarified.
2. The technology of producing hardmetal/cermet powders from used (recycled) hardmetal consisted of preliminary crushing and mechanical size reduction of hardmetal parts and final milling of pretreated product by collision in the disintegrator mill. The dependence of grindability (decrease in particle size) on the specific energy of treatment was studied. Hardmetal powders production with a predicted particle size is available.
3. Angularity parameter SPQ of recycled materials acts differently with decrease of particle size: SPQ of WC-Co is stable, while the SPQ of Cr₃C₂-Ni increases. The divergence of measurements is not significantly different and the confidence of measurements, which is on the order of 5 percent of the SPQ, can be considered at least satisfactory.
4. The size probability density functions of composite powders based on self-fluxing alloys reinforced with hardmetal/cermet particles are narrow and showed sharp maximum values that indicate a small variance of particle size.

Acknowledgments

The authors of the article would like to express their gratitude to Petri Vuoristo from Tampere University of Technology.

This research was supported by the European Social Fund's Doctoral Studies and Internationalisation Programme DoRa and Estonian Ministry of Education and Research (target-financed project SF 01400091s08).

REFERENCES

1. **Kulu, P., Zimakov, S., Goljandin, D., Peetsalu, P.** Novel Thermal Spray Powders for Corrosion and Wear Resistant Coatings *Materials Science (Medžiagotyra)* 8 (4) 2002: pp. 409–412.
2. **Shedd, K. B.** Tungsten Recycling in the United States in 2000. U.S. Geological Survey, Reston, Virginia, 2005. <http://pubs.usgs.gov/of/2005/1028/2005-1028.pdf> (15.05.2011).
3. **Shedd, K. B.** 2008 Minerals Yearbook, Tungsten [advance release]. U.S. Geological Survey, July 2010. <http://minerals.usgs.gov/minerals/pubs/commodity/tungsten/myb1-2008-tungs.pdf> (15.05.2011).
4. **Tymanok, A., Kulu, P.** Treatment of Different Materials by Disintegrator Systems *Proceedings of the Estonian Academy of Sciences Engineering* 5 (3) 1999 pp. 222–242.
5. **Goljandin, D., Kulu, P., Käerdi, H., Bruwier, A.** Disintegrator as Device for Milling of Mineral Ores *Materials Science (Medžiagotyra)* 11 (4) 2005: pp. 398–402.
6. **Mikli, V., Käerdi, H., Kulu, P., Besteri, M.** Characterization of Powder Particle Morphology *Proceedings of the Estonian Academy of Sciences Engineering* 7 2001: pp. 22–34.
7. **Kulu, P., Tymanok, A., Mikli, V., Käerdi, H., Kohutek, I., Besteri, M.** Possibilities of Evaluation of Powder Particle Granulometry and Morphology by Images Analysis *Proceedings of the Estonian Academy of Sciences Engineering* 4 1998: pp. 3–17.
8. **Tamm, B., Tümanok, A.** Impact Grinding and Disintegrators *Proceedings of the Estonian Academy of Sciences Engineering* 2 (2) 1996: pp. 209–223.
9. **Goljandin, D., Kulu, P., Peetsalu, P.** Ultrafine Metal Powder Produced by Grinding from the Industrial Wastes, *Proceedings of TMS 2002 Recycling and Waste Treatment in Mineral and Metal Processing: Technical and Economic Aspects* Sweden 1 2002: pp. 277–284.
10. **Mikli, V., Kulu, P., Käerdi, H., Besteri, M.** Angularity of the Disintegrated Ground Hardmetal Powder Particles *Materials Science (Medžiagotyra)* 8 (4) 2002: pp. 430–433.
11. **Stachowiak, G. B., Stachowiak, G. W.** The Effects of Particle Characteristics on Three-body Abrasive Wear *Wear* 249 2001: pp. 201–207.
12. **Laaneots, R., Mathiesen, O.** An Introduction to Metrology. Tallinn University of Technology Press, 2006.

Presented at the 20th International Conference "Materials Engineering '2011" (Kaunas, Lithuania, October 27–28, 2011)

Publication V

Kers, J., Kulu, P., Goljandin, D., Kaasik, M., Ventsel, T., Vilsaar, K., Mikli, V. (2008). Recycling of Electronic Wastes by Disintegrator Mills and Study of Separation Technique of Different Materials. *Materials Science (Medžiagotyra)*, 14(4), 296 - 300.

Recycling of Electronic Wastes by Disintegrator Mills and Study of the Separation Technique of Different Materials

Jaan KERS^{1*}, Priit KULU¹, Dmitri GOLJANDIN¹, Martin KAASIK¹,
Teet VENTSEL¹, Kristiina VILSAAR¹, Valdek MIKLI²

¹Department of Materials Engineering, Tallinn University of Technology, Ehitajate tee 5, 19086 Tallinn, Estonia

²Centre for Materials Research, Tallinn University of Technology, Ehitajate tee 5, 19086 Tallinn, Estonia

Received 05 June 2008; accepted 30 September 2008

The aim of this work was to study and develop the prospective method and technique for mechanical recycling of printed circuit boards (PCBs). This study describes mechanical reprocessing of PCBs in high-energy disintegrator mills in the direct and selective milling systems. The ferrous metal particles and plastic particles with non-ferrous metal particles were roughly separated by a magnetic separation technique. Several tests were made for air classification of plastic and non-ferrous metal particles. The particle size and distribution were examined by the sieve analysis and laser granulometry analysis (max 300 µm). The chemical composition of the PCB powders was studied by means of the energy dispersive X-ray microanalysis (EDS) with the Link Analytical AN10000 system. The X-ray mapping technique was used to evaluate element distribution inside the powder particles.

Keywords: recycling, electronic wastes, disintegrator milling, plastic powder.

1. INTRODUCTION

Recycling of post-consumer products is becoming increasingly important as an industry response to public demands that resources should be conserved and the environment should be protected. The targets of a minimum reuse, recycling, and recovery on WEEE are settled in the Directive 2002/96/EC that includes all the components, sub-assemblies and consumables that are parts of a product at the time of discarding. RoHS Directive (2002/95/EC) does affect the manufacturers, sellers, distributors, and recyclers of electrical and electronic equipment, which contain lead, mercury, cadmium, hexavalent chromium, or polybrominated diphenyl ethers. Depending upon the use and design of the particular PCB, various other metals may be used in the manufacturing process, including lead, silver, gold, platinum, and mercury. One of the ways of recycling electronic wastes is to produce powdered materials from end-of-life products. Dismantling processes and recycling of PCBs from electronic scrap were discussed in a recent study [1]. Printed circuit boards (PCBs) are common components of many electronic systems built for both military and commercial applications. PCBs are typically manufactured by laminating a dry film on a clean copper foil, which is supported on a fibreglass plate matrix. The film is exposed to the film negative of the circuit board design and an etcher is used to remove the unmasked copper foil from the plate. Solder is then applied over the unetched copper on the board [2].

PCBs are potentially a difficult waste material to process since they generally have no use once they are removed from the electrical component in which they were installed. In addition, they typically consist of the materials classified as a hazardous or “special” waste stream. They must be segregated and handled separately from other non-

hazardous solid waste streams. As an alternative to off-site disposal, PCBs can be handled and processed to recover the value of the raw materials that are used to produce the boards.

For recycling PCBs there are several chemical and mechanical methods available. Chemical methods mainly include:

- pyrolysis and combustion;
- hydration and electrolysis.

The mechanical methods of PCB recycling include:

- size reduction by shredders, hammer mills;
- screening: rotating screen, or trammel, vibratory screening;
- shape, density and magnetic separation;
- electric conductivity based separation, such as Eddy Current separation, corona electrostatic separation, and triboelectric separation;

This work is mainly focused in mechanical recycling methods. The size reduction equipment for mechanical recycling PCBs from the end-of-life durable goods will include the following advantages: it accommodates large amounts of metal, handles tough engineering plastics in reasonable throughputs, liberates moulded-in and well-adhered materials, it does not embed or encapsulate foreign materials, it produces uniform particle shapes and sizes, requires low maintenance costs, it is easy to clean because of the switch-overs of material, it produces low noise and has reasonable power requirements [3].

In addition to traditional mechanical direct contact milling methods (ball-milling, attritor milling, hammer milling, etc.), PCBs can be reprocessed by the collision method.

The fracture of particles in collision with the milling component of one of the rotating rotors is called disintegration. The theoretical studies on milling by the collision method, which were conducted at Tallinn University of Technology (TUT), were followed by the development of the appropriate devices, called disintegrators, and the dif-

*Corresponding author. Tel.: +372-620-3353; fax.: +372-620-319664.
E-mail address: Jaan.Kers@ttu.ee (J. Kers)

ferent types of disintegrator milling, the DS-series systems [4]. Depending on the design of the disintegrator systems, the direct, separative and selective types of milling are available to be used in powder production. Direct milling suits best for testing the properties of materials or producing materials with a wide granulometry, it is used for the treatment of dry, damp and liquid materials. Separative milling is meant only for dry materials, it yields materials with a high degree of fineness and a narrow granulometry [5]. Selective milling is suitable for the treatment of multi-component materials, such as the components of industrial and domestic wastes, etc. The main kinematic parameter in the processing of materials is the specific energy of treatment E_s in kWh per ton, both in view of the size reduction effect and the economic aspect of the process [6]. The size reduction of PCBs as a function of the particle size of the specific energy of treatment was studied.

2. EXPERIMENTAL

2.1. Materials to be reprocessed

Printed circuit boards are mainly produced from thermosetting resin (epoxy or phenolic resin) and reinforced with fibres such as paper, wood, textile, and glass (of high performance).

PCB consists of ~72 wt. % of organic substance and ~28 wt. % of metals (see Fig. 1).



Fig. 1. Preliminarily crushed PCBs separated from dismantled post-consumer electronic equipment

The main composition of the organic substance is the ethoxyline resin bromide or ethoxyline resin chloridate. Many PCBs are made up of either polymer films such as polyimides, or less frequently polyethylene terephthalate or polyethylene naphthalate, or glass fibre composites bonded with a thermoset resin. Common resins include difunctional epoxy resins such as bisphenol, multifunctional epoxy resins such as phenol and creosol based epoxy novolacs, BT epoxy blends, cyanate esters, and polyimides. The most common hardener is dicyanodiamide, diamino-diphenyl sulfone and diamino-diphenyl methane are also used [7].

Depending upon the use and design of the particular PCB, various other metals may be used in the manufacturing process, including lead, silver, gold, platinum, and mercury. The scrap of PCBs contains multi-elements: Al

(2.8 mass %), Cu (10.0 mass %), Pb (1.2 mass %), Zn (1.6 mass %), Ni (0.85 mass %), Ag (280 ppm), Au (110 ppm) [8].

The purity of precious metals in PCBs is more than 10 times higher than that of rich-content minerals. Therefore, recycling of PCBs is an important subject not only from the treatment of waste but also from the recovery of valuable materials [9].

2.2. Reprocessing technology

Milling by collision means that the mechanisms of the particle size reduction of the ductile and brittle materials are different. The milling of brittle materials by collision results in a direct fracture. When milling ductile metallic materials at the initial stage, the metal will be hardened and the fatigue fracture will occur [6]. The separation systems in the DS-series disintegrators are based on the aerodynamic forces. A special inertial classifier with a closed air or gas system has been developed [10]. This system is autonomous and ecologically clean due to the use of kinetic energy in the output material. The system does not need any additional devices of transportation or fans. For various materials and disintegrator milling systems, different inertial classifiers have been designed and developed as an axial inertial classifier and a classifier with a grid formed by the row of blades (see Fig. 2.) [11, 12].

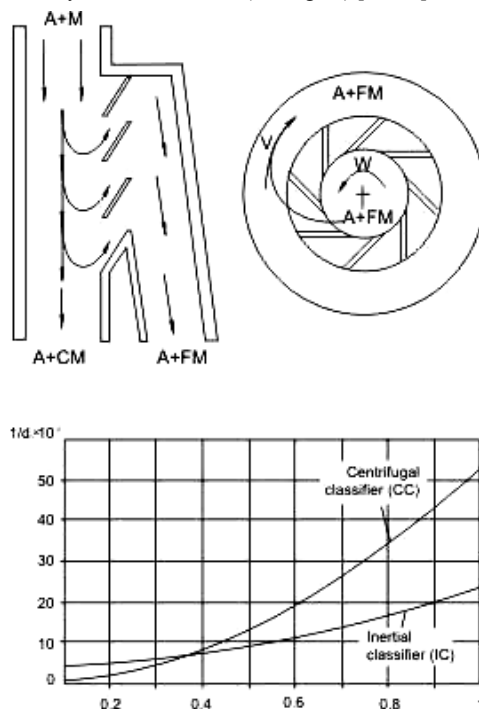


Fig. 2. The principal schemes of the inertial (air) classifier and centrifugal classifier

The reprocessing technology of the PCBs in disintegrators consisted of the following stages:

- the preliminary size reduction of the PCB plates by the experimental DSL-158 disintegrator (up to 2 times);

- the intermediate milling for the size reduction in the semi-industrial disintegrator DSA-2 (up to 6 times);
- the final milling by the DSL-115 disintegrator system in the selective milling conditions to separate the plastic and metallic components.

2.3. Characterization of the milled product

The particle size and distribution in the milled powders were examined with the help of two methods:

- sieve analysis (particle size more than 100 μm);
- laser granulometry analysis by Laser particle sizer Analysette 22 Compact (max particle size 300 μm)

To characterize the material, a scanning electron microscope (SEM) JEOLJSM-840A was used. The chemical composition of the PCB powders was studied by means of the energy dispersive X-ray microanalysis (EDS) with the Link Analytical AN10000 system. The X-ray mapping technique was used to evaluate element distribution inside the powder particles.

3. RESULTS AND DISCUSSION

3.1. Properties of the milled product

The results of the preliminary size reduction, intermediate and final milling are given in Fig 3. The medium particle size of the plastic component from a PCB after a 2-stage milling is about 5 mm–10 mm, after 1–2 times of milling in the disintegrator DSA-2 it is around 1 mm. The subsequent continuous milling (6 times) in DSA-2 reduced the medium particle size to 0.45 mm. As the medium particle size and mass distribution were similar after the 6th and the 8th milling in DSA-2, the new equipment DSL-115 for further size reduction was used. The next remarkable size reduction occurred after the 4th milling in DSL-115, the medium particle size being 0.12 mm.

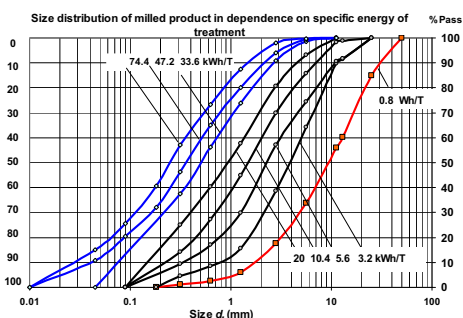


Fig. 3. Dependence of the particle medium size of PCBs on the specific energy of treatment

The powder particles from the PCB after the preliminary size reduction were mainly lamellar after preliminary milling and they stayed lamellar after the multi-stage milling (up to 8 times) in the disintegrator DSL-115. The mechanism of the fracture of PCB particles was the same after preliminary and final milling.

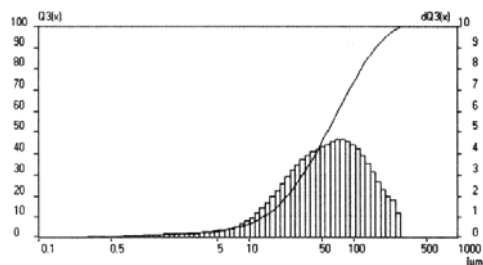


Fig. 4. Laser granulometry of the milled PCB powder

The particle size and distribution of the fine material (70 wt. %) obtained from the 8th milling in DSL-115 (0 mm–0.3 mm) was determined by Laser Granulometry (see Fig. 4). The arithmetic mean diameter of the particle is 74 μm .

3.2. Separation of materials

After two times precruching in DSL-158 disintegrator the 8 wt. % of ferrous metals were separated from milled product by magnet. During the intermediate milling in DSA-2 disintegrator mill the amount of separated ferrous metals was decreasing from 6 wt. % (after 1st milling stage) to 2 wt. % (after 8th milling stage). During the final milling in DSL-115 disintegrator the amount of separated ferrous metals was less than 1 wt. %. It was obvious that the effectiveness of magnetic separation is depending on the size of milled product. AS the particles size of the PMMA powder varied on a large scale, the powder was classified by sieving into 7 fractions: (–0.125 mm; +0.125–0.315 mm; +0.315–0.63 mm; +0.63–1.25 mm; +1.25–2.5 mm; +2.5–5.6 mm and 5.6–11.2 mm) by sieving. The ferrous metals were separated in every fraction by a magnet (except fraction 0–0.125 mm).

The magnetic separation of the ferrous metals gave sufficiently good results (1.2–5 wt. %) for fractions with a larger particle size (see Figs. 5–7), but for fractions less than 0.63 mm the separation was less effective because of the particles were adhering to each other.



Fig. 5. Separated non-ferrous metals and composite plastic from the coarse fraction +1.25–2.5 mm



Fig. 6. Separated ferrous metals from the coarse fraction +1.25 – 2.5 mm

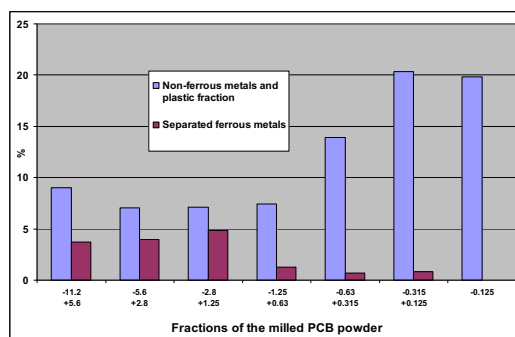


Fig. 7. Results of magnetic separation

The final milling was done by the DSL-115 disintegrator system in the selective milling conditions to

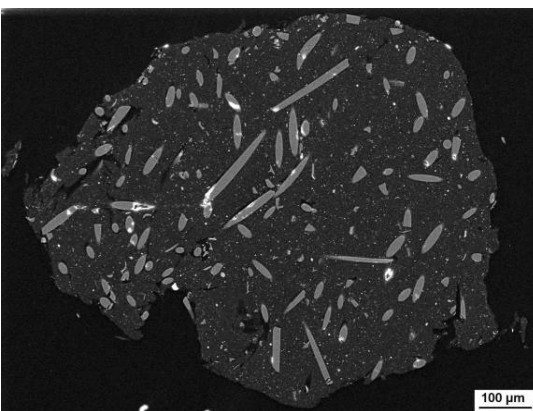
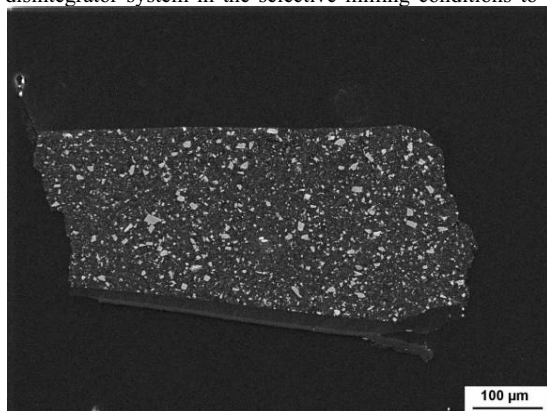


Fig. 9. EDS photos of PCB powder particles: a – green plastic matrix with 5 μm – 10 μm CaCO₃ crystals inside, b – black plastic matrix with Al – 7; Si – 24; Ca – 15 fibre

3.3. EDS analysis of the milled PCB powder

The sample of the PCB milled powder was prepared with the help of SEM. In the sample the plastic and metallic fractions were separated and weighed. The powder contained 29 % metallic content. The micro polish of the sample was made for the EDS analysis. Oxygen was calculated by the difference of 100 %. The chemical composition of the milled PCB powder particles was analyzed by EDS, with the results given in weight percentages.

separate the plastic and metallic components by air classifier.

The separation of plastic and metallic components of the milled PCB powder was not successful, only a small amount of tinfoil and fibres were separated (see Fig. 8).

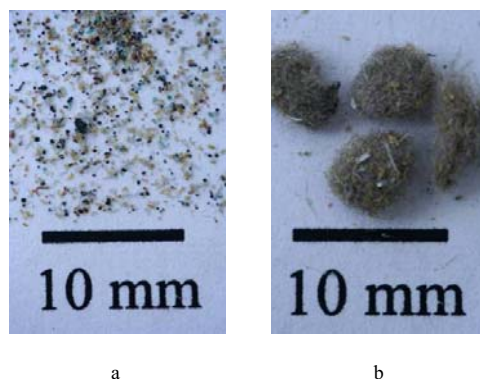


Fig. 8. PCB milled product after 8-time milling in DSL-115: a – separated PCB-powder particles, b – separated glass-fibre

The reason of the poor results could be a small difference in the specific weight of the powder particles. To study the chemical composition of the PCB milled powder the EDS analysis was performed.

As it follows from Table 1, most of the plastic particles are containing different metallic crystals or grains (see Fig. 9).

4. CONCLUSIONS

1. The best results of PCB waste reprocessing by disintegrators will enable a remarkable size reduction after two stages of preliminary crushing and four stages of intermediate milling.

Table 1. Chemical composition of PCB powder particles by EDS analysis

Object No.	Composition, wt %	Description
11	Ca–38; Mg–0.4; O–61.4	Green plastic matrix, 5 µm–10 CaCO ₃ crystals inside
19	Al–33; O–67	Blue plastic matrix, 10 µm–100 µm Al particles inside
23	Si–45; O–55	Black plastic matrix, 10 µm–100 µm SiO ₂ grains inside
25	Al–7; Si–24; Ca–15; Ti–0.4; O–53.6	Black plastic matrix with Al–7; Si–24; Ca–15 fibres
32	Cu–65; Zn–35	CuZn35 brass, on the edge Sn–90; Pb–10
41	Sn–84; Pb–15,8; Al–0,2	Sn80–Pb20 solder
61	Cu–98	20 µm thick Cu stripe with white plastic particle
84	Pure Al	5 µm–10 µm thick Al stripe

- Larger metal particles and thin foil stripes from condensators can be separated by sieving. The ferrous metallic components of coarse fractions can be separated with magnets. For fine fractions (–0.63 mm) the magnetic separation is poor.
- The study of the chemical composition of the PCB powder particles showed that in the plastic particles metallic grains or crystals are in the matrix and because of that they cannot be separated by density separation or the air-classificator system.
- The separation of the plastic and metallic parts of the milled multi-material in the selective milling conditions needs an additional study to determine the optimum milling parameters and in the design of new wet classifiers accounting for the densities of plastic and metallic particles.
- The separated ferrous metals can be recovered by metallurgical methods. For separation and recovery of non-ferrous metals from milled material the pyrometallurgical or hydrometallurgical methods could be applied.
- Tymanok, A., Kulu, P.** Treatment of Different Materials by Disintegrator Systems *Proceedings of Estonian Academy of Sciences, Engineering* 5 1999: pp. 222–242.
- Tymanok, A., Kulu, P., Goljandin, D., Roshchin, S.** Disintegrator as a Machining Device of Metal Chips to Metal Powder *In Proceedings of III ASM International Conference of the Recycling of Metals. Barcelona, 1997:* pp. 513–522.
- Bernardes, I. B. A., Rodriguez, D.** Recycling of Printed Circuit Boards by Melting with Oxidising/Reducing Top Blowing Process *In Proceedings Sessions and Symposia Sponsored by the Extraction and Processing Division, TMS Annual Meeting, B. Mishra, Ed., Orlando, FL, February 9–13, 1997:* pp. 363–375.
- Zhang, S., Forsberg, E.** Electronic Scrap Characterization for Materials Recycling *Journal of Waste Management and Resource Recovery* 3 1997: pp. 157–167.
- Cui, J., Zhang, L.** Metallurgical Recovery of Metals from Electronic Waste: A Review *Journal of Hazardous Materials:* doi:10.1016/j.jhazmat. 2008.02.001, 2008.
- Tymanok, A., Tamm, J., Roes, A.** Flow of Air and Particles Mixture in a Disintegrator *Proceedings of Estonian Academy of Sciences, Physics Mathematics* 43 (4) 1994: pp. 280–292.

REFERENCES

- Hall, W. P.** Separation and Recovery of Materials from Scrap Printed Circuit Boards, Resources Conservation and Recycling (2006), doi:10.1016/j.resconrec.2006.11.010.
- Printed Circuit Board Materials Handbook. McGraw-Hill Professional, 1997, 784 p.
- Biddle, M. B., Dinger, P., Fisher, M. M.** An Overview of Recycling Plastics from Durable Goods: Challenges and Opportunities *Identiplast II Conference Proceedings, APME, Brussels, April 1999.*
- Tamm, B., Tymanok, A.** Impact Grinding and Disintegrators *Proceedings of Estonian Academy of Sciences, Engineering* 2 1996: pp. 209–223.
- Tymanok, A., Kulu, P., Goljandin, D., Roshchin, S.** Disintegrator as a Machining Device of Metal Chips to Metal Powder *In Proceedings of III ASM International Conference of the Recycling of Metals, Barcelona, 1997:* pp. 513–522.
- Tymanok, A., Kulu, P., Goljandin, D.** Metallic Powders Produced by Mechanical Methods *Materials Science (Medžiagotyra)* 9 (2) 1999: pp. 3–7.

Presented at the 17th International Conference
 "Materials Engineering '2008"
 (Kaunas, Lithuania, November 06–07, 2008)

ELULOOKIRJELDUS

1. Isikuandmed

Ees- ja perekonnanimi
Sünniaeg ja -koht
Kodakondsus
E-posti aadress

Dmitri Goljandin
23.03.1973, Tallinn, Estonia
Eesti
dmitri.goljandin@ttu.ee

2. Hariduskäik

Õppeasutus (nimetus lõpetamise ajal)	Lõpetamise aeg	Haridus (eriala/kraad)
Tallinna 40. Keskkool	1990	keskharidus
Tallinna Tehnikaülikool	2002	Tehnikateaduste magister

3. Keelteoskus (alg-, kesk- või kõrgtase)

Keel	Tase
Eesti keel	kõrgtase
Vene keel	emakeel
Inglise keel	kesktase

4. Teenistuskäik

Töötamise aeg	Tööandja nimetus	Ametikoht
1995 - 1998	Tallinna Tehnikaülikool	abitöölaine
1998 - 2002	Tallinna Tehnikaülikool	Erakorraline teadur
2002 - ...	Tallinna Tehnikaülikool	Teadur

5. Teadustegevus

Desintegraatorjahvatuse tehnoloogia (materjalide ülipeen jahvatus, jahvatuse ja materjalide purunemise teooria, separatsiooni ja materjalide klassifitseerimise teooria, tsentrifugaalse klassifikaator-separaatori väljatöötamine jahvatussüsteemidele, autorehvide utiliseerimine jahvatamise teel normaaltemperatuuril)

6. Uurimisprojektides osalemine

Jooksvates projektides:

ETF8850, Isesobituvad adaptiivsed tribomaterjalid mineraalide baasil. 2011-2014

AR12132, Kõrgtehnoloogiliste pinnete ja komposiitmaterjalide arendus kuluosade tarvis. 2012-2014

SF0140091s08, Kõvapinded ja pinnatehnika. 2008-2013

Lõpetatud projektides:

ETF7705, Uus komposiitjäätmete taaskasutustehnoloogia. 2009

V337, Desintegraatori konstrueerimine. 2006-2007

G5881, Nanopulbrid ja nanostruktruursed pinded. 2004-2006

T082, Pihustus- ja sadestuspinded. 2002-2005

V173, Uued kulumis- ja korrosioonikindlad termopinded. 2001-2004

ETF4849, Ülipeened komposiitpulberpindematerjalid. 2001-2003

V176, Laboratoorne desintegraator DSL-160M. 2002

249L, Nioobiumi jahvatustehnoloogia. Tehnoloogilist aparatuuri tugevdav tehnoloogia. 2002

Ilmunud publikatsioone - 32 (allikas: www.etis.ee)

Muud tulemused:

- Ukraina Vabariigi patent nr 20751A (1998) Int.Cl.⁶ B 02 C 13/26
“Desintegraator”, autorid *A.Tümanok, D.Goljandin, O.Tugai, A.Stupnitski*
- Tunnistus nr EE 9700127 Int.Cl.⁶ B 02 C 13/22 “Põrkeveski”
Autorid *D.Goljandin, A.Tümanok*.

CURRICULUM VITAE

1. Personal data

Name	Dmitri Goljandin
Date and place of birth	23.03.1973, Tallinn, Estonia
E-mail	dmitri.goljandin@ttu.ee

2. Education

Educational institution	Graduation year	Education (field of study/degree)
Tallinn Co-education gymnasium	1990	High school
Tallinn University of Technology	2002	Master of Science

3. Language competence/skills (fluent; average, basic skills)

Language	Level
Estonian	Fluent
Russian	Mother tongue
English	average

5. Professional employment

Period	Organisation	Position
1995 - 1998	Tallinn University of Technology	assistant
1998 - 2002	Tallinn University of Technology	visiting fellow
2002 - ...	Tallinn University of Technology	researcher

6. Scientific work

Disintegrator milling systems and milling technology (ultrafine grinding of materials, theory of grinding and impact grinding mechanics, theory of separation and classification of a product, selective grinding, balancing and

systems of automatic balance , utilisation of used tyres by grinding at normal temperature)

7. Main areas of scientific work

Current research topics:

ETF8850, Self-organisation of minerals based adaptive tribomaterials. 2011-2014

AR12132, Development of advanced coatings and polymer – ceramic composites for road construction machinery wear parts (Wear Hard). 2012-2014

SF0140091s08, Hard coatings and surface engineering. 2008-2013

Finished research topics:

ETF7705, New recycling technology for composite plastic scrap. 2009

V337, Design of a disintegrator. 2006-2007

ETF 5881, Nanopowders and nanostructured coatings. 2004-2006

V173, Novel Manufacturing of Wear and Corrosion Resistant Thermally Sprayed. 2001-2004

ETF4849, Ultrafine composite powders for thermal spray. 2001-2003

V176, Laboratory Disintegrator DSL-160M. 2002

249L , Milling technology of niobium. Protection of technological devices by coatings. 2002

Number of publications - 32 (source: www.etis.ee)

Other:

- Patent of the Republic Ukraine nr 20751A (1998) Int.Cl.⁶ B 02 C 13/26 “Desintegraator”, authors: *A.Tümanok, D.Goljandin, O.Tugai, A.Stupnitski*
- Utility model nr EE 9700127 Int.Cl.⁶ B 02 C 13/22 “Pörkeveski”
Authors: D.Goljandin, A.Tümanok,

**DISSERTATIONS DEFENDED AT
TALLINN UNIVERSITY OF TECHNOLOGY ON
*MECHANICAL ENGINEERING***

1. **Jakob Kübarsepp**. Steel-Bonded Hardmetals. 1992.
2. **Jakub Kõo**. Determination of Residual Stresses in Coatings & Coated Parts. 1994.
3. **Mart Tamre**. Tribocharacteristics of Journal Bearings Unlocated Axis. 1995.
4. **Paul Kallas**. Abrasive Erosion of Powder Materials. 1996.
5. **Jüri Pirso**. Titanium and Chromium Carbide Based Cermets. 1996.
6. **Heinrich Reshetnyak**. Hard Metals Serviceability in Sheet Metal Forming Operations. 1996.
7. **Arvi Kruusing**. Magnetic Microdevices and Their Fabrication methods. 1997.
8. **Roberto Carmona Davila**. Some Contributions to the Quality Control in Motor Car Industry. 1999.
9. **Harri Annuka**. Characterization and Application of TiC-Based Iron Alloys Bonded Cermets. 1999.
10. **Irina Hussainova**. Investigation of Particle-Wall Collision and Erosion Prediction. 1999.
11. **Edi Kulderknuip**. Reliability and Uncertainty of Quality Measurement. 2000.
12. **Vitali Podgurski**. Laser Ablation and Thermal Evaporation of Thin Films and Structures. 2001.
13. **Igor Penkov**. Strength Investigation of Threaded Joints Under Static and Dynamic Loading. 2001.
14. **Martin Eerme**. Structural Modelling of Engineering Products and Realisation of Computer-Based Environment for Product Development. 2001.
15. **Toivo Tähemaa**. Assurance of Synergy and Competitive Dependability at Non-Safety-Critical Mechatronics Systems design. 2002.
16. **Jüri Resev**. Virtual Differential as Torque Distribution Control Unit in Automotive Propulsion Systems. 2002.
17. **Toomas Pihl**. Powder Coatings for Abrasive Wear. 2002.
18. **Sergei Letunovitš**. Tribology of Fine-Grained Cermets. 2003.
19. **Tatyana Karaulova**. Development of the Modelling Tool for the Analysis of the Production Process and its Entities for the SME. 2004.
20. **Grigori Nekrassov**. Development of an Intelligent Integrated Environment for Computer. 2004.

21. **Sergei Zimakov**. Novel Wear Resistant WC-Based Thermal Sprayed Coatings. 2004.
22. **Irina Preis**. Fatigue Performance and Mechanical Reliability of Cemented Carbides. 2004.
23. **Medhat Hussainov**. Effect of Solid Particles on Turbulence of Gas in Two-Phase Flows. 2005.
24. **Frid Kaljas**. Synergy-Based Approach to Design of the Interdisciplinary Systems. 2005.
25. **Dmitri Neshumayev**. Experimental and Numerical Investigation of Combined Heat Transfer Enhancement Technique in Gas-Heated Channels. 2005.
26. **Renno Veinthal**. Characterization and Modelling of Erosion Wear of Powder Composite Materials and Coatings. 2005.
27. **Sergei Tisler**. Deposition of Solid Particles from Aerosol Flow in Laminar Flat-Plate Boundary Layer. 2006.
28. **Tauno Otto**. Models for Monitoring of Technological Processes and Production Systems. 2006.
29. **Maksim Antonov**. Assessment of Cermets Performance in Aggressive Media. 2006.
30. **Tatjana Barashkova**. Research of the Effect of Correlation at the Measurement of Alternating Voltage. 2006.
31. **Jaan Kers**. Recycling of Composite Plastics. 2006.
32. **Raivo Sell**. Model Based Mechatronic Systems Modeling Methodology in Conceptual Design Stage. 2007.
33. **Hans Rämmal**. Experimental Methods for Sound Propagation Studies in Automotive Duct Systems. 2007.
34. **Meelis Pohlak**. Rapid Prototyping of Sheet Metal Components with Incremental Sheet Forming Technology. 2007.
35. **Priidu Peetsalu**. Microstructural Aspects of Thermal Sprayed WC-Co Coatings and Ni-Cr Coated Steels. 2007.
36. **Lauri Kollo**. Sinter/HIP Technology of TiC-Based Cermets. 2007.
37. **Andrei Dedov**. Assessment of Metal Condition and Remaining Life of In-service Power Plant Components Operating at High Temperature. 2007.
38. **Fjodor Sergejev**. Investigation of the Fatigue Mechanics Aspects of PM Hardmetals and Cermets. 2007.
39. **Eduard Ševtšenko**. Intelligent Decision Support System for the Network of Collaborative SME-s. 2007.
40. **Rünno Lumiste**. Networks and Innovation in Machinery and Electronics Industry and Enterprises (Estonian Case Studies). 2008.

41. **Kristo Karjust.** Integrated Product Development and Production Technology of Large Composite Plastic Products. 2008.
42. **Mart Saarna.** Fatigue Characteristics of PM Steels. 2008.
43. **Eduard Kimmari.** Exothermically Synthesized B₄C-Al Composites for Dry Sliding. 2008.
44. **Indrek Abiline.** Calibration Methods of Coating Thickness Gauges. 2008.
45. **Tiit Hindreus.** Synergy-Based Approach to Quality Assurance. 2009.
46. **Karl Raba.** Uncertainty Focused Product Improvement Models. 2009.
47. **Riho Tarbe.** Abrasive Impact Wear: Tester, Wear and Grindability Studies. 2009.
48. **Kristjan Juhani.** Reactive Sintered Chromium and Titanium Carbide-Based Cermets. 2009.
49. **Nadežda Dementjeva.** Energy Planning Model Analysis and Their Adaptability for Estonian Energy Sector. 2009.
50. **Igor Krupenski.** Numerical Simulation of Two-Phase Turbulent Flows in Ash Circulating Fluidized Bed. 2010.
51. **Aleksandr Hlebnikov.** The Analysis of Efficiency and Optimization of District Heating Networks in Estonia. 2010.
52. **Andres Petritšenko.** Vibration of Ladder Frames. 2010.
53. **Renee Joost.** Novel Methods for Hardmetal Production and Recycling. 2010.
54. **Andre Gregor.** Hard PVD Coatings for Tooling. 2010.
55. **Tõnu Roosaar.** Wear Performance of WC- and TiC-Based Ceramic-Metallic Composites. 2010.
56. **Alina Sivitski.** Sliding Wear of PVD Hard Coatings: Fatigue and Measurement Aspects. 2010.
57. **Sergei Kramanenko.** Fractal Approach for Multiple Project Management in Manufacturing Enterprises. 2010.
58. **Eduard Latõsov.** Model for the Analysis of Combined Heat and Power Production. 2011.
59. **Jürgen Riim.** Calibration Methods of Coating Thickness Standards. 2011.
60. **Andrei Surzhenkov.** Duplex Treatment of Steel Surface. 2011.
61. **Steffen Dahms.** Diffusion Welding of Different Materials. 2011.
62. **Birthe Matsi.** Research of Innovation Capacity Monitoring Methodology for Engineering Industry. 2011.
63. **Peeter Ross.** Data Sharing and Shared Workflow in Medical Imaging. 2011.
64. **Siim Link.** Reactivity of Woody and Herbaceous Biomass Chars. 2011.

65. **Kristjan Plamus**. The Impact of Oil Shale Calorific Value on CFB Boiler Thermal Efficiency and Environment. 2012.
66. **Aleksei Tšinjan**. Performance of Tool Materials in Blanking. 2012.
67. **Martinš Sarkans**. Synergy Deployment at Early Evaluation of Modularity of the Multi-Agent Production Systems. 2012.
68. **Sven Seiler**. Laboratory as a Service – A Holistic Framework for Remote and Virtual Labs. 2012.
69. **Tarmo Velsker**. Design Optimization of Steel and Glass Structures. 2012.
70. **Madis Tiik**. Access Rights and Organizational Management in Implementation of Estonian Electronic Health Record System. 2012.
71. **Marina Kostina**. Reliability Management of Manufacturing Processes in Machinery Enterprises. 2012.
72. **Robert Hudjakov**. Long-Range Navigation for Unmanned Off-Road Ground Vehicle. 2012.
73. **Arkadi Zikin**. Advanced Multiphase Tribo-Functional PTA Hardfacings. 2013.
74. **Alar Konist**. Environmental Aspects of Oil Shale Power Production. 2013.
75. **Inge Roos**. Methodology for Calculating CO₂ Emissions from Estonian Shale Oil Industry. 2013.
76. **Dmitri Shvarts**. Global 3D Map Merging Methods for Robot Navigation. 2013.
77. **Kaia Lõun**. Company's Strategy Based Formation of e-Workplace Performance in the Engineering Industry. 2013.